

INVESTIGATION OF THE EFFECT OF REACTOR SIZE
ON THE NETT RATE OF FORMATION OF HYDRAZINE
FROM AMMONIA IN A GLOW DISCHARGE.

Submitted in part fulfilment of
the Degree of Doctor of Philosophy
in the Faculty of Applied Science,
in the University of Newcastle-
upon-Tyne.

R. A. RIELLEY, BSc.

1973.

BEST COPY

AVAILABLE

Variable print quality

SUMMARY.

The effect of reactor size on the nett rate of formation of hydrazine in an electrical discharge in ammonia gas has been studied. Three geometrically similar reactor units, the largest of which was greater in volume by a factor of 64:1 compared to the smallest, were used in this work.

The nett rate of formation of hydrazine has been found to be inversely proportional to reactor size. Evidence has been provided which suggests that changing the reaction tube size results in a change in the concentration of atomic hydrogen in the reaction zone. As the reaction tube diameter is increased the rate of diffusion of atomic hydrogen to the reaction tube surface is decreased. This results in a decrease in the rate of recombination of atomic hydrogen at the reaction tube surface, and consequently an increase in the concentration of atomic hydrogen in the reaction zone. In turn this leads to an increase in the rate of destruction of hydrazine by atomic hydrogen attack and as a result, a decrease in the nett rate of formation of hydrazine.

Attempts to minimise the concentration of atomic hydrogen in a large scale reactor, by packing the reactor with a quartz surface (wool), failed due to field distortion with subsequent discharge constriction, and also due to the catalytic nature of the quartz surface employed.

In the early experimental work several of the major reactor design problems encountered in scale up were identified. One of these was the constriction of the discharge zone into a narrow beam thereby allowing some of the gas to by-pass this zone completely. Because of this, the early work was directed towards obtaining a set of reactor units, in

which the discharge occupied the entire volume between the electrodes over a wide range of operating conditions. In this work it was found that under dc discharge conditions, electrodes of diameter greater than a critical size which is dependent upon a number of interdependent factors viz.

- a) the nature of the reactant gas
- b) reactor unit geometry
- c) electrode material and electrode profile
- d) the flow pattern of the gaseous reactant
- e) electrical and operating conditions - of which the most important are electric current density, operating pressure, and gas flow rate

give rise to non-uniform constricted discharges.

In chapter 2.3 the hypothesis that physical similarity (similarity in the physics of the discharge) in two geometrically similar discharges of different size, ensures chemical similarity has been examined.

This was done by testing whether or not the ' similarity principle ' could be applied to electrical discharges in which chemical reactions occur.

The results of this investigation show that while discharge processes depending on single electron impact activation follow the ' similarity principle ', the relationship does not hold for chemical reactions where secondary processes are of primary importance. Consequently semi-theoretical methods of investigation have been used in this work and an equation of the form -

$$\left(\frac{r D^3}{FC} \right) \propto \left(\frac{V_p D^4}{F^3 C} \right)^\alpha \left(\frac{D^4 P}{F^2 C} \right)^b \left(\frac{L}{D} \right)^c$$

where r: nett rate of formation of hydrazine

D: reaction tube diameter

F: ammonia gas flow rate

C: ammonia gas concentration

V_p : potential difference across the reaction zone (positive column) of the discharge

I : discharge current

L : length of the reaction zone (positive column)

p : pressure in the reaction zone (positive column)

a, b, c : constants

which was derived using the technique of dimensional analysis, has been used to correlate the experimental results satisfactorily.

Finally during the course of the experimental work it was discovered that the nett rate of formation of hydrazine depended on the reactor unit ' age ', and consequently a small amount of work was carried out to investigate this phenomenon. The results of this research indicate that the effect of reactor unit ' age ' is primarily due to a change in either the catalytic and/or adsorption properties of the reaction tube surface, and not due to changes in the electrode surface as was previously believed.

ACKNOWLEDGEMENTS.

The author wishes to express his gratitude to the following -

Professor J. D. Thornton for his supervision, advice and encouragement throughout this work and especially for the manner in which this was given.

Professor J. M. Coulson in whose laboratories this work was carried out.

Dr. C. R. Howarth and Dr. F. H. Haji for countless stimulating discussions.

Mr. C. A. Currie and his staff and in particular Mr. G. Doherty for assistance in the design and construction of the experimental equipment.

Mr. R. R. Randle, for the photographic work.

Margaret, my wife, for her patience, understanding and support throughout the course of this work.

The Science Research Council for their financial support.

DEDICATION.

This thesis is dedicated to the memory of my brother Terence

George Rielley.

CONTENTS.

PAGE. NO.

Summary.	
Acknowledgements and Dedication.	
Contents.	
<u>1.0.</u> Introduction.	1
1.1. General Introduction.	1
1.2. Gas Discharge.	4
<u>2.0.</u> Survey of Previous Work.	13
2.1. Reactor Development - Engineering Design and Criteria.	14
2.2. Derivation and Application of the Similarity Principle to Electrical Discharges.	19
2.3. Chemical Studies of the Electrical Discharge Synthesis of Hydrazine from Ammonia.	30
<u>3.0.</u> Scope of Present Investigation.	44
<u>4.0.</u> Experimental Work.	47
4.1. Experimental Equipment.	47
4.1.1. Design, Construction and Arrangement.	47
4.1.2. Flow System.	48
4.1.3. Discharge Reactors.	51
4.1.4. Hydrazine Sampling and Analytical Equipment.	53
4.1.5. Electrical Equipment.	53
4.2. Materials used in Experiments.	57
4.3. Experimental Procedure.	57
4.4. Measurements and Chemical Analysis.	61

	<u>PAGE. NO.</u>
4.4.1. Analysis of Products.	61
4.4.2. Power Measurement.	64
4.4.3. Flow rate Measurement.	64
<u>5.0.</u> Experimental Results and Discussion.	64
5.1. Design, Development and Testing of Chemical Discharge Reactors.	69
5.1.1. Experimental Programme.	69
5.1.2. Results and Discussion.	70
5.2. Investigation of the Effect of Reactor Size on the Nett Rate of Formation of Hyarazine.	77
5.2.1. Experimental Programme and Operating Conditions.	77
5.2.2. Presentation of Experimental Results.	81
5.2.3. Results and Discussion.	86
5.3. Investigation of the effect of Reactor Unit ' Age ' on the Nett Rate of Formation of Hydrazine.	90
<u>6.0.</u> Interpretation of Results.	97
<u>7.0.</u> Recommendations for Future Work.	111
<u>8.0.</u> Conclusions.	114
<u>9.0.</u> Nomenclature.	119
<u>10.0.</u> Literature Cited.	122
<u>Appendicies.</u>	
Appendix 1. Gas Chromatography Work.	128
Appendix 2. Hydrazine Analysis.	131
Appendix 3. Flowmeter calibration Results.	139
Appendix 4. Tabulated Results.	143
Appendix 5. Dimensional Analysis	152
Appendix 6. Method of Estimation of the Abnormal Cathode Fall of Potential and the Length of the Positive Column.	155
Appendix 7. Specimen Calculations.	159

CHAPTER I .O.

1.0. INTRODUCTION

1.1. General Introduction

The powerful reducing character of hydrazine has made it a useful analytical reagent. It may be used to separate and precipitate certain metallic ions as the free metals and it also precipitates complex compounds of nickel, cobalt, and cadmium and can be used for the quantitative determination of these substances. In addition hydrazine is now being used in the development of new drugs and various biochemicals and dyes.

There is little doubt however, that the present high cost of hydrazine is a major obstacle to its more extensive commercial development. If a cheaper method of hydrazine production could be developed then its very unusual chemical properties could find application in fluxes, photographic developing agents, explosives, insecticides, dyes, pharmaceuticals and many other areas.

Currently hydrazine is only produced commercially by the Raschig process (first developed in 1907) in which ammonia or urea is oxidised by sodium hypochlorite in aqueous solution. Unfortunately this process involves a number of inherent expensive separation, purification and concentration steps which are necessary to obtain hydrazine which meets commercial specifications.

The search therefore, for a reduction in the cost of hydrazine has moved towards the development of alternative methods of synthesis rather than improvement of the existing process.

At present methods of hydrazine synthesis can be placed into three categories which are:-

- 1) Reduction of compounds containing a nitrogen-to-nitrogen linkage.
- 2) Partial oxidation of ammonia or ammonia derivatives such as urea.
- 3) Decomposition of ammonia.

In the last category hydrazine has been obtained by pyrolysis photo-decomposition, electron bombardment and the action of an electrical discharge. Of these methods the discharge route appears to have more commercial potentialities because of the lower energy costs involved.

In the past the use of electrical discharges for chemical synthesis has received limited commercial exploitation. Although this means of chemical synthesis has been recognised for over one hundred years its use has been confined to the production of ozone (first synthesised as far back as 1857) hydrogen peroxide and the electrocracking of hydrocarbons to give olefins and acetylene. More recently it has found application in surface polymerisation processes for the coating of metals and plastics.

Wider commercial development however without doubt has been hindered by the lack of understanding of both the chemical reactions which occur in the discharge and the actual discharge itself. This lack of understanding has persisted until recently for a number of reasons viz:-

1. The discharge reactions and the actual discharge itself are extremely complex. When a molecular gas is subjected to an electrical discharge a complex mixture of gas molecules unchanged by the discharge, initial, intermediate and final reaction products including ions and electrons result.
2. The electrical and chemical characteristics of the discharge are not independent. For example changing the reaction tube diameter changes the surface to volume ratio in the discharge which in turn may change the fraction of chemical reactions occurring on the walls to that occurring in the gas phase. Not only does this add to the complexity of the discharge, but also it makes optimisation of discharge chemical synthesis extremely difficult if not impossible.

3. There is an absence of fundamental discharge data. If for a particular chemical synthesis information such as the particle energy and density distributions, the processes involved and their rates and cross sections was available, then it would be possible to predict the effects of the discharge. In practice very little of this information is known, and only a small amount of that which is known, is applicable to the conditions normally found in commercial discharge reactors.

4. There has been a lack of systematic investigations. Despite the numerous investigations of the past, only a fraction have helped to clarify the effects of discharge and operational variables upon chemical reactions. Apart from the factors outlined above the main reason for this, has been that in the past no systematic studies were carried out in which all of the variables which effect discharge chemical synthesis, were studied for a single system.

In the last twenty years a number of developments (for example the manufacture of more sophisticated and dependable electrical generating equipment and the possibility of a reduction in the relative cost of electrical power (with the advent of nuclear reactors)) have occurred which have significantly increased the commercial potential of the discharge route of chemical synthesis. This has triggered a resurgence of interest in the electrical discharge and in the last decade systematic studies have been undertaken, resulting in a greater understanding of the factors which influence discharge chemical reactions. In particular increased knowledge of the optimum conditions for the synthesis of hydrazine has established that both high conversions and yields of hydrazine

can be obtained (Savage(1970)). Up to the present time however these commercially attractive results have been achieved using laboratory scale reactors and the way in which they depend upon scale-up parameters has not been determined. This is the object of the experimental studies outlined in this thesis which to the author's knowledge is the first systematic investigation of these effects.

1.2. Gas Discharge

1.2.1. General Features.

The term gas discharge is used to describe the flow of electric current through a gaseous medium. This requires that some of the gas particles should be ionised, by some means, and that there should be an electric field to drive the charged particles produced to form a current.

Gas discharges can take place over a very wide range of pressure and carry currents ranging from scarcely measurable values to over 10^6 Amps.

Three distinct types of discharges can be formed which are the Dark or Townsend discharge, the Glow discharge and the Arc discharge (see Fig. 1.1.). The form of these discharges depends to a small extent on whether a direct current (dc), alternating current (ac), high frequency (hf), radio frequency (rf) or microwave discharge system is employed, or in other words on the frequency of the applied voltage used. In addition, the type of discharge formed varies with the nature of the gas, pressure, dimensions of the reactor and the type, size, separation and material of the electrodes.

The discharge system used in the research presented here was a.d.c. glow discharge system and this is discussed in further detail below.

1.2.2. The dc glow discharge.

The gas in a discharge tube always contains a few stray electrons which have been formed as a result of gas ionization by cosmic or other background radiation.

The glow discharge originates with the applied voltage accelerating these electrons, which acquire kinetic energy as they are attracted towards the positive electrode. Their passage through the electrode gap is interrupted by collisions with molecules after which they are re-accelerated towards the anode.

As the voltage is increased some of these electrons gain sufficient energy to ionise the gas molecules on collision. The ions produced drift towards the cathode, becoming sources of more electrons by secondary emission when they hit the cathode. In addition photons emitted as a result of ion-electron recombination and metastable atoms formed through collisions in the discharge also extract electrons from the cathode. These secondary emitted electrons are capable of further gas molecule collisions, and the sequence of events repeats itself. As a result the discharge current is increased and a point is reached where breakdown occurs and the self-sustaining discharge called the Townsend or Dark discharge is formed (see Fig. 1.1.). When the applied voltage is further increased the current becomes large enough ($\sim 10^{-4}$ Amp) to bring about the transition from the Dark discharge into the more complex form known as the glow discharge, and the potential across the discharge tube falls to a constant value.

If the gas pressure is above the arbitrary level of 20 mmHg, the visible nature of the discharge alters into glowing streamers, or striations and the term silent discharge is used. If in this discharge

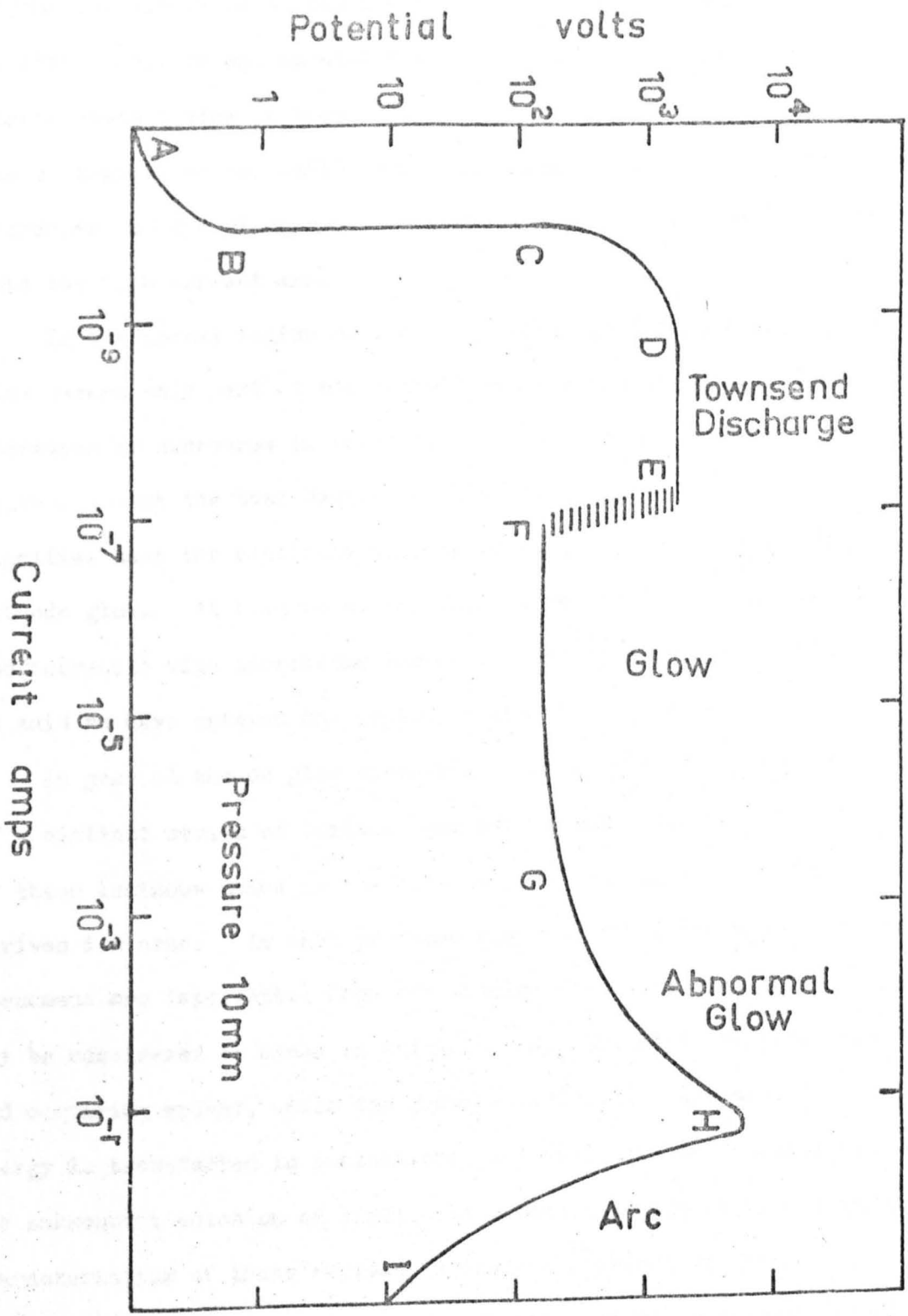


FIG 14

region the electrode surfaces are highly curved a non-homogeneous electric field is set up near the highly curved electrode and the discharge plasma concentrates in this region forming a corona discharge. As the voltage is raised still further the intensity of the visible plasma increases and the discharge enters the abnormal region before passing into the high current arc.

In the normal region of the glow discharge (Fig. 1.1.) the cathode glow covers only part of the cathode surface and the area covered increases or decreases in proportion to the current flowing. When the voltage across the tube begins to rise with increasing current this signifies that the electrode surface is completely covered by the cathode glow. At this point the current density is no longer constant and increases with increasing current. When this occurs the discharge is said to have entered the region of the abnormal glow.

In general the dc glow discharge is characterised by the presence of a distinct series of luminous and dark zones (see Fig. 1.2.). One of these luminous zones is the cathode glow from which the glow discharge derives its name. In each of these regions of the discharge different phenomena are important. From the physical point of view the dark spaces may be considered as areas in which charged particles are accelerating and acquiring energy, while the glowing regions are the areas where this energy is transferred in ionisational and excitational collisions, with the subsequent emission of light. As a result of the different physical characteristics of these regions, different chemical reactions proceed preferentially in one region or other in the discharge. In the case of the nitrogen-hydrogen discharge for example ammonia and

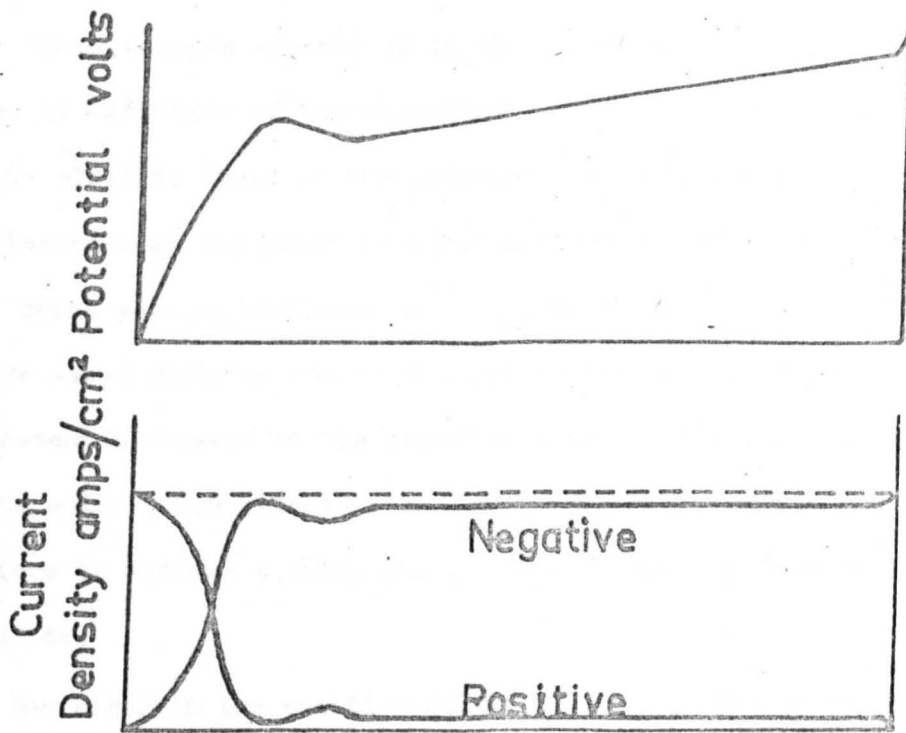
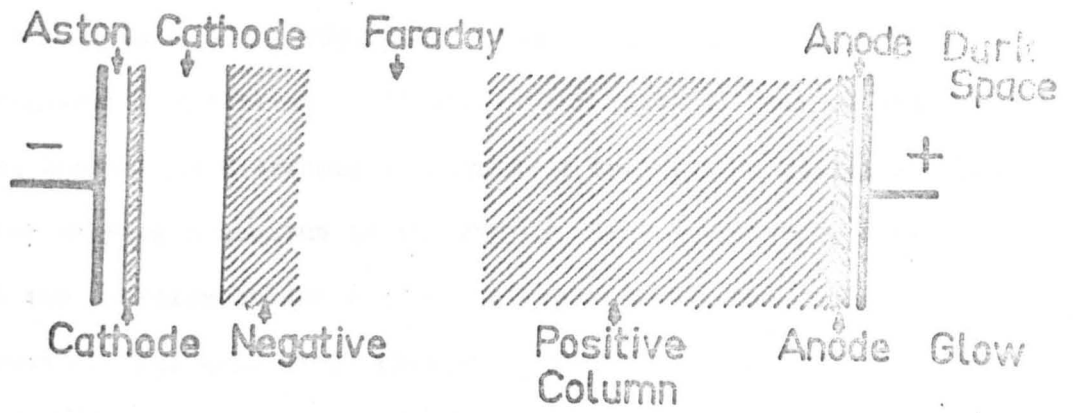


FIG 1.2

hydrazine are formed preferentially in the negative glow and positive column respectively. (Westhaver (1929) (1930)).

As the voltage across the discharge does not vary linearly (because of space charge) as a function of the distance from one of the electrodes, (see Fig. 1.2.) the electric field in each of these regions is different. Initially the field is high at the cathode, however it decreases in magnitude towards the negative glow, and after passing a minimum in the Faraday dark space stays constant through the positive column and only rises again at the anode. Inspection of Fig. 1.2. shows that most of the applied potential is dissipated in the cathode dark space. The potential drop across the cathode dark space is known as the cathode drop or fall.

Space charges are set up in the discharge due to the different rates of diffusion of the electrons (-ve) and positive ions (+ ve). As the electric field in the positive column is constant the concentration of electrons at any point is equal to that of positive ions. If both these species diffused freely to the tube walls a positive space charge would build up due to the faster electron diffusion. This is prevented however as the negative space charge which accumulates on the walls gives rise to a radial field, which forces electrons and ions to diffuse equally fast. This is called ambipolar diffusion.

The field in the positive column is several orders of magnitude smaller than that found in the dark spaces. This, as well as the uniform appearance of the positive column, indicates that the electrons

gain sufficient energy for ionisation in this part of the discharge, as a result of the large random velocity they acquire by elastic collisions: rather than from their drift velocity gained under the action of the field.

If the electrodes in the glow discharge are moved together the positive column disappears indicating that it is not essential to the existence of the discharge. When the distance between the electrodes increases the length of the negative zones remains unchanged while the length of the positive column varies. In practice the positive column can be extended to any length provided the voltage for initiating and maintaining the discharge is sufficiently large.

As the gas pressure in the discharge is increased the negative zones of the discharge contract towards the cathode (above 100 mmHg only the Faraday Dark space is clearly visible) and the positive column expands to fill the vacant space. At higher pressures however radial contraction of the positive column occurs.

1.2.3. Chemical Activation

Activation in a gaseous discharge depends largely on collisions of electrons and gas molecules. Essentially an electron can undergo two types of collision, which have been designated elastic and inelastic collisions.

An elastic collision involves a small change of kinetic energy only, between the colliding particles, whereas an inelastic collision results in a change in the internal energy of the particles. Thus encounters in which excitation or ionisation occur are inelastic, since some of the kinetic energy of the striking electron is transformed into potential energy of the molecule.

In order to make an inelastic collision an electron must acquire sufficient energy to exceed the excitation or ionisation potential of the particle it collides with. Obviously not all electrons acquire this level of energy, and in practice, a distribution of electron energy exists in the discharge, the form of which primarily determines the probability of a certain type of collision (Fig. 1.3. illustrates an example of a theoretically calculated energy distribution. Normally this distribution is concentrated around a definite maximum which depends on field strength, gas pressure and collision frequency). This probability is often represented as a cross-section, for example, (Q_i) is the cross-section for ionisation (see Fig. 1.4.) and similarly (Q_{ex}) is the cross-section for excitation. The total cross-section (Q) for all collisions is simply the sum of the particular cross-sections for particular types of collision.

Normally the electron energy distribution can be broken down into three different energy classes depending on the origin of the electrons. In general the electrons from each of these classes predominantly take part in a particular type of reaction.

The first group of electrons consists of high energy electrons emitted from the electrodes as a result of the impact of positive ions and other species. These electrons form the high energy tail of the electron energy distribution and are primarily responsible for ionisation in the discharge. In the second group the electrons are of lower energy and are released from the gas molecules as they are ionised. These electrons rarely acquire enough energy to ionise gas molecules on single impact but play a predominant role in other activation phenomena leading to chemical reaction.

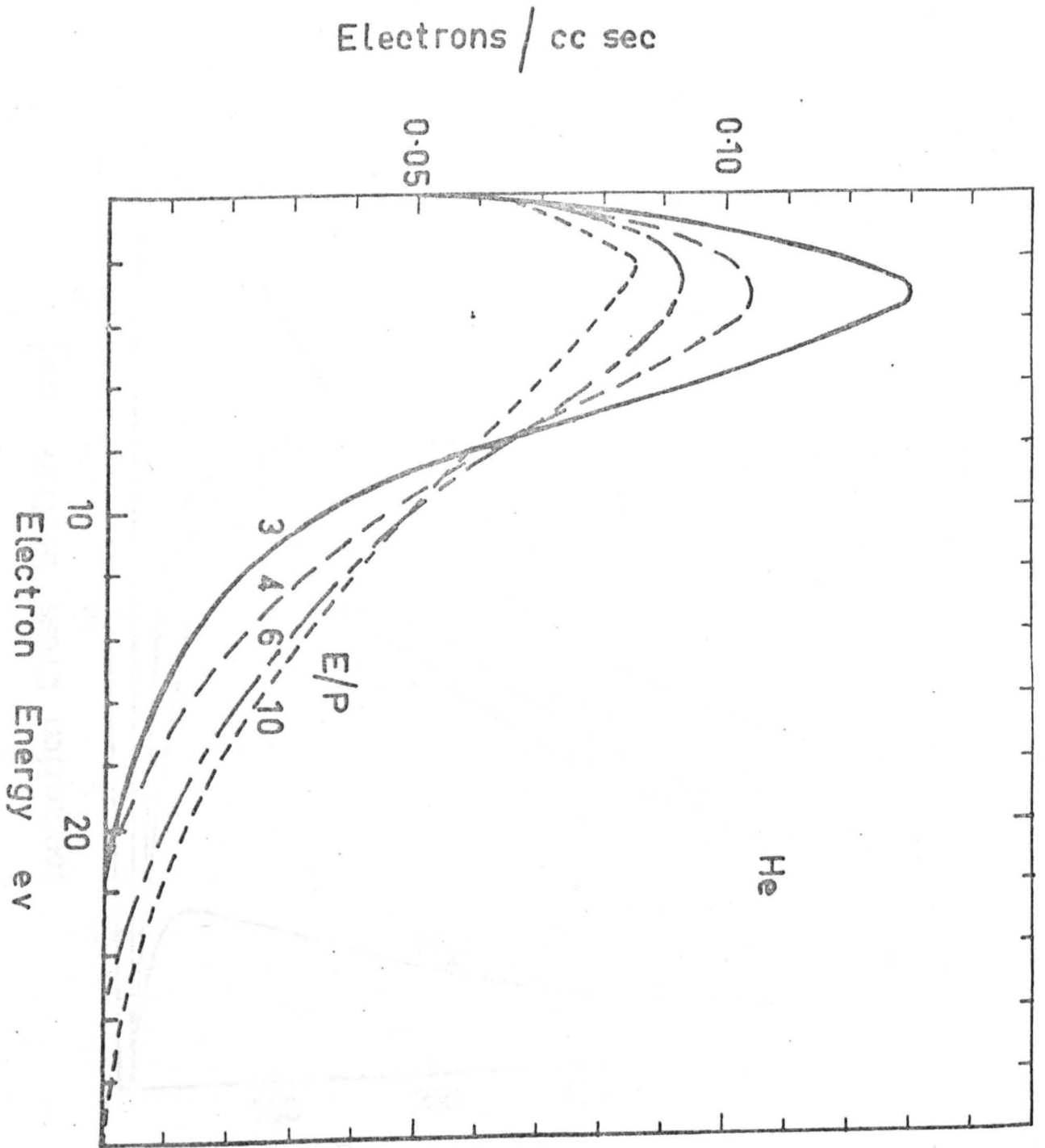


FIG 13

FIG 14

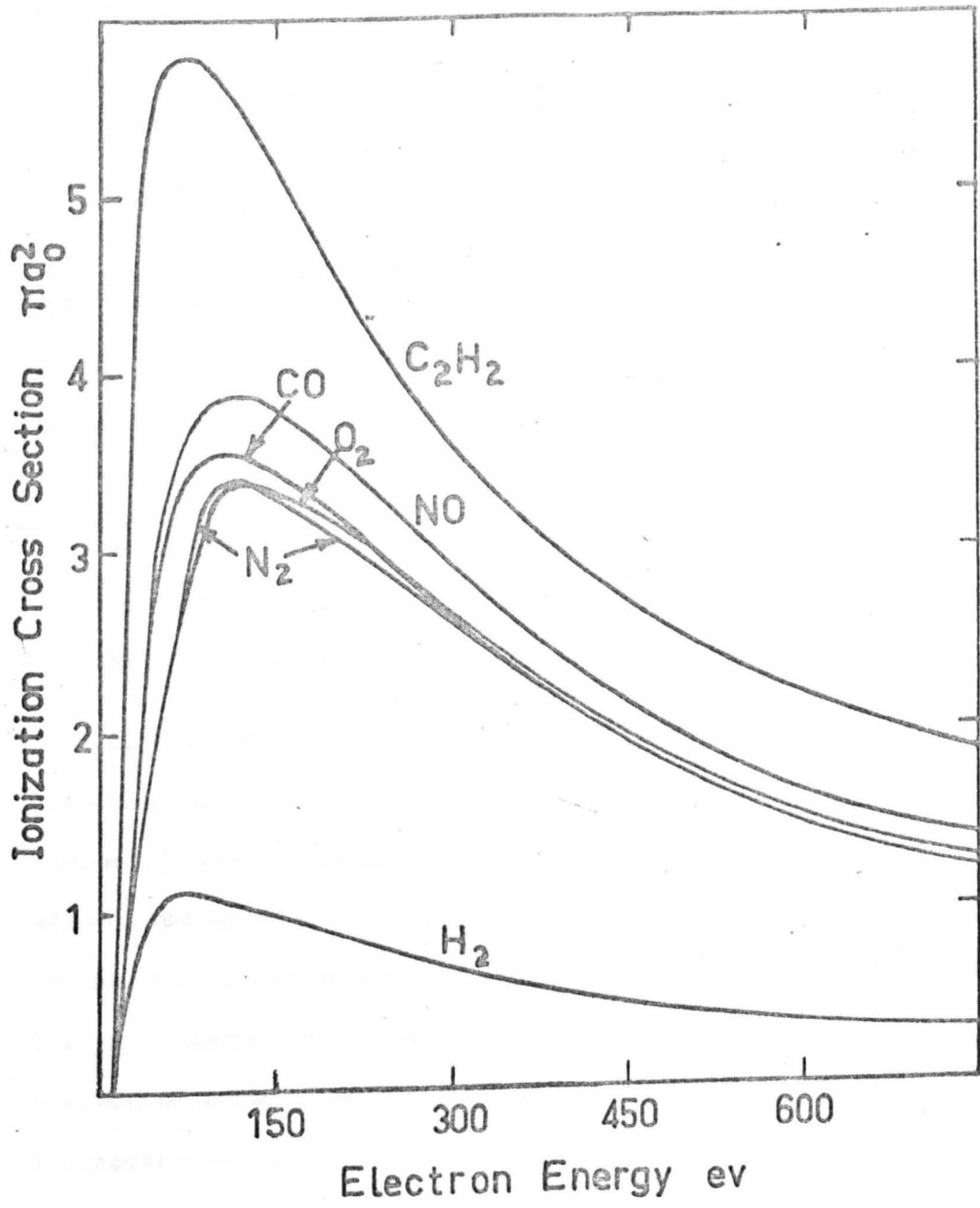


FIG 1.4

Finally in the third group there are low energy electrons which originate from other secondary processes.

When an effective collision occurs between an electron of suitable energy and a molecule (or atom) the conversion of electron energy may give rise to an excited or ionised molecule (or atom) or else molecular dissociation may occur with the consequent production of atoms, radicals, or ions.

Similarly activation may result from molecular or atomic impact with fast ions and neutral atoms, the latter usually resulting from charge transfer processes involving ions and gas molecules. Again the following possibilities arise:-

- 1) Atomic and molecular excitation.
- 2) Atomic and molecular ionisation..
- 3) Charge transfer processes resulting in the formation of neutral atoms.
- 4) Molecular dissociation into atoms, radicals or ions.

In the glow discharge the energies of ionic species are only of the order of tens of volts and consequently the cross-sections for ionisation and excitation are very small. In contrast although the average energy of the electrons in the discharge is only about 2-3 ev, the cross-section for electron ionisation and excitation are much larger. Therefore, as mentioned previously, in most instances activation arises from electronic impacts and ionic impacts play only a secondary role.

Furthermore only a small fraction of electrons in discharge have sufficient energy to bring about molecular ionisation, consequently in regard to chemical synthesis, the primary gaseous processes of importance are excitations.

When a molecule is excited by electron impact, the excited species or a molecular fragment resulting from its spontaneous decomposition (i.e. atoms, radicals and ions) may then react with the numerous other species present forming eventually a final product. In a molecule many different excited states can be generated by electron impact, each involving a different energy change. Thus in a discharge where the electrons have a distribution of energy, which depends on the gas and on the discharge parameters, many different electron impact reactions may be occurring simultaneously, with the result that a whole spectrum of products exists. This is one reason why the chemical reactions in a discharge are so complex and so difficult to understand.

In addition further complications arise if the desired product can be destroyed in the discharge. Thus for example in the case of hydrazine synthesis it is reported in section 2.2. that degradation of hydrazine or its precursor, in an electrical discharge, may occur by both electron and atomic hydrogen attack.

Consequently, the rate of synthesis of a particular product may depend not only upon the extent to which the distribution of electron energy in the discharge coincides with the energy range required to initiate the primary reactions which lead to the formation of this product, but also upon the attainment of favourable conditions which ensure that the species formed by primary reaction are consumed mainly in reactions leading to the desired product, and also that no significant loss of product occurs before it is removed from the discharge zone and isolated.

Finally with reference to the effect of reaction tube size on chemical synthesis it will be shown in section 2.2. that both the nature and ' active area ' of the reaction tube surface may influence the chemical reactions which occur. This is extremely important as the ratio of reactor surface area to volume varies in geometrically similar reactors of different size.

CHAPTER 2.0.

2.0. SURVEY OF PREVIOUS WORK.

Normally the original investigation of a chemical process is carried out in the laboratory on a small unit. Before chemical production of the process can be realised methods of increasing throughput must be investigated.

In the case of chemical synthesis in electrical discharge reactors there are basically two ways in which this can be achieved, by reactor scale-up and by a step-up technique using an appropriate number of parallel discharges each of similar dimensions to the laboratory scale reactor. The work in this thesis is concerned only with the first of these methods.

A large scale reactor may be considered similar to a laboratory unit if the nett rate of formation of product per unit volume is the same in each case. This situation would only be expected to arise if the following conditions were satisfied.

- 1) The discharge in each reactor was uniform occupying the entire volume of the reaction zone.
- 2) Physical and chemical similarity existed in each reactor.

The first of these conditions is necessary to ensure both uniform activation intensity of the discharge and no by-passing of the reaction zone by the reactant gas. Thus a large proportion of the experimental work reported in this thesis, involved the development of a set of reactor units in which these requirements could be maintained over a wide range of experimental conditions. A discussion of the engineering design criteria associated with this work is presented in the first section of this chapter.

In the second section of this chapter physical similarity and the application of the 'similarity principle' to electrical discharges in which chemical synthesis occur is discussed. In the present study physical similarity is defined as similarity in the physics of the discharge. (The physics of a discharge determine the activation phenomena which lead to chemical reactions).

Finally in the third section of this chapter a summary of the chemistry of hydrazine formation and destruction in a glow discharge is outlined. (A comprehensive review of the chemistry of hydrazine synthesis in a glow discharge can be found in the work of (Savage (1970)). Also a small amount of work dealing with the effect of reaction tube size on the decomposition of ammonia and the synthesis of hydrazine in a glow discharge is reviewed. Reference to photochemical and radiolysis studies has been made in this section where the results of such work support important discharge findings, or provide new ideas which have not been examined in discharge studies.

2.1. Reactor development - engineering design and criteria.

Thornton (1966) has put forward a classification of the different gas discharge reactors the main types of which are shown in (Fig. 2.1.). Two principal classes have been recognised, single phase homogeneous reactors and multiple phase heterogeneous reactors.

Only reactor types of the first series in which a single gaseous phase is present in the reactor were suitable for the work outlined in this thesis, and only these will be discussed.

Of these, the double electrode discharge (see Fig. 2.1(a)) is the only reactor which operates solely with dc power ('continuous' or 'pulsed').

The main advantage of using other types of power is that the discharge is normally of a more uniform nature than the dc glow discharge.

In the case of the electrodeless discharge (Fig. 2.1. (f)) additional advantages may result from the fact that it contains no metal electrodes in the reaction zone.

The main disadvantages (at the time this study commenced) of using power other than continuous dc were:-

- 1) Although power measurement with continuous dc is reasonably simple and accurate this is not the case for alternative modes of power supply.
- 2) In the context of this study the use of other types of power would introduce new factors (for example, frequency if a h.f. discharge was used) the effect of which little or nothing is known.
- 3) With pulsed dc power in addition to the reasons outlined above even if desired, this could not be used as a suitable generator for this type of power is not available.

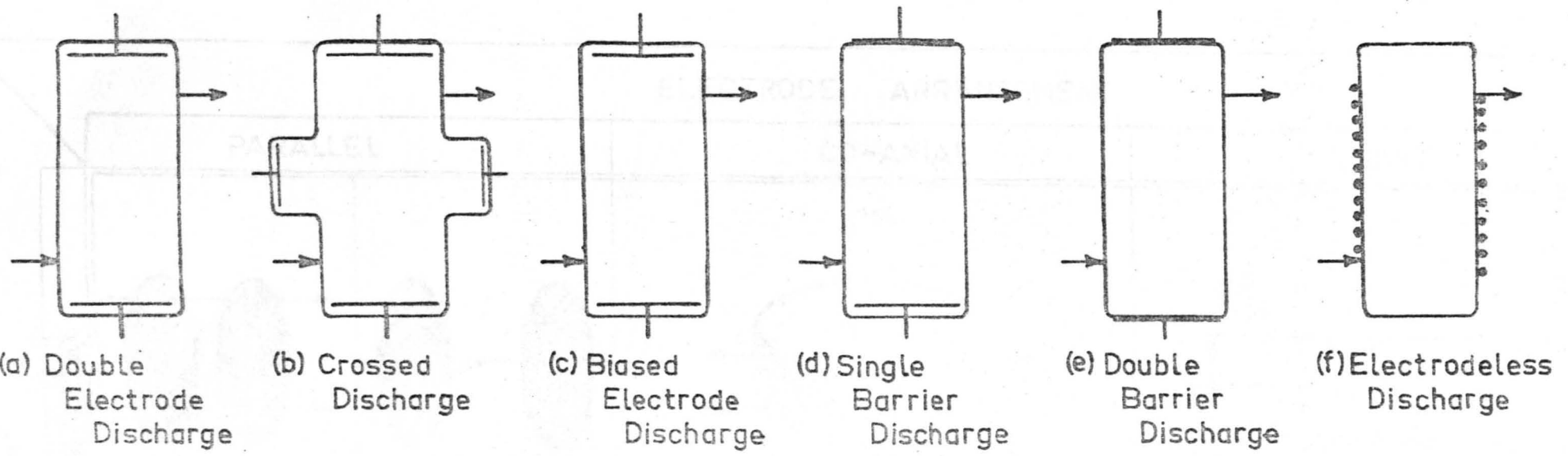
Thus the double electrode discharge reactor was chosen for this study and the engineering design criteria discussed is pertinent only to this type of reactor.

Once the type of reactor to be used is decided, the next important step involves the selection of the correct electrode configuration, and direction of flow of reactant gas, to meet the criteria of ' uniform discharge ' and ' no reactant gas by-passing '.

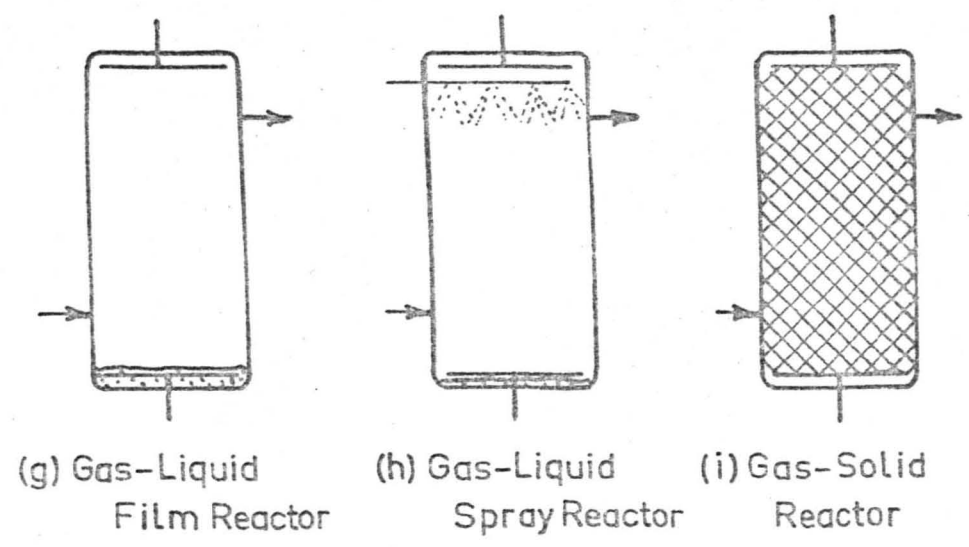
Thornton (1966) has detailed the various electrode and flow arrangements (Fig. 2.2.) electrodes may consist of parallel plates,

HOMOGENEOUS REACTORS

FIG 2.1



HETEROGENEOUS REACTORS

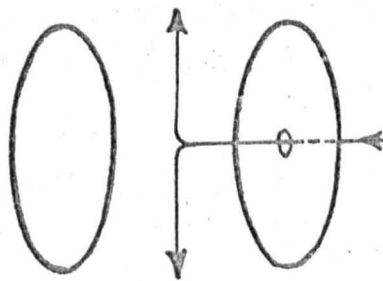
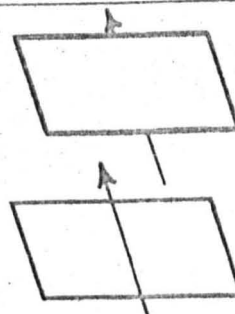
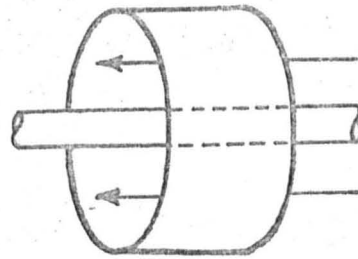
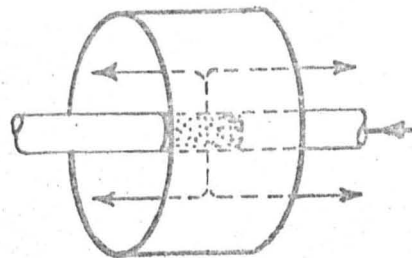
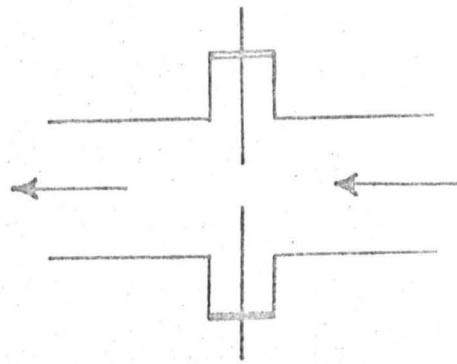
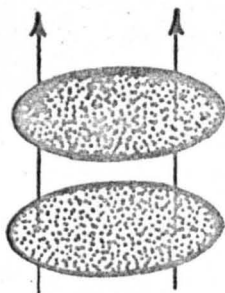
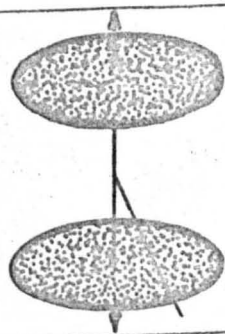
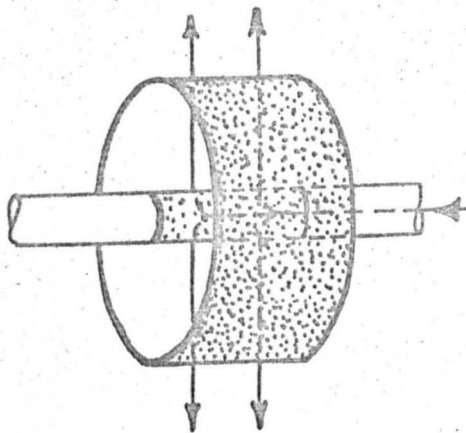
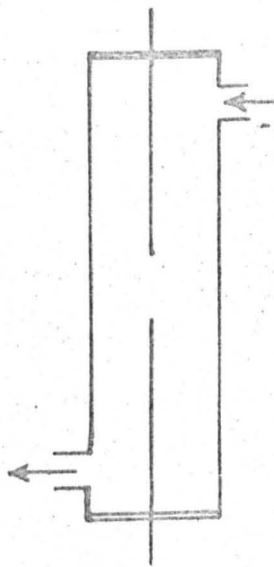


ELECTRODE ARRANGEMENT

POINT

CO-AXIAL

PARALLEL



PARALLEL

CROSS

FLOW OF REACTANT

FIG 2.2

4

9

3

8

2

6

1

5

7

co-axial cylinders or a pair of points, whilst the gas flow may be parallel or at right angles to the plane of the discharge.

In relation to the present study some of these systems were not considered to be worth testing because of their inherent unsuitability. For example it is obvious that the point electrode configuration is associated with considerable and variable by-passing of the discharge zone.

Co-axial electrode arrangements are normally associated with non-uniform electric fields. If the radius of the co-axial electrodes is very different from unity, the field intensity will be higher around the inner electrode, and the activation intensity of the discharge will vary across the interelectrode gap.

Fortunately this can be partially rectified if the interelectrode distance is minimised. In this way the field intensity can be made to approximate that of a uniform field. Although this imposes severe restrictions it nevertheless allows the use of this configuration over a certain range of conditions. This is important as the use of co-axial systems in which the reactant flows through the annular space between the electrodes is the simplest way of meeting the 'no by-passing' requirement.

The choice of correct electrode configuration and direction of gas flow can be influenced by other considerations. In particular any electrode configuration and direction of gas flow may be influenced by the shape and profile of the electrodes, and also the shape of the reaction zone (Eremin (1965)).

Non-uniform electric fields are set up about the edges of electrodes unless they are suitably profiled. To minimise this effect the physical size of the electrodes can be made very large to help reduce the boundary to surface area ratio of the electrode.

Different electrode shapes show different effects. An electrode shape of the nozzle type might lead to a decrease in discharge uniformity resulting in increased by-passing and variation in activation intensity. Likewise a change in the discharge shape e.g. venturi shape instead of a cylindrical one could have similar effects.

In respect to chemical synthesis it is important to note that as well as variation in discharge uniformity (discharge activation intensity) and degree of ' by-passing ', electrode and reactor shape can also influence the electro-aerodynamic discharge conditions by affecting; the power requirements to sustain the discharge, and also both residence time and residence time distribution.

Thus if the necessary type of reactor, the correct electrode configuration and direction of reactant flow, and the correct electrode profile and shape and reactor shape, could be identified; then all the necessary ' engineering design ' criteria to meet the conditions of ' uniform discharge ' and ' no by-passing ' would be satisfied.

Unfortunately this in itself would not guarantee that these latter conditions would be satisfied as it has been shown that other factors may significantly effect the discharge characteristics.

Work on the dc discharge (Bruce (1949)), (Pearson et al (1969)) and (Goshō (1969)) has shown that together with engineering design considerations, gas pressure, gas linear flow rate and distribution, and location of the reactor walls effect the stability of a discharge system.

It will be shown later that these observations have been confirmed in the present study. In addition it has been found that discharge constrictions (i.e. formation of non-uniform discharge) may also depend upon the discharge current.

Constriction phenomena are complex and as yet not well understood however since completing of this experimental study Woolsey (1970A) (1970B) has published some detailed work in this area.

According to Woolsey three types of constriction or contraction of the positive column of a dc discharge can occur. The first is a gradual contraction which appears to occur in most discharges. The second is a constriction of the entire discharge down to a diameter of 1-2 mm; this takes place suddenly at a critical current which depends on the pressure and gas properties. This effect gives rise to a bright mobile discharge thread with a sharp boundary. The third type of contraction changes the uniform positive column to one containing a bright cone 1-2 cm in diameter with an outer diffuse region extending to the tube wall. This effect is common in electronegative gas such as iodine vapour. (Woolsey (1970B)).

Finally in passing it is unfortunate to note that in spite of the extensive investigations into the glow discharge synthesis of hydrazine in which:-

- 1) A number of different reactor and electrode configurations have been used over a wide range of experimental conditions.
- 2) The use of low work function metal cathodes (Manion (1958)) (Rummel (1940)) e.g. tantalum, caesium coated tungsten.
- 3) The use of various metal electrodes - nickel, aluminium, stainless steel or electrodes coated with thin metallic

films e.g. gold, silver (Eremin et al (1966) (1968)) have been examined, in all of this work little or no reference is made to the nature of the discharges obtained.

2.2. Derivation and application of the 'Similarity Principle' to electrical discharges.

Any chosen property of a discharge, for example the potential (V) depends on a number of others, the current (I) gas pressure (P), size of the vessel and electrodes. The dependence is often complicated, and sometimes cannot be expressed analytically at all but only in the form of curves (theoretical or experimental), linking various parameters.

Obviously, an infinite number of such curves would be required to describe every possible state of the discharge, given by every combination of dimensions, current, pressure etc. Fortunately, this can be simplified by grouping together some of these parameters for example the breakdown potential (V_s) of a gas between plane parallel electrodes depends upon the inter-electrode distance (d) and on the pressure. Experimentally V_s does not change if the product pd is kept constant (except at very high pressures) i.e. $V_s = f(pd)$ for any one combination of gas and electrode material

The importance of such groupings was first realised by De La Rue and Muller (1880) and later by Paschen (1889), Townsend (1915) and others who noted that $(E\lambda)$ represents the energy gained by an electron moving along a free path (λ) and pd is proportional to the number of molecules between two electrodes of given size.

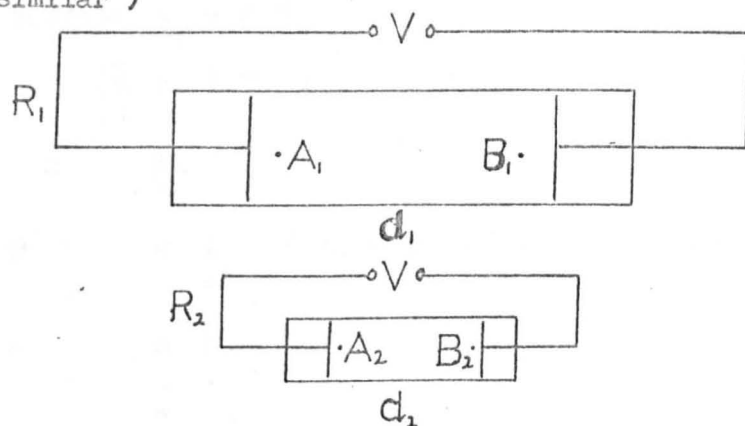
where p is any pressure, measured

Thus if $(E\lambda)$ or (E/p) and pd are maintained constant multiplication of electrons between the electrodes is fixed.

These groups of parameters and others can be deduced more generally as shown below, partly following the treatments of Holm (1924), Von Engel (1925), Steenback (1932) and Dallenback (1925).

Derivation of Similarity Relations.

Consider two discharges in the same gas with the same electrode material in which all the corresponding linear dimensions are different by a factor a (see Fig. 2.3.). This includes the vessel, electrodes and the properties of the gas e.g. mean free path (but not the mean distance between the molecules). Assume that the gas temperature is the same in both, and that corresponding points (e.g. $A_1, A_2; B_1, B_2$) have the same potential difference between them; the potential across the electrodes is V . Such discharges are called similar (i.e. physically similar)



then the following relations hold for corresponding points in the two discharges. For the linear dimensions of vessel and electrodes

$$d_1 = a d_2$$

$$r_1 = a r_2$$

$$R_1 = a R_2$$

where r is any radially measured distance.

For elements of area $dA_1 = a^2 dA_2$

For the mean free paths of electrons, ions or molecules in the gas.

$$\lambda_1 = a \lambda_2$$

Hence the gas density (number of molecules per cm^3).

$$n_1 = \frac{n_2}{a}$$

since by definition the temperature is the same in both, pressure $p \propto n$, hence for the pressure.

$$p_1 = \frac{p_2}{a}$$

The potential $V_1 = V_2$ by definition.

$$\text{The electric field } E_x = - \frac{\partial V}{\partial x}$$

$$\text{Hence } E_1 = \frac{E_2}{a}$$

Surface and volume charge densities σ , ρ nett, can be derived from

$$E \text{ surface} = 4 \pi \sigma$$

$$\frac{\partial E}{\partial x} = 4 \pi (\rho^+ - \rho^-)$$

whence $\sigma_1 = \frac{\sigma_2}{a}$

$$\text{and } (\rho_1^+ - \rho_1^-) = \frac{1}{a^2} (\rho_2^+ - \rho_2^-) \quad (2-1)$$

$$\text{from which } E_1 \lambda_1 = E_2 \lambda_2$$

$$\frac{E_1}{p_1} = \frac{E_2}{p_2}$$

may be derived.

Relations involving current.

Relations between the nett space charge densities have already been found.

$$(\rho^+ - \rho^-)_1 = \frac{1}{a^2} (\rho^+ - \rho^-)_2$$

ρ^- includes both electrons and negative ions.

The general expression for the total current density is

$$j = \rho^+ v^+ + \rho^- v^- = (\rho^+ - \rho^-) (v^+ - v^-) + \rho^- v^+ + \rho^+ v^- \dots$$

To find the relation between j_1 and j_2 the second form of the above equation is used adding the appropriate suffixes 1 and 2. Then using equation (2 - 1) and assuming only single stage processes so that $v_1 = v_2$ it can be seen that a simple proportionality between j_1 and j_2 can arise only when

$$\rho_1^- v_1^+ + \rho_1^+ v_1^- = \frac{1}{a^2} (\rho_2^- v_2^+ + \rho_2^+ v_2^-)$$

which together with equation (2 - 1) results in

$$\rho_1^+ = \frac{1}{a^2} \rho_2^+ ; \quad \rho_1^- = \frac{1}{a^2} \rho_2^-$$

Particle and current densities are thus related by

$$N_1^+ = \frac{1}{a^2} N_2^+ ; \quad N_1^- = \frac{1}{a^2} N_2^-$$

$$j_1 = \frac{1}{a^2} j_2$$

and, since areas transform by the factor a^2 , total current is

$$i_1 = j_1 dA_1 = \frac{1}{a^2} j_2 a^2 dA_2 = i_2$$

This equality of current in two discharges is used by most writers as part of the definition of similar discharges, i.e. two discharges are defined as (physically) similar when the potential and current at corresponding points are equal and all linear dimensions are different by a factor a .

In the above paragraphs the similarity transformations of a number of discharge parameters have been presented. The results of the transformation of a number of other parameters are given in table 2.1.

TABLE 2.1.

<u>System</u>	<u>1</u>	<u>2</u>
Linear Dimension	K	aK
Gas density or pressure	P	P/a
Interelectrode potential	V	V
Field Strength	E	E/a
Surface charge density	σ	σ/a
Total mass of gas between electrodes	M	M/a ²
Total electric charge in gas	e	e a
Ratio of density of ionised to neutral molecules	N_i/N_N	$N_i/N_N a$
Electric current	I	I
Current density	J	J/a ²
Voltage current characteristic	V.I	V.I
Temporal growth rate of current	$\partial I/\partial t$	$\partial I/\partial t$
Space charge density	ρ	ρ/a^2

It follows from what has been said (and the transformations presented in table 2.1.) that the discharges in two geometrically similar reactors of different size, can be made physically similar if the reduced field strength (E/p) is made the same in both. This condition may be achieved by varying either the operating pressure or the voltage.

In turn it follows that if the rate of those discharge physical processes (activation etc.) upon which chemical synthesis depend are solely dependent upon (E/p), then it would be possible to make two geometrically similar discharges of different size chemically similar by making the reduced field strength the same in both (i.e. by making them physically similar).

In order to test the feasibility of this approach it is necessary to identify those fundamental discharge processes which follow the similarity principle and consequently are solely dependent upon (E/p). This has in fact been carried out by Francis (1960) and thus it is only necessary here to present a few examples for illustration. Before doing this however it is helpful to define the meaning of the terms ' permitted ' and ' forbidden ' in the context of the similarity principle.

Thus those processes which conform to the similarity principle are referred to as ' permitted ' while those which do not are distinguished as ' forbidden '. It should be realised, however, that these terms refer only to whether or not a process obeys the similarity principle, and have no bearing on whether or not a process can physically occur in the discharge.

Examples of Permitted and Forbidden Processes

The concentration N of any type of charged particle, at any point in a steady state discharge, can be derived by equating the rates of production and loss at that point.

Thus in accordance with the similarity principle N_1 must equal

$(\frac{1}{a^2})N_2$ and dt_1 must equal adt_2 then

$$\left(\frac{dN}{dt}\right)_1 = \frac{1}{a^3} \left(\frac{dN}{dt}\right)_2 \quad (2-2)$$

where $\frac{dN}{dt}$ is the sum of the rates of production by a number of elementary processes e.g.

$$\left(\frac{dN}{dt}\right)_{\text{total}} = \left(\frac{\partial N}{\partial t}\right)_{\text{collision}} + \left(\frac{\partial N}{\partial t}\right)_{\text{drift}} + \left(\frac{\partial N}{\partial t}\right)_{\text{diffusion}} + \left(\frac{\partial N}{\partial t}\right)_{\text{photoionisation}} + \dots$$

Each process whether gain or loss must transform by the factor $\frac{1}{a^3}$

in order that equation (2-2) is satisfied. Considering processes separately reference is made always to corresponding points or small volumes in the two discharges.

Ionisation by Single electron collision

The rate of ionisation by single collisions of electrons with gas molecules depends on the concentration N_e , of electrons and their energy, and on the concentration n of gas molecules.

Assuming that the electron energy is the same in both discharges the rate of production of ions and electrons is

$$\left(\frac{\partial N}{\partial t}\right)_1 = C N_{e1} n_1 = C \frac{N_{e2}}{a^2} \frac{n_2}{a} = \frac{1}{a^3} \left(\frac{\partial N}{\partial t}\right)_2$$

This process is therefore permitted. The constant C and in the following equations C_1, C_2, \dots merely indicate proportionality.

Secondary collision processes.

Stepwise Ionisation: (collision of the second kind)

Ionisation by these processes can occur when the electron hits

an already excited molecule, when two excited molecules collide, or when an excited (metastable) molecule of one gas hits and ionises a neutral molecule of another (Penning effect). This last process can occur only when the excitation potential of the one gas exceeds the ionisation potential of the other.

The equilibrium concentration N^* of excited molecules is given by equating rates of production and loss, assuming that electrons produce, by single collisions, excited states having an average life τ

$$\left(\frac{\partial N}{\partial t} \right)_{\text{production}} \propto N_e n \quad (\text{where } N_e = \text{concentration of electrons.})$$

$$\left(\frac{\partial N^*}{\partial t} \right)_{\text{loss}} \propto \frac{N^*}{\tau} \quad (n = \text{concentration of gas molecules}).$$

hence $\frac{N^*}{\tau} \propto N_e n$

For excited molecules which simply radiate within about 10^{-8} seconds and whose radiation is not absorbed in the gas, τ is much shorter than the time between collisions and is therefore a constant.

This gives $N^* \propto N_e n$

i.e. $N_1^* = \frac{1}{a_1} N_1$ (2 - 4)

$$(N_1^* = N_e, n_1 = \frac{N_1}{a_1}, \frac{n_1}{a} = \frac{1}{a^2} N_1^*)$$

as $N_2^* = N_e n_1$

For metastable atoms or molecules (concentration N_m^*) destroyed by collision with gas molecules (their own gas or impurities) or on the walls $\tau \propto \frac{1}{n}$ or $\tau \propto R$ hence

$$(N_m^*)_1 \propto \tau N_e n$$

$$\frac{N_e n_1}{\tau_1} = \frac{N_e}{a^2} \frac{n_1}{a} a \tau_1 = \frac{1}{a^2} (N_m^*)_2 \quad (2 - 5)$$

This is true provided that no metastables are produced by electrons

falling from higher levels.

In conditions where resonance radiation is appreciably absorbed and re-emitted in travelling through the gas the rate of production of resonance states (N_r^*) in any given volume is determined by the nett flow of resonance photons through this volume, as well as by equation (2 - 4). These photons come from other parts of the discharge and the nett flow in any one direction (e.g. x) is proportional to $\frac{\partial}{\partial x} \left(\frac{N_r^*}{\tau} \right)$

hence for resonance states

$$\frac{N_r^*}{\tau} \propto N_e n + \text{const} \frac{\partial}{\partial x} \left(\frac{N_r^*}{\tau} \right)$$

and taking $\tau = \text{constant}$

$$N_r^* \propto N_e n + \text{const} \frac{\partial N_r^*}{\partial x}$$

From this it follows that N_r^* does not transform with any simple factor of a, in particular

$$(N_r^*)_1 \neq \frac{1}{a^2} (N_r^*)_2 \quad (2 - 6)$$

The rate of ionisation caused by electrons hitting these excited molecules is proportional to the concentrations of both. Equations (2 - 4) and (2 - 5) and (2 - 6) may be used to determine the following. For ionisation by electrons - excited molecules

$$\left(\frac{\partial N}{\partial t} \right)_1 = C_1 N_e N_1^* = \frac{1}{a^5} \left(\frac{\partial N}{\partial t} \right)_2$$

electrons - metastable molecules

$$\left(\frac{\partial N}{\partial t} \right)_1 = C_1 N_e (N_m^*)_1 = \frac{1}{a^4} \left(\frac{\partial N}{\partial t} \right)_2$$

electrons - resonance states

$$\left(\frac{\partial N}{\partial t} \right)_1 = C_2 N_e (N_r^*)_1 \neq \frac{1}{a^3} \left(\frac{\partial N}{\partial t} \right)_2$$

All these processes do not therefore conform to the similarity principle.

The rate of ionisation by the collision of two excited molecules is proportional to the concentrations of both i.e.

$$\left(\frac{\partial N}{\partial t}\right)_1 = C_4 N_A^* N_B^* \neq \frac{1}{a^3} \left(\frac{\partial N}{\partial t}\right)_2$$

where $N_A^* N_B^*$ is any combination of N^* , N_M^* , N_r^* , hence all possible processes of this kind do not conform to the similarity principle.

Recombination

Recombination between positive and negative ions follows the law

$$\left(\frac{\partial N}{\partial t}\right) = -\alpha N^+ N^-$$

where α is the recombination coefficient. At high pressure α is proportional to $\frac{1}{p}$ and so transforms with factor a , while N^+ , N^- each transform with $\frac{1}{a^2}$ thus finally $\frac{\partial N}{\partial t}$ transforms with $\frac{1}{a^3}$. The process therefore obeys the similarity principle. At low pressures α is proportional to p , and $\frac{\partial N}{\partial t}$ transforms with $\frac{1}{a^5}$ and the process does not conform to the similarity principle.

For recombination between electrons and positive ions α is never proportional to $\frac{1}{p}$, but rather is proportional to $p^{\frac{1}{2}}$, hence $\frac{\partial N}{\partial t}$ never transforms with $\frac{1}{a^3}$ and the process never conforms with the similarity principle.

The results of the transformations of the most important discharge processes are summarised in table 2.2. (after Francis (1960)).

Inspection of table 2.2. reveals that the application of the similarity principle to electrical discharges in which chemical synthesis takes place is limited to those synthesis where primary reactions arising from single stage physical activation phenomena (permitted processes) control the rate of synthesis. In practice as noted in section 1.2. chemical synthesis depends upon secondary processes (i.e. two stage processes - forbidden processes) and thus having two physically similar

discharges will not ensure that the chemistry of these discharges will follow suit. It is still a matter of speculation as to which parameters control these secondary processes and hence should be preserved in scale-up. * Also the role of solid surfaces adjacent to the discharge is still not clear. This is important in that the surface area per unit volume varies in geometrically similar reactors of different size, however one way of overcoming this may be by packing the larger reactors with solid material. This procedure has been examined in the present study and is discussed in chapter 5.0.

TABLE 2.2.

<u>PERMITTED PROCESSES</u>	<u>FORBIDDEN PROCESSES</u>
In the gas ionisation by single electron collision	All stepwise ionisations, collisions of second kind except Penning effect.
Penning effect.	Photo-ionisation.
Electron attachment and detachment.	Charge transfer: fast neutral \rightarrow ion*.
Drift Self repulsion } of charges Diffusion	All recombination except ion - ion at high pressure.
Charge transfer ion \rightarrow fast neutral recombination ion - ion at high pressure	Thermal ionisation.
On the walls secondary emission by impact of: Electrons (δ) Ions (f_i) Non-resonance photons (f_p) Metastables (f_m) Fast neutrals (f_n)	Electrons emitted by fast ions formed by charge transfer* Photo-electric effect by diffusing resonance photons. Field emission.
* Fast neutral molecules are assumed to be those already formed by charge transfer at some other point in the discharge.	

2.3. Chemical studies of the electrical discharge synthesis of hydrazine from ammonia

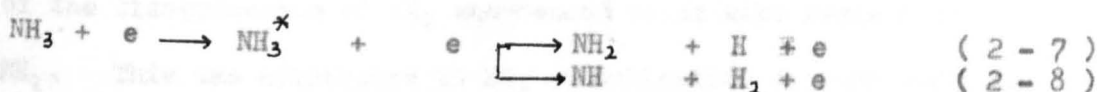
Most of the early studies of discharge chemical reactions were aimed at identifying the reaction mechanism. Two principal mechanisms were put forward - that of Lind (1928) in which ionic reactions only were proposed and that of Lunt and Mills (1925) who interpreted the reactions on a free radical basis. Although support for both these views can be deduced from experimental data from various reactions, it is clear that the mechanism of chemical reactions in discharges do not all follow the same pattern.

In the synthesis of hydrazine from ammonia in a glow discharge although Westhaver (1933) favoured the ionic mechanism the majority of workers (e.g. Ouchi (1949) (1952) (1953), Anderson et al (1959)) have preferred the free radical mechanism, and a large amount of evidence supporting this view has been obtained. For example (1) Devins and Burton (1954) have shown that relative to the number of electrons adequate to excite ammonia (to the lowest excited state in light absorption ~ 5.1 e.v.) the fraction of electrons with energy adequate to ionise ammonia is $\sim 1.8 \times 10^{-2}$. (2) Anderson et al (1959) (in their work in which the rate of ammonia decomposition was related to a theoretical model of the discharge) have shown that the electron energy in the discharge is approximately 4.2 e.v. which is not sufficient to ionise ammonia gas (10.2 e.v.) on a single collision.

Hydrazine Formation.

In the free radical mechanism of hydrazine formation ammonia gas molecules are first excited by electrons and then undergo dissociation into free radicals. Two principal ammonia decomposition steps have been

put forward viz.



These free radicals are the precursors for hydrazine formation.

Most workers (e.g. Devins and Burton (1954) Skorokhodov (1961)) have favoured (2 - 7) (which requires an activation energy of 4.52 e.v.) with the subsequent formation of hydrazine by the reaction



although Ouchi (1953) suggested that the reaction



was the primary reaction for hydrazine formation.

A great deal of photochemical evidence favours (2 - 7) and (2 - 9).

Different wavelengths of light have associated with them corresponding energies hence by conducting experiments at various wavelengths the threshold energies for dissociation reactions can be found.

In this way it has been shown that the NH radical only appears with light of wavelength below 1600 Å (i.e. above 7.8 e.v.) but NH₂ radicals appear above and below 1600 Å (Schnepf and Dressler (1960) Bayes et al (1963)).

Further evidence for (2 - 7) and (2 - 9) has been obtained from the work of McCarthy and Robinson (1959) who positively identified the NH₂ radical in high frequency discharge products trapped in an argon matrix at 4.2 °K and by Haines and Bair (1963). These workers made photolytic measurements of NH₂ absorption as a function of time following a radio frequency discharge pulse through ammonia. They observed that NH₂ radicals appeared much earlier (after fewer pulses) than NH radicals indicating that NH₂ radicals were the primary product of ammonia decomposition.

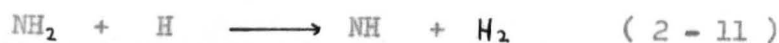
They also showed that under the proper conditions the kinetics

of the reaction between NH₂ and NH radicals (1954) and

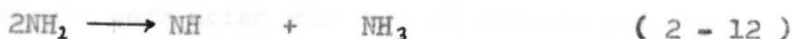
and in experiments in which the concentration of NH₂ radicals

of the disappearance of NH_2 was second order with respect of NH_2 . This was attributed to NH_2 recombination to form hydrazine by the reaction (2 - 9), rather than NH_2 recombination to form ammonia.

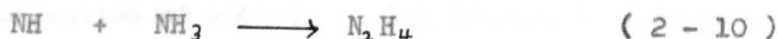
Recently Mantei and Bair (1968) studied the flash photolysis of ammonia and showed that the NH radical is formed by a secondary reaction, either



or



and it decays by the insertion reaction



This work proves conclusively that although hydrazine can be formed from both NH (2 - 10) and NH_2 (2 - 9) radicals, the formation of the NH_2 radical (2 - 7) is the primary reaction in each case.

Hydrazine Decomposition.

The majority of studies into the decomposition of hydrazine have been concerned with investigating whether -

- 1) Hydrazine decomposition takes place via atomic hydrogen attack and/or electron collision.
- 2) The decomposition takes place via N - N bond fission and/or N - H bond splitting.

Evidence of hydrazine destruction by atomic hydrogen was obtained in 1932 by Dixon who found that when atomic hydrogen and hydrazine were reacted together in a flow reactor hydrazine decomposition occurred.

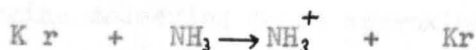
Further evidence of this mode of hydrazine (or its precursor) destruction was obtained from the extensive photochemical work of McDonald, Khan and Gunning (1954) and McDonald and Gunning (1955), and in experiments in which the concentration of atomic hydrogen

was decreased with a resultant increase in the yield of hydrazine.

The concentration of atomic hydrogen can be reduced by either (or both) of two approaches -

- a) prevent H atom formation
- b) selectively scavenge H atoms with appropriately reactive substances.

The first of these approaches was used by Lampe et al (1967) in his radiolysis work using mixtures of ammonia and Krypton. According to Lampe if the rare gas absorbed all the radiation energy the ionisation of ammonia (with Krypton) would be -



and the decomposition path with Krypton should lead to fewer H atoms than with pure ammonia.

The second approach involved either the introduction of special catalysts e.g. platinum (Devins and Burton (1954) Rathsack (1961) Eremin et al (1966) (1968) which favoured hydrogen recombination) or the use of various scavenging agents e.g. ethylene (Manion (1958)).

In all these experiments evidence of increased hydrazine yields were obtained indicating that hydrazine yield is influenced by atomic hydrogen attack. Whether this attack is upon hydrazine itself (i.e. destruction) or upon hydrazine precursors (e.g. NH_2) (i.e. prevention of hydrazine formation) was not established.

Electron attack of hydrazine has also been shown to occur by several workers (e.g. Logan et al (1969)). Logan et al studied the electrical discharge decomposition of hydrazine and concluded that decomposition could occur by collisions with electrons, possessing energy greater than the dissociation

energy of hydrazine (3.3 e.v.(Foner (1958)).

In a glow discharge in ammonia since the energy required to rupture the (N - H) bond in hydrazine is only 3.3 ev. as compared with 4.5 ev. required to dissociate ammonia (Altshuller (1954)) into NH_2 and H - atoms the number of electrons capable of dissociating hydrazine is greater than that for ammonia dissociation. By assuming a Maxwellian distribution of energies in the positive column of an ammonia glow discharge with mean electron energy of 1.25 ev. Savage (1970) found that about 6.5% of the electrons present had enough energy to break the ($\text{NH}_2 - \text{H}$) bond while 25% had sufficient energy to break the ($\text{H}_2\text{NNH} - \text{H}$) bond. By further assuming the area of hydrazine molecules to be approximately twice that of ammonia he was able to give a first estimate of the relative rates of reactions between electrons and hydrazine and electrons and ammonia as 7.7: 1. A similar analysis was carried out by Barker (1970) for a microwave discharge using an estimated electron energy of 1.0. ev. A ratio of 5:1 was obtained.

Another indication of the relative rates of reactions between electrons, hydrazine and ammonia maybe deduced from the work of Takahashi (1960) using 100 to 250 MHz discharge. From the initial slopes of her data and assuming no difference between electron energies in the 8.4 mmHg and 11.0. mmHg discharges it can be seen that with a 100 MHz discharge the rate of reaction of hydrazine with electrons is 10.0 times faster than that of the reaction of electrons with ammonia. This agrees reasonable well with the previous estimates despite the inherent assumptions of both methods.

Using this data in a simple kinetic model of the discharge Savage has compared the relative importance of hydrazine decomposition by atomic hydrogen attack with electron - induced destruction of hydrazine. Savage concluded that atomic hydrogen attack is the primary mode of decomposition of hydrazine although some electron destruction occurs.

Barker (1970) also attempted to determine the relative importance of these two destruction mechanisms and reasoned that this could be achieved by the use of atomic hydrogen scavengers (e.g. Allyl alcohol). Addition of sufficient scavenger should remove all the H atoms allowing the study of any other important destruction mechanisms that are present.

In this way Barker established that the mode of decrease in hydrazine yield varied with the power input. At lower powers (2.5 - 10.2 watts.) atomic hydrogen attack of hydrazine predominated whereas at higher powers (50 - 100 watts.) electron destruction of either hydrazine or its precursor NH_2 was more significant.

The second main area of investigation involving the decomposition of hydrazine has centred on elucidating whether decomposition is by N - H bond fission and/or N - H bond splitting. Attempts to identify the hydrazine decomposition products and their subsequent reactions have only been partially successful due to the complex nature of the reactions taking place.

Evidence of both modes of decomposition has been obtained by several workers including -

Bamford (1939), Birse and Melville (1940), Schiavello and Volpi (1962), Diesen (1963), Gray and Thymne (1964) etc. (N - H bond splitting) and Ramsey (1953), Hussain and Nourish (1963) etc. (N - N bond fission.)

Some of the most extensive investigations were carried out by Stief and DeCarlo (1965), (1966), (1967A), (1967B), (1968), who demonstrated that approximately 80% of the nitrogen formed in the direct photolysis of hydrazine resulted from reactions which did not involve the fission of the N - N bond.

Jones and Lossing (1969) have carried out the most recent work in this area. These workers obtained evidence to suggest that both types of breakdown occur in the photochemical decomposition of hydrazine. They tentatively suggested that the reaction involving N - N bond fission was approximately twice as fast as the reaction involving N - H bond splitting.

Thus it can be seen that despite the numerous investigations which have been carried out the exact mechanism of hydrazine formation and destruction in the discharge has not been elucidated. Consequently it is still not clear which factors control the reaction kinetics and hence should be preserved in scale-up.

In view of this it is not surprising that the scale-up of discharge chemical reactors for hydrazine synthesis has received little attention, and practically no data is available on the effect of reactor size on reaction yields.

Only two references dealing with the effect of reactor size on the decomposition of ammonia in an electrical discharge have been traced in the literature. In 1935 Wiig studied the photo-decomposition of ammonia and showed that the quantum yield (the

number of ammonia molecules decomposed per absorbed quanta of radiation) decreased with decreasing pressure. Wiig associated this with an increase in the adsorption of NH_2 radicals (formed in the decomposition of ammonia) on the silica surface, and subsequent recombination with H atoms to form ammonia. Wiig postulated that if this process occurred then it should be decreased by increasing the size of the reaction vessel. In 1937 he showed that the quantum yield did in fact increase under these conditions. Hydrazine synthesis or the effect of reactor size on the formation of hydrazine was not mentioned in this work.

Devins and Burton (1954) carried out a small number of experiments in which reaction tube diameter was varied. The influence of this parameter on the reduced field (E/p) was measured and found to agree with the theoretical analysis of Engel and Steenback (1939). The yield of hydrazine however was found to be a function of tube radius as well as (E/p). This strongly suggested that the discharge surface as well as the discharge characteristics influenced the chemical reactions. Devins and Burton found that the yield of hydrazine decreased with decreasing value of the product of pressure x tube radius, however no explanation of this was given.

The implication that reactor surfaces effect the reactions occurring in the discharge is extremely important with reference to the study of the effects of reactor size, in that the ratio of surface area per unit volume varies in geometrically similar reactors of different size.

Therefore together with some other important developments in the glow discharge synthesis of hydrazine a summary of the work dealing

with the effect of discharge surfaces follows.

One of the most significant developments in the study of the synthesis of hydrazine in a glow discharge has been the discovery by Westhaver (1933) and later confirmed by Devins and Burton (1954) and Rathsack (1957, 1960, 1961) that hydrazine is formed only in the positive column of a glow discharge.

It is important to realise this means that it is the reaction conditions in the positive column of the discharge which determines the nett rate of formation of hydrazine. In the past unfortunately, almost without exception investigators have used electron energies based upon the mean electric field strength of the discharge instead of the electric field strength in the positive column (which is much smaller), for correlation and discussion of their experimental data. This has ofcourse lead to misleading conclusions.

Similarly the residence time of the gas molecules in the total discharge volume has been considered, instead of the residence time of the gas molecules in the positive column (providing gas flow is in the direction of cathode to anode). This is especially important in experimental work in which either the discharge current and/or pressure were varied since the length of the positive column is a function of both these parameters as well as interelectrode separation.

Westhaver (1933) was also responsible for the discovery of another unknown characteristic of the glow discharge namely the ' working in ' of the cathode. He reported that a freshly machined cathode gave a far greater rate of ammonia decomposition than an aged one. AS the cathode aged the voltage increased while the rate decreased for

a period of about three hours after which the conditions remained fairly constant.

Running the discharge in pure oxygen or hydrogen had no effect on the worked in conditions although a discharge in water vapour readily restored the original freshly machined characteristics.

Westhaver concluded that this was due to the reduction of a nitride film on the cathode, the formation of which was responsible for the ageing effect. With a freshly machined cathode an abnormally low cathode potential drop was observed and he attributed this to the adsorption of ammonia on the surface.

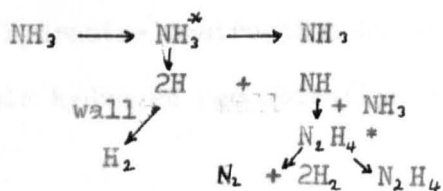
Brewer (1930) demonstrated that the work function of a surface could be lowered from a third to a half by the adsorption of ammonia: due to the dissociation of ammonia into ions by the surface forces. Since the lowering of the work function increases the ease with which the electrons are emitted from the cathode it should enhance the efficiency of the discharge.

A further possibility of accounting for the abnormally high rates on fresh surfaces was put forward by Brewer who found that ammonia adsorbed on the metallic surfaces could undergo decomposition at a temperature as low as 250°C. In most glow discharges 'cold cathodes' are used however it is quite possible that the bombardment by positive ions, atoms, and metastable molecules received by the cathode during the discharge could be as efficient as a hot surface in dissociating adsorbed ammonia.

Devins and Burton (1954) also noted the effect of surfaces upon the chemical reactions occurring in the discharge. In some of their experiments platinum probes were used in the discharge and these

greatly increased the yield of hydrazine but when placed just outside the discharge they had no effect. By coating the discharge walls with platinum they yield of hydrazine was increased significantly, but the yield of nitrogen was only slightly effected. This is rather surprising as nitrogen is considered to be a product of degradation of hydrazine. If, as proposed in their work the platinum walls prevent the degradation of hydrazine by promoting the recombination reaction $H + H \rightarrow H_2$ and hence inhibiting the proposed reaction $H + N_2H_4 \rightarrow NH_2 + NH_3$ it would be expected that the nitrogen yield would fall. Thus because this effect was not noted it may be concluded that this work did not establish whether the improvement in hydrazine yield was due to prevention of its destruction by hydrogen atoms or the catalysis of its formation.

Rathsack extended Devins and Burton's work and showed the effect wall surfaces and metals acting as catalysts had on the formation of hydrazine. It was known that hydrogen atom recombination was retarded by coating the reaction vessel walls with phosphoric acid so experiments were carried out with and without this treatment. With the reactor treated to prevent hydrogen recombination yields and conversion to hydrazine were only one fifth of those from the untreated reactor, clearly showing that hydrogen atoms either prevented the formation of hydrazine or degraded it. Rathsack also put forward the possibility that hydrazine was also formed on the reactor walls explaining his theory in terms of Ouchi's reaction mechanism viz.



This reaction mechanism fitted his results and also explained why the yield of hydrazine fell when the reactor walls overheated.

By using electrodes made of different metals Rath sack demonstrated that the increase in yield of hydrazine was not due to a change in the work function of the electrode or electrical characteristics of the discharge but was caused by the catalytic effect of the electrode materials. Platinum was found to be the best electrode material in agreement with Devins and Burton.

Still further indications of the effects of discharge surfaces upon the hydrazine yields was obtained by Schueler (1959) who used a reactor lined with fused glass powder and by Eremin et al (1966), (1968) who confirmed that the effect of thin metallic films in the discharge zone was to accelerate the recombination of hydrogen atoms.

Williams (1967) obtained increased yields of hydrazine by irradiating gaseous ammonia in the presence of a solid e.g. Zeolites (' which attracted and incorporated H atoms by chemisorption with the result that less destruction of hydrazine or its precursor - NH_2 radical was apt to occur through H atom attack ').

The most recent evidence of surface effects was obtained by Savage (1970) who showed that packing the positive column of a dc glow discharge with glass wool approximately doubled the yield and conversion to hydrazine. Savage proposed that these increases were due to a decrease in hydrazine destruction by atomic hydrogen attack because of increased atomic hydrogen recombination on the extra surface in the discharge.

To summarise it follows from the work which has been reviewed that the introduction of a catalyst into the reaction zone does increase the nett rate of formation of hydrazine, but the exact role of this catalyst in the overall kinetics of the process remains to be established.

In addition to the catalytic effect of discharge surfaces another important surface effect which adds to the complexity of the discharge reactions, is the adsorption of discharge products by the reaction tube walls.

In 1932 Gedye and Allibone working upon ammonia decomposition showed that 'out gassing' by an electric discharge altered the catalytic activity of the glass surface.

Srikantan (1935) investigated the kinetics of ammonia decomposition in a high frequency electrodeless discharge at low pressures and found that reproduceable results could not be obtained due to the effects of the vessel walls. Ammonia was more rapidly adsorbed by the walls of highly evacuated glass tubes than was hydrogen. When the walls of the vessel were saturated with ammonia, the extra gas supplied decomposed into nitrogen and hydrogen. In the presence of the discharge the hydrogen was adsorbed leaving only nitrogen. Ammonia adsorption was found to be irreversible under the influence of the discharge but hydrogen could be adsorbed as well as desorbed from the surface by the discharge.

One very important aspect of discharge surfaces which appears not to have been considered is the possible effect resulting from the migration of loosely bound species in the material of construction of the reaction tubes.

to speculation and until further work is done on the surface will remain a matter of conjecture. The chemistry,

Most reaction tubes used in the glow discharge studies have been made of quartz or silica.

Details of the methods by which vitreous silicas are manufactured are proprietary but four basic types can be recognised (Hetherington (1962 (1963)) with differences based principally upon hydroxyl and metallic impurity concentration and on methods of fusing.

At present very little is known about the effect of high field gradients in the region near the surface of a quartz reactor, however Hetherington (1965) has suggested that inside quartz there are a number of loosely bound species which could possibly migrate under the influence of the field.

As different types of quartz contain varying amounts of OH and metallic impurities it is possible that migration of these species to or from discharge surface might significantly increase or decrease the catalytic efficiency of the surface.

As far back as 1922, Wood in his work on the dissociation of hydrogen in a low frequency discharge concluded that water vapour or oxygen reduced the ability of the walls to catalyse H atoms recombination. Recently a large amount of work has been carried out on the catalytic production of atomic H in a discharge when small amounts of H_2O or O_2 are added. Increases of H atom yield by factors of ten or so when switching from dry H_2 to H_2 containing 0.1 - 0.3% H_2O have been noted (Kaufman (1969)).

Thus the presence of OH in the discharge could significantly inhibit the recombination of atomic H and the presence of metallic impurities could catalyse this recombination.

At present surface effects are poorly understood and are open to speculation and until further work is undertaken the role of the surface will remain a bottleneck in the understanding of discharge chemistry.

CHAPTER 3.0.

3.0. Scope of present investigation.

The primary aim of the experimental work presented in this thesis was to investigate the effect of reactor size on the nett rate of formation of hydrazine in an electrical discharge in ammonia gas. In the course of this work however it was found that the nett rate of formation of hydrazine depended on the reactor unit 'age' and consequently a small amount of work was carried out to investigate this phenomenon.

The experimental work can be summarised in three main parts as follows: -

1) The design, development and testing of suitable reactor units.

A number of homogeneous double electrode discharge chemical reactors employing various electrodes, and electrode configurations, were investigated in order to develop a set of reactor units in which the discharge occupied the entire volume between the electrodes (i.e. the reaction zone) and in which no by-passing of the discharge zone by the reactant gas occurred. Thus for example electrode configurations of co-axial, point, and cylindrical parallel plate design were studied. In addition basic electrode design features were investigated involving the use of electrodes of various shapes, and material of construction, (for example porous circular electrodes of both aluminium and steel, multipoint branched copper electrodes and many others).

2) Investigation of the effect of reactor size on the nett rate of formation of hydrazine.

Three geometrically similar parallel plate reactor units of different size were used in this experimental work.

These reactors have been designated large, intermediate and small, the volume of the large unit (50.7 cm³) being eight, and sixty four times, that of the intermediate and small units respectively.

In each reactor three sets of experiments were carried out to determine the effect of reactor size when the operating conditions of residence time, current density, and reduced electric field strength (E/p) were varied. An equation of the form:-

$$\left(\frac{r D^3}{FC} \right) \propto \left(\frac{V I D^4}{F^3 C} \right)^a \left(\frac{D^4 p}{F^2 C} \right)^b \left(\frac{L}{D} \right)^c$$

where: r: nett rate of formation of hydrazine (ML³T⁻¹)(GMCM³SEC⁻¹)

D: reaction tube diameter (L)(CM)

F: ammonia gas flow rate (L³T⁻¹)(CM³SEC⁻¹)

C: ammonia gas concentration (ML⁻³)(GMCM⁻³)

V_p: potential difference across the reaction zone of the discharge (ML²T⁻²Q⁻¹)(VOLTS)

I: discharge current (QT⁻¹)(MAMPS)

L: length of the reaction zone (positive column)(L)(CM)

P: pressure in the reaction zone (ML⁻¹T⁻²)(MM.HG)

a, b, c : constants

which was derived using the technique of dimensional analysis was found to correlate the experimental results obtained satisfactorily. Inspection of this equation reveals that the nett rate of formation of hydrazine decreases with increasing reaction tube size.

One explanation of this is that the rate of destruction of hydrazine by atomic hydrogen increases with increasing reaction tube size. In order to test this hypothesis, a few ~~few~~ experiments were carried out, in which a large surface area in the form of

quartz wool was introduced into the **positive** column of the intermediate and large reactors. In this way it was hoped to increase the rate of recombination of atomic hydrogen at the discharge surface and consequently decrease the concentration of atomic hydrogen available for hydrazine destruction.

3) Investigation of the effect of reactor unit age on the nett rate of formation of hydrazine.

Two sets of experiments were carried out in this work. In the first set the effect of electrode age was studied and in the second set the effect of reaction tube age was investigated. The results of this research indicate that the age effect (on the nett rate of formation of hydrazine) is primarily due to a change in either the catalytic and/or adsorption properties of the reaction tube surface and not due to changes in the electrode surface as was previously believed.

CHAPTER 4.0.

4.0. EXPERIMENTAL

4.1. EXPERIMENTAL EQUIPMENT

4.1.1. Design, Construction and Arrangement.

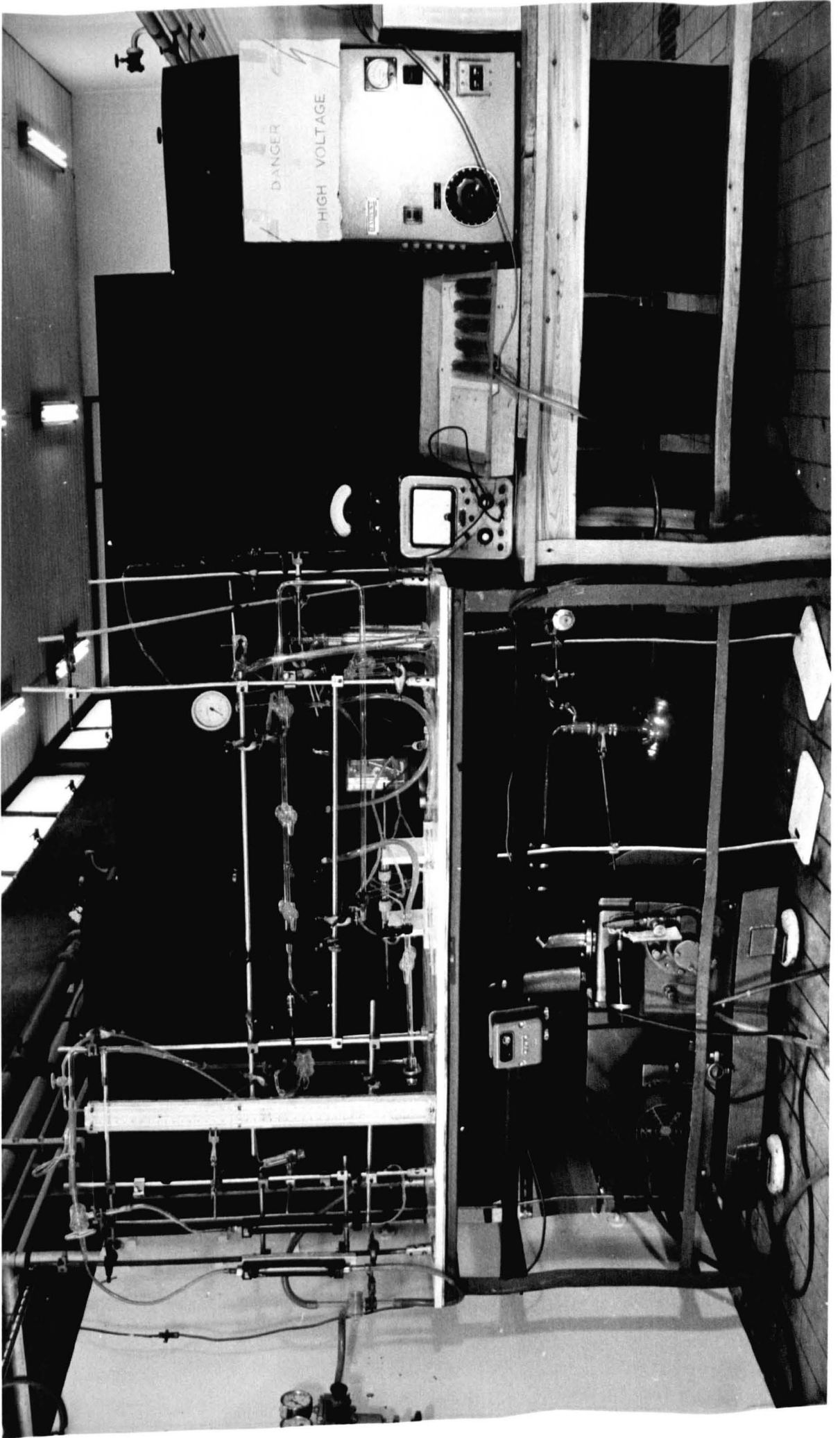
The equipment was designed to study the effects of reactor size on the synthesis of hydrazine in a glow discharge. A general view of the equipment is shown in Fig. 4.1.

In the design and construction of the flow system and reactors, particular attention was paid to the maintenance of high vacuum and prevention of air leaks. Whenever possible glass sections and quickfit ground glass cone and socket joints were used. Where these were impracticable, such as the rotameter (s) connections, fluted stainless steel nozzles which could be screwed onto the rotameter (s) and sealed with Neoprene O - rings were employed. High vacuum stop cocks and glass valves were welded into the flow line where practicable. If metallic valves were necessary stainless steel valves (to prevent corrosion by ammonia) with polythene tubing sealed onto them were used.

Gas flow lines to and from the reactor (s) consisted of polythene tubing which was carefully sealed to the reactor (s) inlet and outlet ports. For those parts of the equipment which were frequently dismantled for cleaning and maintenance etc. ' Q ' sealing compound or quickfit screw joints were preferred.

Apezion high vacuum grease (Types M and N) was used throughout the flow system where applicable, and to minimise pressure drops large bore (> 10mm) polythene tubing was incorporated wherever possible.

FIG. 4.1



Most of the equipment was assembled on a firm Dexion framed bench giving ready access to all parts of it. Lablox stands and retorts were used to support glass pipelines and flow-meters, and manometers were assembled on 1/2" wooden panels clipped onto lablox stands.

Instruments were situated at the front of the rig or in a prominent position to facilitate easy reading. For safety the generator was positioned so as to ensure a minimum length of high voltage lead to the reactor (s). Ballast resistors were housed in a suitably insulated container and all electrical connections to the reactors were routed under the bench to prevent accidental contact.

Following each experiment, after switching off, the electrical apparatus was discharged by placing a suitably insulated length of high tension cable between the high tension and earth sides.

The gas sampling vessel for chromatographic analysis was a separate, detachable unit, which could be connected to the exit ports of the reactor (s).

All switches and controls were positioned such that operation of the rig could be controlled from one area.

4.1.2. Flow system

A line diagram and a photograph of this section of the apparatus is shown in Figs. 4.2. and 4.3. respectively. Reactors could be easily removed or plugged into the system and the use of quickfit joints (vacuum tight to 10^{-2} Torr) facilitated both reactor and flow system modification. Only one cylinder of distilled anhydrous ammonia containing less than 200 ppm impurities of mainly oil and water, was used for all the experiments, so the gas composition can be considered as constant.

At the entrances to the metering system, high pressure ammonia gas from a cylinder was reduced to a pressure slightly above atmospheric by a pressure reducing unit (2).

Depending upon the magnitude of the gas flow (a number of different sized flow meters were required over the range of flow studied) the ammonia could be directed through a three way stop cock into one of two flow paths.

In the flow path 1, the gas was metered through a previously calibrated rotameter at a known temperature and pressure (indicated by a mercury manometer (4) fitted with a mercury trap (5) (in case of blow outs). The small flows encountered were regulated by a high vacuum stainless steel needle valve (6); and adjustment of this valve in conjunction with the pressure reducing valve (2) permitted regulation of the pressure in this section of the system. In order to allow direct reading, the flow meters (which were calibrated at 762 mmHg pressure) were maintained at the calibration pressure of the flow meters.

In flow system 2 the stainless steel needle valve (6) was replaced by a glass valve (7A) which enabled flows of up to 12 litres minute⁻¹ at S.T.P. to be used. Pressure regulation of this section of the system could be controlled by adjustment of valves (2) and (7a).

Regardless of which flow system was used ammonia gas emerged into the vacuum side of the equipment where it was directed through the reactor (8) and then bubbled through three absorption bottles (12). The last two bottles contained ethylene glycol, to remove any hydrazine which had been formed. The first absorption bottle was empty and acted as a trap to prevent suck back into the reactor and other parts of the equipment.

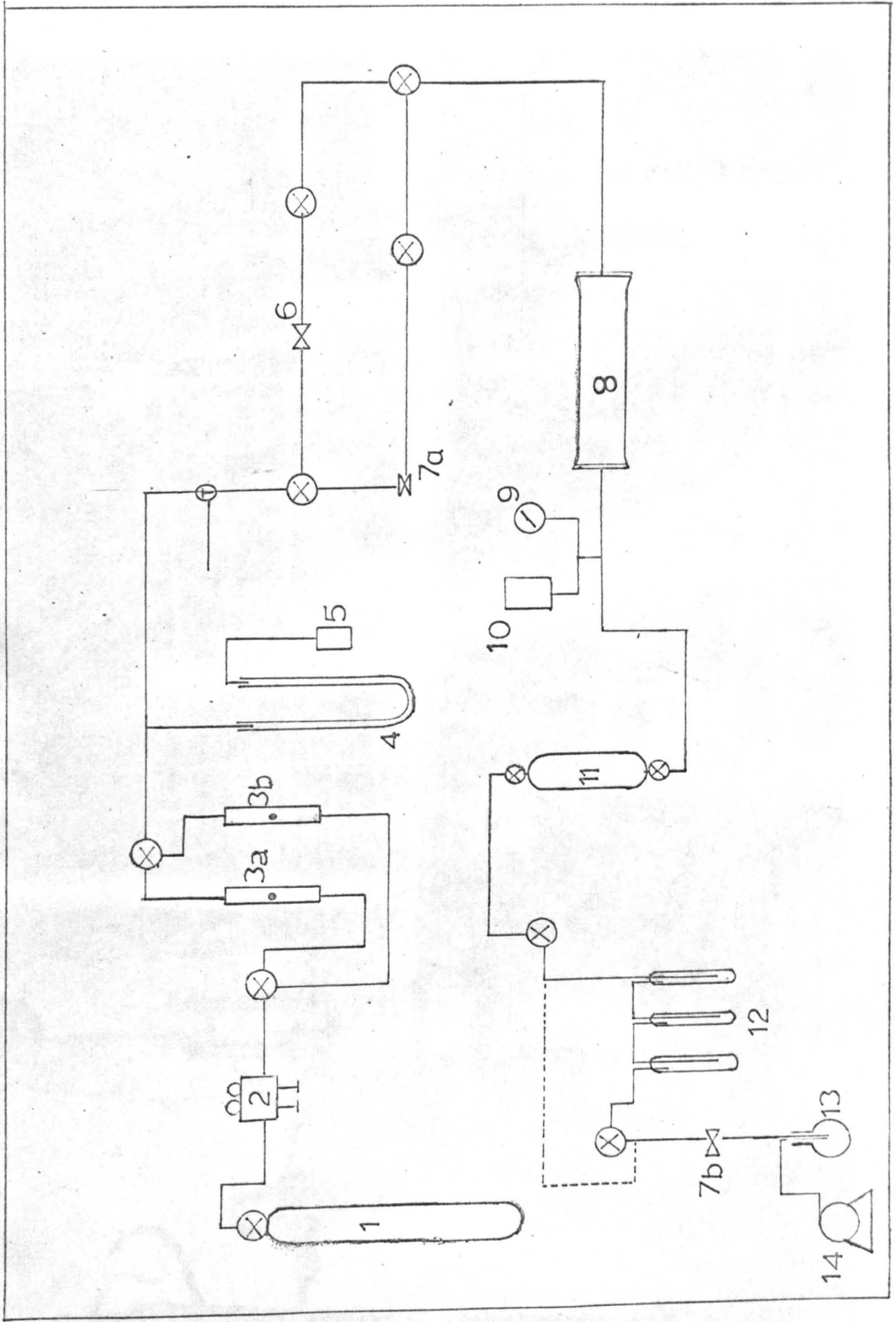
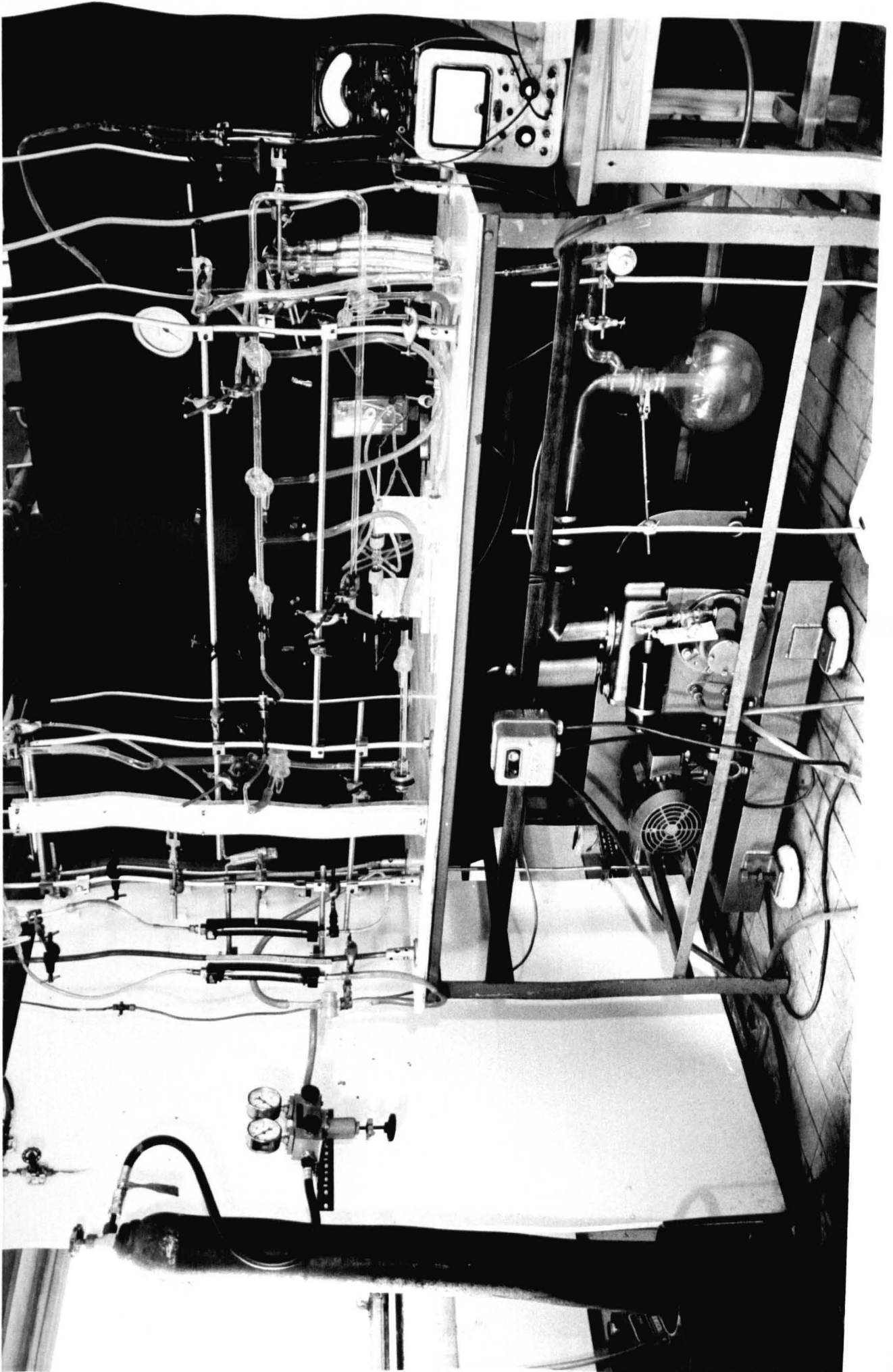


FIG 4.2 FLOW SYSTEM

FIG 4.3



Vacuum flow of ammonia was maintained by a Edwards high vacuum pump (14) fitted to the exit side of the analytical system. The pump displacement at normal speed was 980 litres minute⁻¹ and pump operation was controlled by an auto-memota starter (2.0 - 4.0 amp.). All the effluent gas was discharged directly to the atmosphere.

KEY TO FIGS. 4.2. and 4.3.

1. Ammonia cylinder manufactured by Agricultural Division, ICI ltd.
2. Ammonia pressure reduction unit (MK 2) code no. A5.
- 3a) and 3b) flowmeters.
4. Mercury manometers.
5. Mercury trap.
6. Edwards high vacuum stainless steel needle valve.
- 7a) and 7b) Glass valves.
8. Reactor - (small, intermediate and large).
9. Barometrically compensated Speedivac pressure gauge - type CG3.
10. McCleod gauge (0 - 10 Torr) - type K2470.
11. Two litre, glass detachable gas collection vessel, fitted with high vacuum glass taps at each end used for chromatographic samples.
12. Adsorption train (quickfit B19/26 cone and socket joints).
13. Five litre surge flask fitted with quickfit B/55/44 cone and socket joints.
14. Edwards high vacuum pump/(Speedivac model I.S.C. 900. Single stage gas ballast rotary pump).
15. Gas input line.
16. Gas output line.
17. Pump starter.
- ⊕ 0 - 50°C Thermometer inserted in glass sleeve.
- ⊗ Quickfit three-way high vacuum taps (12mm bore).

--- Absorption train by-pass.

Flow path 1. 2, 3a, 6.

Flow path 2. 2, 3b, 7a.

Gas flow rates were measured by three Fischer and Porter flat meters.

In experiments where gas samples for chromatographic analysis were required the sample collection vessel (11) was placed between the reactor and the absorption traps.

The pressure in the reactor was regulated by a valve (7b) and measured just downstream of the reactor by both a McCleod gauge and a Speedivac pressure gauge. Pressure fluctuations were reduced with a 5 litre surge flask (13) and a by-pass system was incorporated to allow product gases from the reactor to by-pass the absorption train.

4.1.3. Discharge Reactors.

A considerable number of reactors which are described in Chapter 5.1. were tested before a suitable unit was obtained in which no by-passing of the discharge by the ammonia gas occurred.

Three geometrically similar reactors of different size were used in the experimental work. Figs. 4.4 and 4.5 show a diagram and a photograph of the intermediate sized reactor. The important dimensions of the three reactors are listed in Table 4.1.

Each reactor consisted of a cylindrical quartz tube containing a 'push fit' electrode (to allow for expansion) positioned at each end of the reaction tube. The electrodes which were made from stainless steel were highly polished and suitably profiled to reduce edge effects. Ammonia gas was fed into the reactor through four inlets fixed at right angles to each other and the reaction tube and re-emerged through four identical correspondingly positioned outlets. These inlet and outlet ports were connected so that the pressure drop along each 'arm' was the same. This facilitated a uniform gas flow through the reactor which enabled a uniform diffuse glow discharge to be maintained over a fairly wide range of flow conditions.

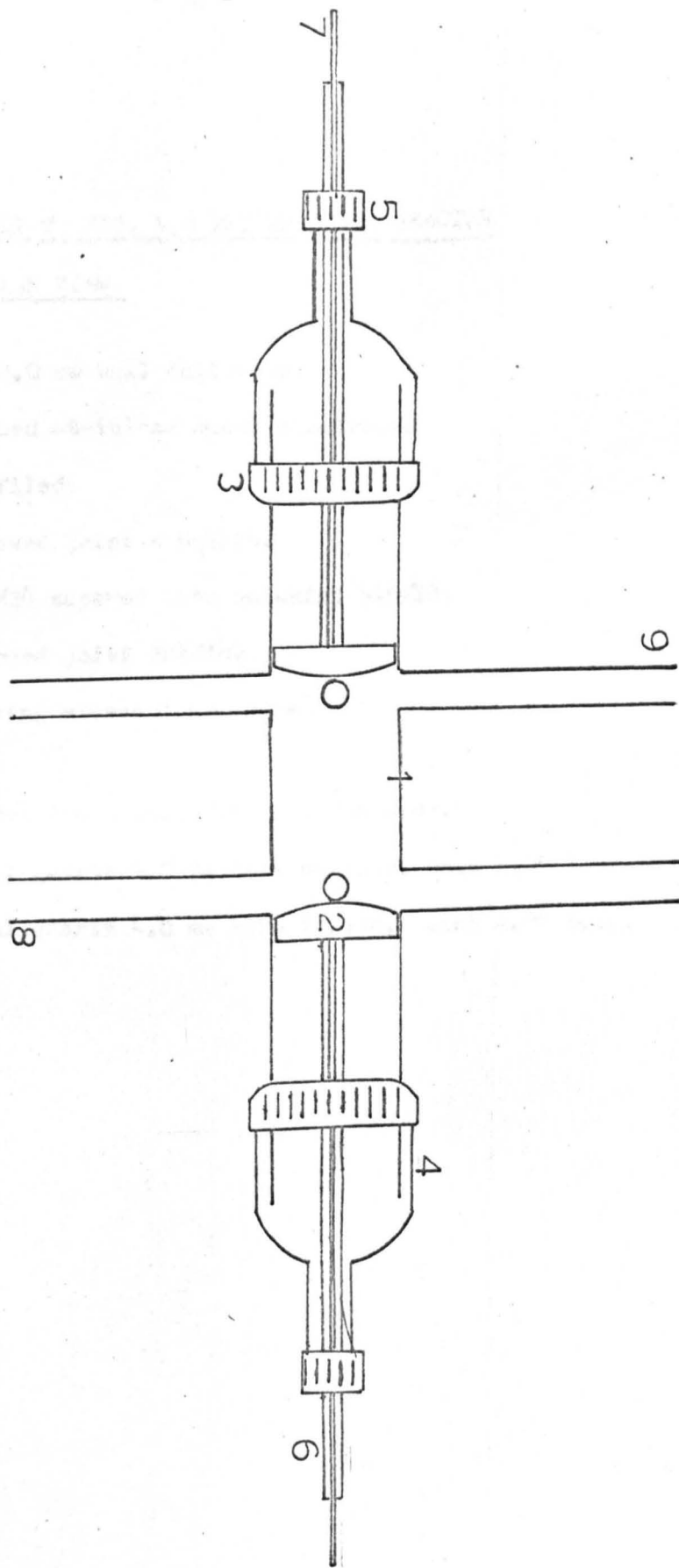


FIG 4.4 INTERMEDIATE REACTOR

KEY TO FIG. 4.4 INTERMEDIATE REACTOR

PLAN VIEW

1. Quartz tube 2.0 mm wall thickness.
2. Highly polished stainless steel electrodes suitably profiled.
3. Quickfit screwed joint - SQ4/24.
4. Quickfit SQ4/24 tapered into quickfit SQ4/18.
5. Quickfit screwed joint SQ4/18.
6. Glass insulating sleeve ' araldited ' into position.
7. Stainless steel conductor, 0.635 cm diameter.
8. Four identical quartz 4.0 mm bore outlets, each 2.0" long.
9. Four identical quartz 4.0 mm bore inlets, each 2.0" long.

FIG 4.5

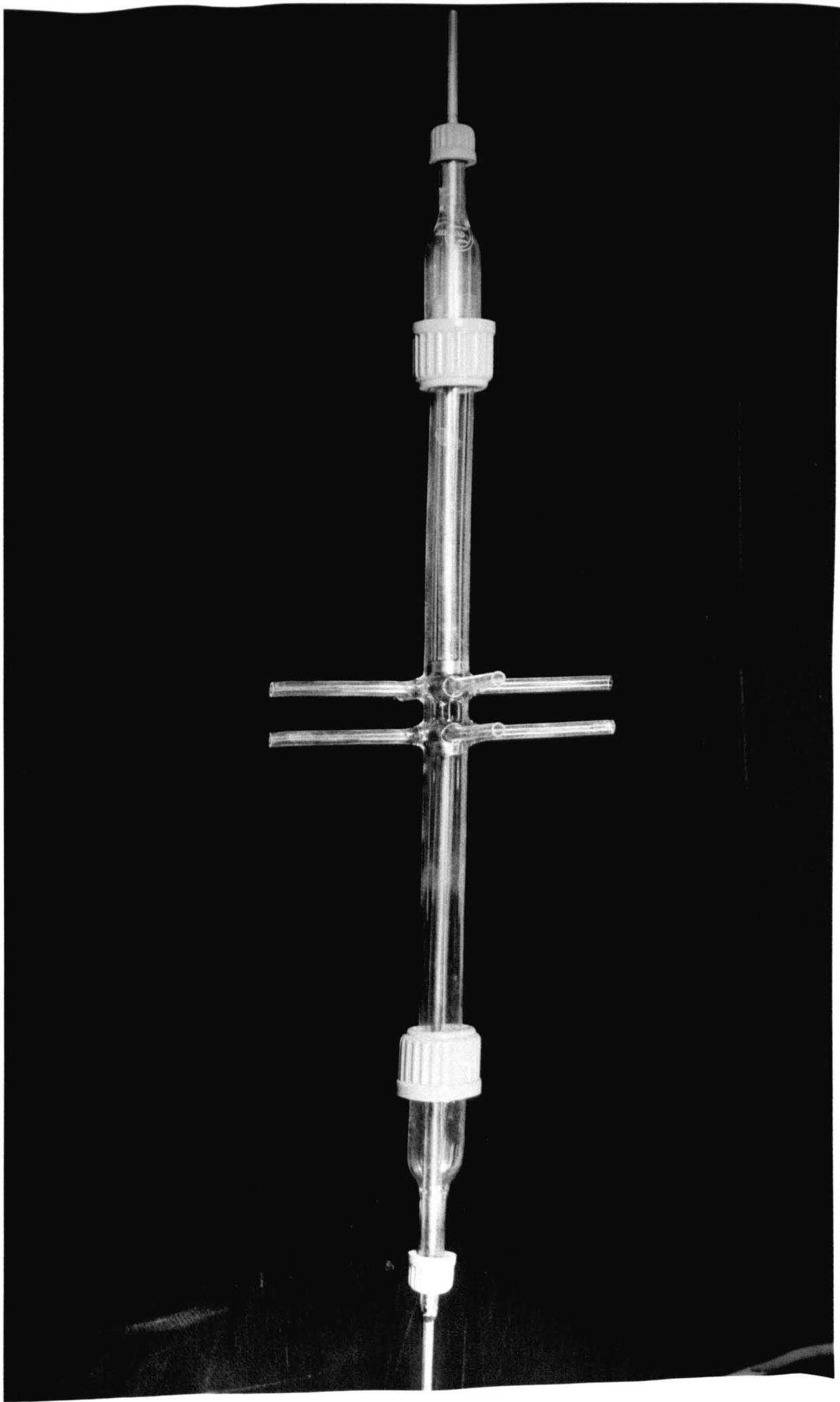


TABLE 4.1. Dimensions of Discharge Reactors.

REACTOR	Quartz Tube Internal Diameter	Electrode Thickness	Electrode Spacing	Discharge Volume	Discharge Surface Area	Electrode Diameter
	(cm)	(cm)	(cm)	(cm ³)	(cm ²)	(cm)
LARGE	3.15	0.635	6.50	50.66	60.308	3.110
INTER- MEDIATE	1.575	0.635	3.25	6.33	15.075	1.565
SMALL	0.794	0.635	1.625	0.805	3.803	0.756

4.1.4. Hydrazine Sampling and Analytical Equipment

Hydrazine formed during the discharge operation was absorbed in ethylene glycol, and analysed colorimetrically. Transmittancy measurements were made with Unicam SP 600 (series 2) spectrophotometer. The instrument incorporated a tungsten filament lamp as the light source two vacuum photocells (blue and red) and two light filters (clear glass and OX7 filter). The setting of the required wave length (458 m μ) was achieved by using the blue photocell in conjunction with the glass filter.

Samples for chromatographic analysis were collected in a detachable 2 litre gas collection vessel (situated just down stream of the reactor) and transferred to the chromatograph at the end of each experiment. The unit is shown in Fig. A1.1*. A description of this unit, its operation and the column operating conditions employed is outlined in Appendix 1.

4.1.5. Electrical Equipment.

The electrical system consisted of a modified hf power supply, valve volt meter coupled to a dc multiplier, milliammeter and ballast resistors. A diagram of the electrical circuit is shown

* throughout this thesis table or figure numbers prefixed by the letter A indicate that this table or figure is located in the appendix of that number.

in Fig. 4.6. and a photograph of the electrical equipment in Fig. 4.7.

The dc power was supplied by a modified Cl2/BRadayne generator with output transformer capable of 4.2 kv. The HT output was tapped off after rectification and then fed to a 'smoothing system' before passing to the reactor. By the combined use of 'choke' coils in series with the load and condensers in parallel with the load, it was possible to reduce time amplitude of the ac 'ripple' so that it was of the order of only 1% or less of the dc component. The current and voltage signals from the system were periodically checked on a dual trace oscilloscope. The electric circuit of the power supply is shown in Fig. 4.8.

An insulated airmec dc multiplier (factor X 1000) was used in conjunction with a multirange valve voltmeter (Airmec Type 314) to measure voltage up to 4.0 kv. A.25.0k Ω (Welwyn c47) ballast resistor was used in series with the reactor(s) in order to limit the current and thus prevent the glow discharge from developing into an arc discharge. The current was measured by either a universal Ivometer (model 8 Mk III) or one of three E.I.C. moving coil milliammeters (0 - 20, 0 - 100, 0 - 200 milliamps.) depending upon the current magnitude.

Polythene insulated 14/.0076 plain core with outer sheaf of P.V.C. extra high tension cable (safe up to 18 kv.) was used for circuit connections.

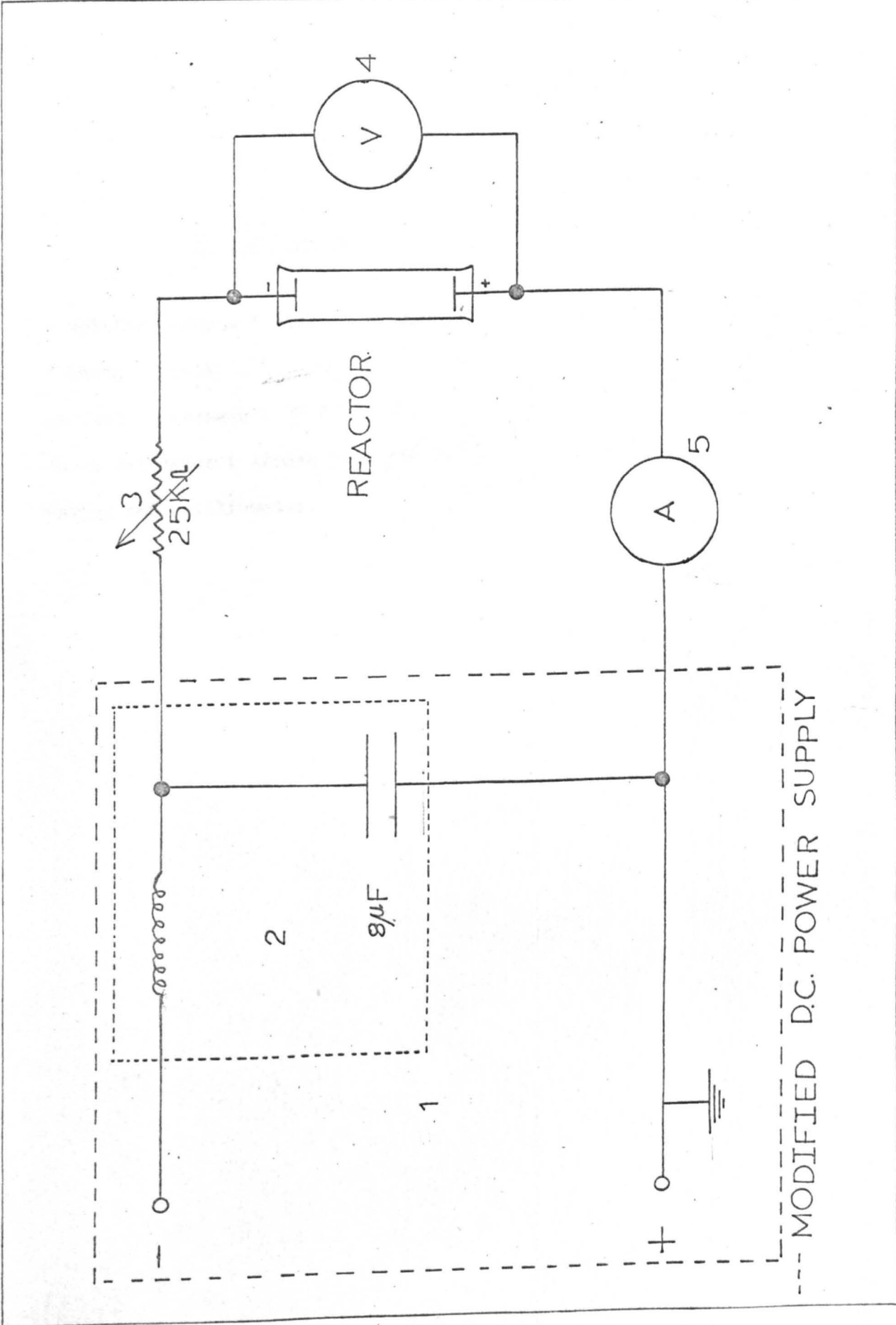


FIG 4.6 ELECTRICAL CIRCUIT

KEY TO FIG. 4.6.

1. ' Modified Radyne ' d.c. power supply.
2. ' Choke circuit '.
3. Ballast resistance (25 K Ω).
4. Valve voltmeter (Airmec type 314).
5. Moving coil milliammeter.

FIG. 4.7

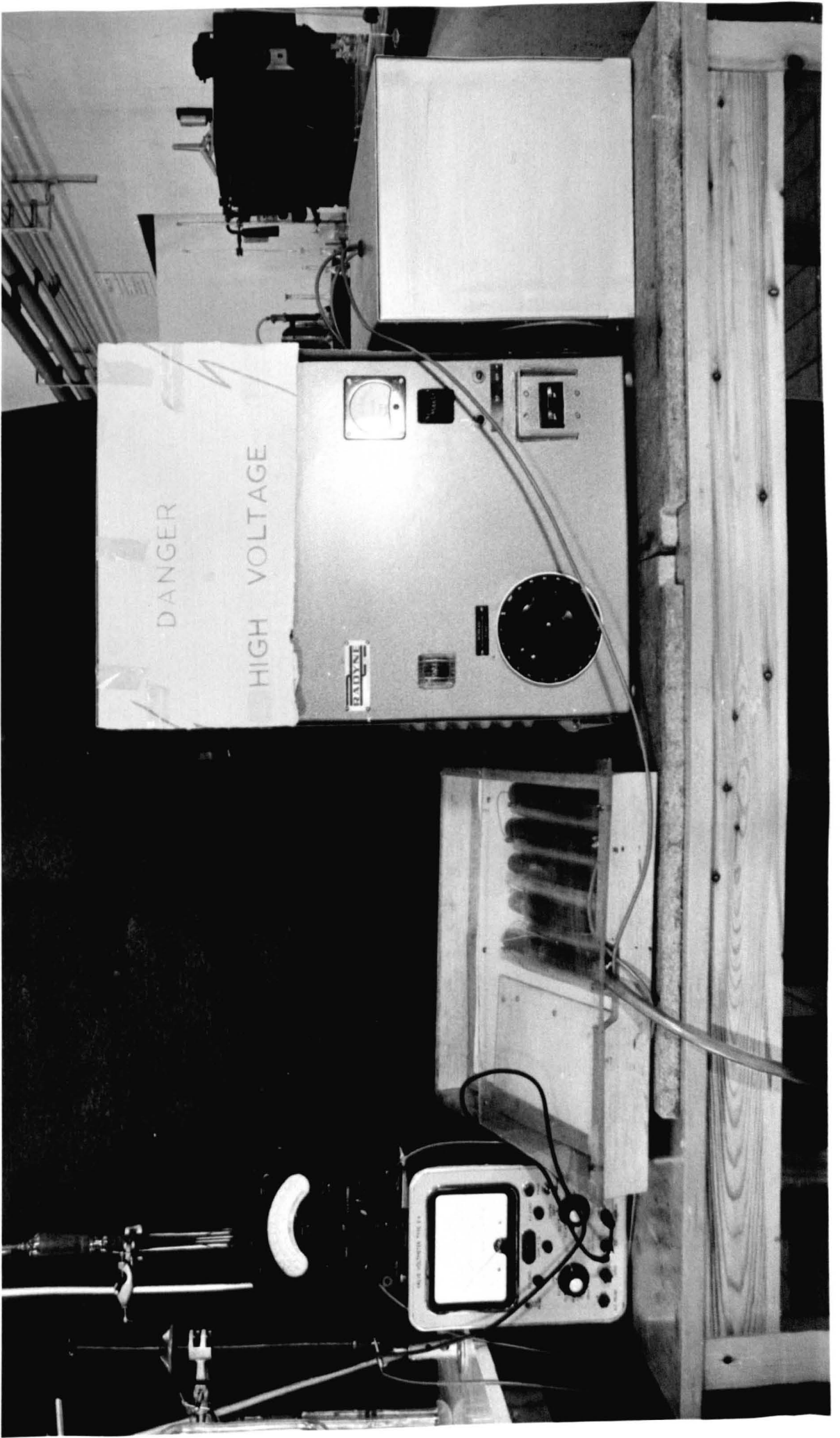
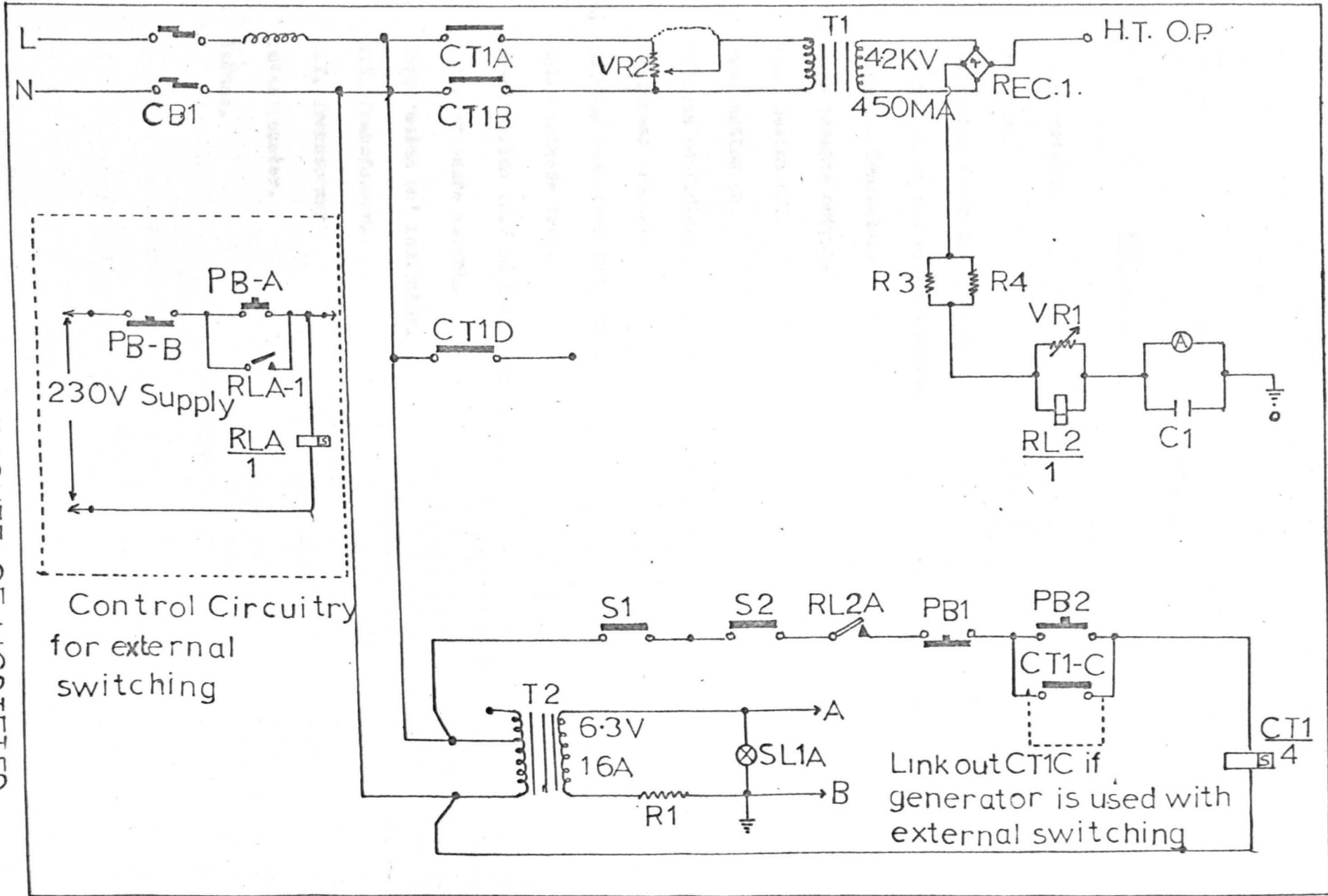


FIG.4.8 ELECTRIC CIRCUIT OF MODIFIED RADYNE GENERATOR



KEY TO FIG. 4.8.

- A. Meter output.
- Ⓐ Ammeter.
- C1. Capacitor meter by-pass: 0.01μ F.
- CB1. Mains switch and circuit breaker.
- CT1. A,B,C,D: Contactor.
- H.T.Op. High tension output.
- PB1. Push button off.
- PB2. Push button on.
- REC1. Silicon rectifiers.
- R1. Filament dropper.
- R3-R4. Cathode resistors 150 10W.
- RL2. Relay cathode trip.
- S1. Panel switch (H.7 on indicator).
- S2. Water pressure switch.
- SLIA. Lamp 'mains on' indicator.
- T1. H.T. Transformer.
- T2. L.T. Transformer
- VRL. Potentiometer.
- VR2. Variac.

4.2. Materials used in experiments.

The chemicals which were used as reactants, absorbents and for chromatographic analysis are listed in this section. Reagents used in analysis of the products are detailed later in the description of the appropriate analytical method.

1. Ammonia - Commercial Grade (99.5%) ' Distilled Anhydrous' ammonia.
2. Ethylene Glycol - BDH Reagent Grade.
3. Nitrogen - 99.5% pure was supplied by the British Oxygen Co.
4. Hydrogen - 99.5% pure was supplied by the British Oxygen Co.
5. Helium - 99.9% pure <1.0 ppm oxygen supplied by British Oxygen Co.

4.3. Experimental procedure

In the small number of experiments* in which chromatographic analysis was carried out each experimental run was performed twice under identical operating conditions. Both these runs the first with liquid absorption of the hydrazine and the second to collect the gaseous products for chromatographic analysis, involved routines which were identical. In the remaining experiments for which it was not possible to carry out chromatographic analysis only one experimental run was necessary.

The apparatus referred to in this section are identified in Fig. 4.2.

4.3.1. Description of an experiment using liquid absorbent.

The first step in a normal routine involved switching on all

* Originally it was planned to carry out chromatographic analysis of the reaction products for all of the experimental runs. Unfortunately however as it was not possible to obtain stable conditions continuously in the chromatographic unit, analysis was limited to a few runs carried out in the small reactor, during a short period when the chromatographic column appeared stable.

of the electrical instruments according to the Manufacturer's recommendations. Following this the absorption traps were filled with ethylene glycol (50.0 ml.).

With the valves (6, 7a) which connect the input lines to the reactor closed the vacuum pump was switched on and the system evacuated down to 1.0 mmHg pressure. The system was then held in this state for about 10 minutes in order to warm up the pump oil (using full gas ballast) to assist in preventing vapour condensation in the pump and to completely de-gas the system. During this time the pump was inspected to check that-

- 1) The oil level was not below the upper limit of the lower sight glass - if it was the oil was topped up and once every three months it was changed.
- 2) The cooling water flow rate was above 0.5 litres min^{-1} .

The three way trap situated between valve (7b) and the absorption traps (12) was closed and the system tested for leaks. From time to time it was necessary to recoat the stop cock keys with high vacuum grease. Also the rubber vacuum seals in the pump, glass valves and the pressure gauges were checked periodically. In the absence of detectable leaks the Speedivac gauge (9) remained at zero over a period of minutes (the pressure was checked at the beginning and end of this period with the McCleod Gauge (10)).

Regulation of Flow and Pressure.

The gas input line was connected to the reactor and the apparatus was flushed with ammonia, until the glycol in the absorption traps was saturated, and then allowed to come to the required temperature and pressure (fine control of the pressure in this section was achieved by adjustment of the valves (2) and (6) or (7a) (depending upon the range of flow desired).

The pressure in the reactor was controlled by valve (7b). In early experiments the absorption traps were switched out, the compressed air from the mains supply blown onto the ballist resistors and the discharge switched on and allowed to come to steady conditions. As the discharge reached a steady form, almost immediately, the by-pass was not used in later experiments.

The power input to the reactors was controlled by adjustment of the generator variac control. With the product gases passing through the absorption train where any hydrazine which had been formed was removed, the discharge current and voltage were noted and then the discharge switched off after a fixed time. The flow rate readings and the temperature and pressure at the measuring points were recorded.

Finally, the system was returned to atmospheric pressure, by closing valves (2) and (6) or (7a) (depending upon which flow system was used) and opening the vacuum tap situated between the absorption traps and valve (7b), to the atmosphere with the pump switched out. The pump which was now isolated from the system was allowed to run for a further fifteen minutes, with maximum gas ballast flow, to remove any corrosive ammonia vapours. During this time the absorption traps were removed and the contents thoroughly mixed, sampled and analysed by the methods described in section (4.4).

Fluctuations of the Experimental Variables.

Unavoidable fluctuations of the experimental variables occurred during a run. Readjustment was necessary during the preparation

period, but the magnitude of the fluctuations during the discharge operation were very small:

- 1) The movement of the float in the flowmeters was very much reduced by trial and error adjustments of the pressure in the input lines. It was more serious at low gas flow rates in which the oscillation of the float could vary to 5% of the desired flow rate.
- 2) Fluctuation of the reactor pressure due to pumping, operating conditions, and heating of the cathode were negligible however, (estimated at 1.0%), and readjustment was not attempted during the short operating times involved. This effect was more pronounced in the smaller reactor.
- 3) Also due to cathode heating small changes in current and voltage were noticed (estimated at 1.0%) and again readjustment was not attempted.

4.3.2. Description of an experiment to collect samples for Chromatographic Analysis.

The chromatograph was left running continuously from the time that the desired operating conditions were achieved and samples could be analysed at any time.

Experimental procedure was identical to that described for using liquid absorbents except that immediately before switching off the discharge the gas sample collection vessel was sealed off by closing taps (2) and (3) Fig. A1.1. At the end of the run the collection vessel was transferred to the chromatograph, and connected as shown in Fig. (4.9). The lines from the injection point to the collection vessel were then

evacuated and flushed with helium several times, then finally, evacuated and the sample injected and analysed. The whole procedure occupied seven to ten minutes.

Fluctuation of the Experimental Variables.

During discharge operation these were identical to those for the absorption experiments. In addition leakage occurred during the transfer of the collection vessel and the preparation period for sample injection. Fine control of sample injection pressure was achieved by use of the three way tap (Y) Fig. (4.9), however, variations occurred resulting in differences in sample volume and hence peak height. Errors in measurement of peak height and variation of detector sensitivity contributed to an overall apparent error of $\pm 6 - 8\%$ for the small concentrations involved.

4.4. Measurements and Chemical Analysis

In this section the analytical procedure and the calibration of instruments are described. Reference is made to sources of error and where possible an estimate is made.

4.4.1. Analysis of Products.

In the few experiments in which the exit gases from the reactor were analysed a Perkin Elmer 452 gas chromatograph was used, which employed a molecular sieve 5A to facilitate separation and analysis of nitrogen and hydrogen. The column also showed the presence of air from leaks as oxygen peak. Helium was used as the carrier gas.

Chromatographic determination of ammonia was not attempted as it was more accurate to calculate ammonia by difference than by

direct analysis, for the small percentage decomposition obtained (Carburgh (1967)). For the same reason colorimetric determination of the small concentrations of hydrazine encountered was preferred to chromatographic analysis.

Chromatograph Calibration Procedure.

Various mixtures of nitrogen, hydrogen and ammonia were prepared in an apparatus especially constructed for this purpose (Fig. 4.9). These mixtures were injected into the chromatograph at a constant injection pressure of 6.0 mmHg. Fine control of this injection pressure was achieved by use of the three way stopcock (X). Fig. Al.2 shows an example of a chromatographic trace obtained from one of these mixtures.

Calibration curves of percent nitrogen versus nitrogen peak height (Fig. Al. 3) and percent hydrogen versus hydrogen peak height (Fig. Al.4) were plotted from these results which are tabulated in Table Al.1.

In the experimental runs the collection vessel was sealed off and then transferred to the chromatograph. Any air leakage which occurred during transfer showed as an oxygen peak from which a nitrogen correction to give the actual percent nitrogen in the sample could be calculated.

A chromatographic trace obtained from an experimental run is shown in Fig. A.1.5. The apparatus used for injecting samples of air or gas samples from the experimental runs is shown in Fig. 4.9.

Sources of error in Chromatographic Analysis

Errors arose due to : -

- a) Base line drift at low range settings.
- b) Noise interference resulting in a distorted base line at low range settings.

- c) Because of the similar retention times of nitrogen and hydrogen the attenuation range had to be the same for both gases. This resulted in a greater error in the measurement of the small hydrogen peaks.
- d) The use of peak height rather than the area under the peak as the basis for measurement of the component concentrations in the gas samples.
- e) Reduced accuracy of pressure gauge at low pressures leading to variations in the injection pressure volumes of the samples injected.
- f) Reading of instruments etc.

Analysis of Hydrazine.

A detailed description of the method used, standardisation of the solutions employed and experimental procedure used is contained in Appendix 2.0.

Basically the hydrazine in the exit gas from the reactor was absorbed in ethylene glycol and then analysed. The concentration of hydrazine in the ethylene glycol, was only of the order of a few parts per million so a colorimetric method of analysis using p - dimethylaminobenzaldehyde was used.

A standard hydrazine solution was prepared using hydrazine sulphate, quantitatively analysed by titration against standard potassium iodate with chloroform as indicator. The hydrazine solution was then carefully diluted to the concentration range required, 0.01 to 0.2 ppm for the colorimetric analysis. A calibration curve of absorption at 458μ against ppm hydrazine was plotted using these standard solutions in a Unicam SP 600 (series 2) spectrophotometer see Fig. A2.1. The experimental solutions could then be determined against this curve.

Although analytical grade p - dimethylamino benzaldelyde was used, its appearance and colour developing properties varied slightly from batch to batch, so new colour solutions were always recalibrated. Colour solutions and standard hydrazine solutions could be kept for about one month without deterioration.

Analysis of Ammonia.

Literature indicated that ammonia conversion could be estimated by bubbling the ammonia from the exit gas through acid and backtitrating any unneutralised acid.

Savage (1969) reported that this method did not give reproducible results and consequently it was not used.

4.4.2. Power Measurement.

Power was supplied by a modified Radyne hf generator. A choke coil operated in series with the generator was used to reduce any ' ripple ' to the order of 1% or less of the d.C. component.

The current which was measured by an universal Ivometer or an appropriate milliammeter depending upon current magnitude, was limited (to prevent arc formation) with a 25 K Ω ballast resistor placed in series with the reactor.

Voltage was measured by using an Airmec dc multiplier (factor X 1000) in conjunction with an Airmec valve voltmeter (type 314). Power supplied to the discharge was computed as the product of amps x volts = watts for all experimental results. The estimated accuracy of the power measurement was \pm 5%.

4.4.3. Flowrate Measurements.

The flowrates of gases were measured with Fischer and Porter rotameters of 1/8" and 1/16" nominal diameters using spherical stainless

steel and/or tantalum floats, individually calibrated to read:-

Ammonia: 0.1 → 3.0 cm³ sec⁻¹ (@ 15.6 °C and 762 mmHg Press)
FP-1/16-10-6-5/84 stainless steel float.

Ammonia: 3.0 → 12.0 cm³ sec⁻¹ (@ 15.6 °C and 762 mmHg Press)
FP-1/16-16-G-5/84 tantalum float.

Ammonia: 13.3 → 66.0 cm³ sec⁻¹ (@ 15.6 °C and 762 mmHg Press)
FP - 1/8-20-G-5/84 stainless steel float.

The meters were calibrated to a method described by the manufacturers (the results were checked with results obtained from calibration procedures involving the use of a soap bubble burette and also a wet air meter).

The reproducibility of the flowrate determination with the soap bubble burette indicated an accuracy of the order of: ± 3 - 4%.

1. Soap Bubble Method.

In this method operating pressure was maintained constant throughout the calibration procedure. By timing the flow of a soap bubble between two graduated marks on a soap bubble burette, a table of volumetric gas flow rates was computed over the range for a particular tube at an operating condition R_1, T_1 . The temperature T_1 being the inlet temperature of the gas to the flow meter. A plot of volume flow rate of ammonia (@ 15.6 °C and 762 mmHg) as a function of flowmeter scale reading was then constructed. This method was only suitable for low flowrates (0.1 → 3.0 cm³ sec⁻¹).

2. Fischer & Porter Calibration Procedure.

In this method the flowrate is related to the flowmeter conditions by the equation:

$$F = C B ((\rho_f - \rho_{opt}) \rho_{opt})^{\frac{1}{2}} \quad (4 - 1)$$

where F = calculated flowrate at operating pressure and temperature

ρ_f = density of float gm cm⁻³

ρ_{opt} = density of gas at operating temperature and pressure gm cm⁻³

B = constant for each tube

C = 'flow co-efficient' given by the manufacturers as a function of tube dimensions, scale reading and 'viscous influence number N

$$N = \frac{A}{\mu_{opt}} ((\rho_f - \rho_{opt}) \rho_{opt})^{\frac{1}{2}} \quad (4 - 2)$$

A = constant for each tube

Table 6, F & P Manual gives values of ρ_{opt} and μ_{opt} as a function of temperature.

Table 7, F & P Manual gives values for size factors A and B for various tube sizes.

Procedure.

- 1) From equation (4 - 2) calculate viscous influence number N.
- 2) Using the float characteristic curve (Fig. 11 F & P Manual) for the relevant tube values of C over the scale range can be calculated for the computed value of N.
- 3) Determine the value of F (gm min⁻¹) using equation (4 - 1) for each C value determined.
- 4) The corresponding values of flowrates at some standard temperature and pressure can be computed from conversion formula:

$$\text{S.T.P. cm}^3 \text{ min.}^{-1} = \frac{\text{grams min}^{-1}}{\rho \text{ S.T.P.}} \quad (4 - 3)$$

The results and calibration curves and an example of the calibration procedure are given in Appendix 3. The estimated accuracy of flow measurement by this method was $\pm 3\%$ (however at low flows the error could be up to $\pm 5\%$).

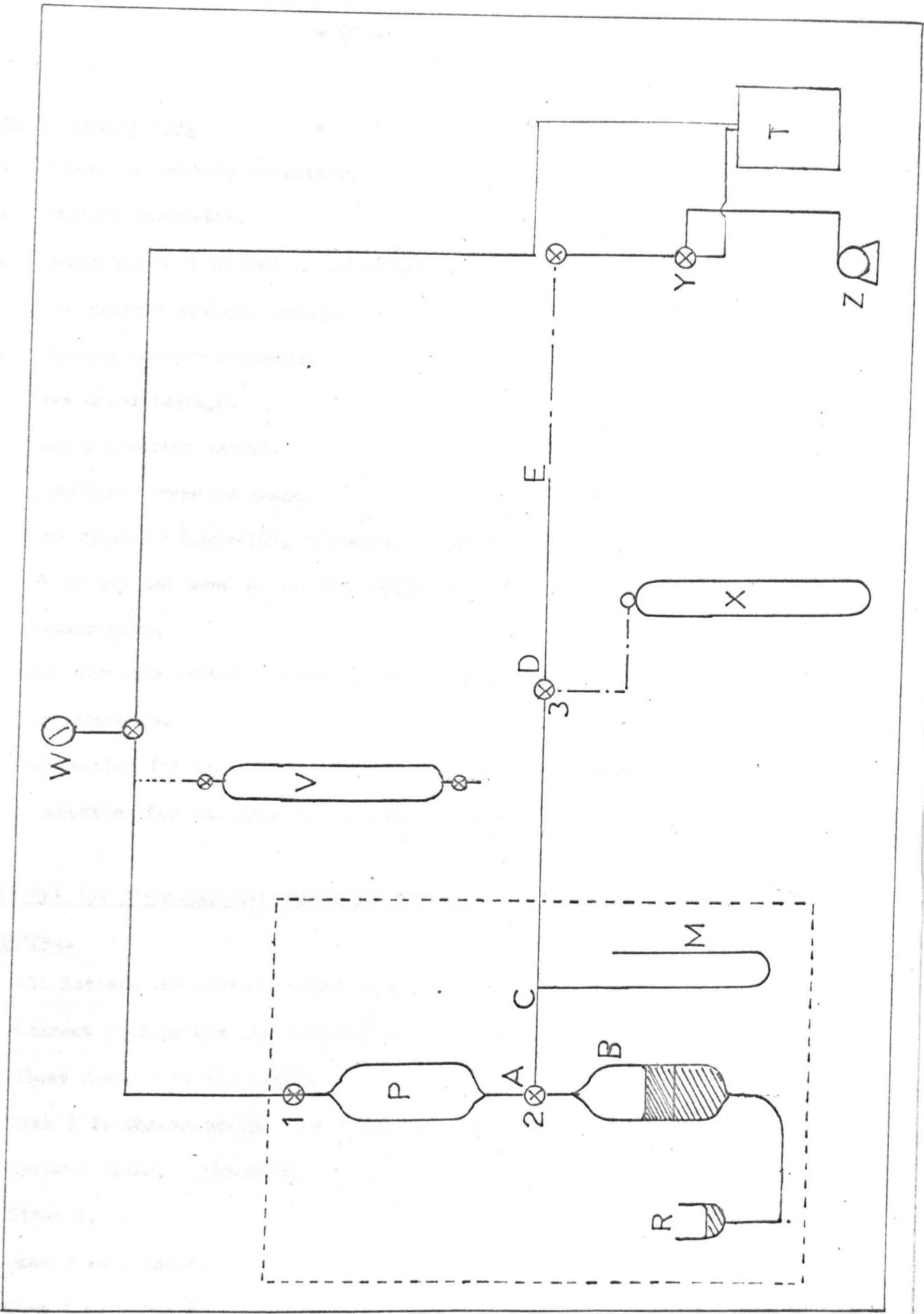



FIG 4.9

Key to Figure 4.9.

- B. Graduated mercury container.
- M. Mercury Manometer.
- Q. Graduated mark etched on container B.
- P. Gas mixture storage vessel.
- R. Movable mercury container.
- T. Gas chromatograph.
- V. Gas collection vessel.
- W. Speedivac Pressure gauge.
- X. Gas cylinder (ammonia, nitrogen, or hydrogen).
- Y. Three way tap used to control sample injection pressure.
- Z. Vacuum pump.
-  Gas burette system for making precision gas mixtures at low pressure.
- Connection for analysis of samples from discharge experiments.
- Connection for analysis of air and precision gas mixtures.

Procedure for preparing and analysing precision gas mixtures at low pressures.

All letters and numbers refer to Fig. (4.9.)..

1. Connect appropriate gas cylinder and pump with vacuum tubing.
2. Close 2 and 3 to all limbs.
3. Open 1 to chromatograph line flush out with helium and evacuate several times. Evacuate.
4. Close 1.
5. Open 2 to A and C.
6. Open 3 to C and D.

7. Raise gas pressure to approximately 1/2 atmosphere.
8. Connect A and B on 2.
9. Raise R to fill B with mercury.
10. Switch 2 to connect A and C.
11. Open 3 to C,D and E.
12. Switch on vacuum pump to evacuate apparatus and gas line.
13. Switch off 2 by rotating 45 anticlockwise.
14. Switch 3 to connect D and C.
15. Raise gas pressure to slightly over 1 atmosphere.
16. Connect B and C by rapid anticlockwise rotation of 2.
17. Lower mercury in B to lower mark Q.
18. Keep volume in B constant while gas pressure is adjusted to desired value by use of 3.
19. Switch off 3.
20. Connect A and B by clockwise rotation of 2.
21. Raise R to fill A and B.
22. Switch off 2 anticlockwise.
23. Connect new gas supply to D.
24. Connect C, D and E on 3 evacuate the system.
25. Go to instruction 13 for next gas.

CHAPTER 5.0.

5.0. Experimental results and discussion.

The experimental studies are reported in three sections.

- 5.1. The design, development and testing of a set of geometrically similar homogeneous double electrode discharge reactor units in which the discharge in each reactor occupied the entire volume of the reaction zone ensuring that no by-passing of the reaction zone by the gaseous reactant occurred.
- 5.2. Investigation of the effect of reactor size on the nett rate of formation of hydrazine in an electrical discharge.
- 5.3. Investigation of the effect of reactor unit 'age' on the nett rate of formation of hydrazine in an electrical discharge.

5.1. Design, development and testing of chemical discharge reactors.

5.1.1. Experimental Programme.

The various factors effecting the design and operation of reactors in which the conditions of 'uniform discharge' (no radial contraction) and ' no reactant gas by-passing ' have been outlined in chapter 2.1.

In the experimental work several different reactor units were tested. Once a suitable design of reactor unit was obtained in which the above requirements were satisfied, larger size units were constructed and tested. In the design of these units the following specifications with reference to the small initial test reactor were used.

- 1) Geometric similarity (i.e. both reactor and electrode configuration).
- 2) Identical material of construction (for all of the reactors tested quartz tubing was used. Electrodes of various metals were investigated).

5.1.2. Results and Discussion

The first ' reactor set ' tested employed a co-axial electrode configuration with stainless steel electrodes (see Fig. 5.1.a.). The electrodes were profiled with the boundary to surface area ratio kept to a minimum to remove ' edge ' effects.

Even with the interelectrode distance reduced to 2.0 mm the discharge in ammonia gas constricted into a thin pencil beam.

' Cleaning ' and ' polishing ' the electrodes (on several occasions) showed no improvement, nor did substituting aluminium electrodes (in place of the stainless steel electrodes).

Four possible reasons were put forward to explain these observations:

- 1) A high spot (due to surface roughness or some other factor) existed which reduced the work function of the material resulting in an electron avalanche at this point.
- 2) The presence of the earthed reactor walls distorted the discharge field. (Harrison (1967) reported this effect to be negligible).
- 3) The magnitude and variation in flow of the ammonia gas.
- 4) The nature of the ammonia gas.

Each time the discharge was switched on the pencil beam struck from a different point which suggested that neither surface roughness, nor hot spots, contributed to the pencilling effect (it was not possible with this reactor to verify this by rotation of the electrodes - i.e. if surface hot spots were responsible for the constriction the discharge point would not move over the electrode surface).

PAGE

NUMBERING

AS ORIGINAL

The fact that no improvement was obtained by using lower work function electrodes (aluminium) suggested that this also did not account for the pencilling (it should be noted however that aluminium cannot be ' polished ' as well as stainless steel). When air was used as the (stationary) reactant gas a uniform diffuse discharge was obtained even at increasing inter-electrode distances.

In order to test the effects of variation in the flow pattern of the ammonia gas a distributor was fitted into the smallest reactor. Operation at very low pressures and flow resulted in a slight broadening of the constricted discharge, but the pencil beam still only occupied a small fraction of the electrode surface.

Significantly the discharge point appeared only at the gas exit end of the reactor indicating that the flow magnitude and pattern was responsible for the non-uniformity. It was concluded that this type of reactor design was unsuitable.

The next reactor (test number 4 Table 5.2.) consisted of a cylindrical reaction tube with push fit (no by-passing) porous aluminium parallel discharge electrodes (see Fig. 5.1b). Again a radially contracted discharge was obtained however experimentally it was established that a diffuse discharge existed at conditions of -

- 1) Very low flow rates and pressures (of the order of 5.0 mmHg) at higher pressure the discharge became striated.
- 2) Reduced electrode perforation diameter.
- 3) Reduced number of perforations.
- 4) Reduced electrode gap.

FIG 5.1

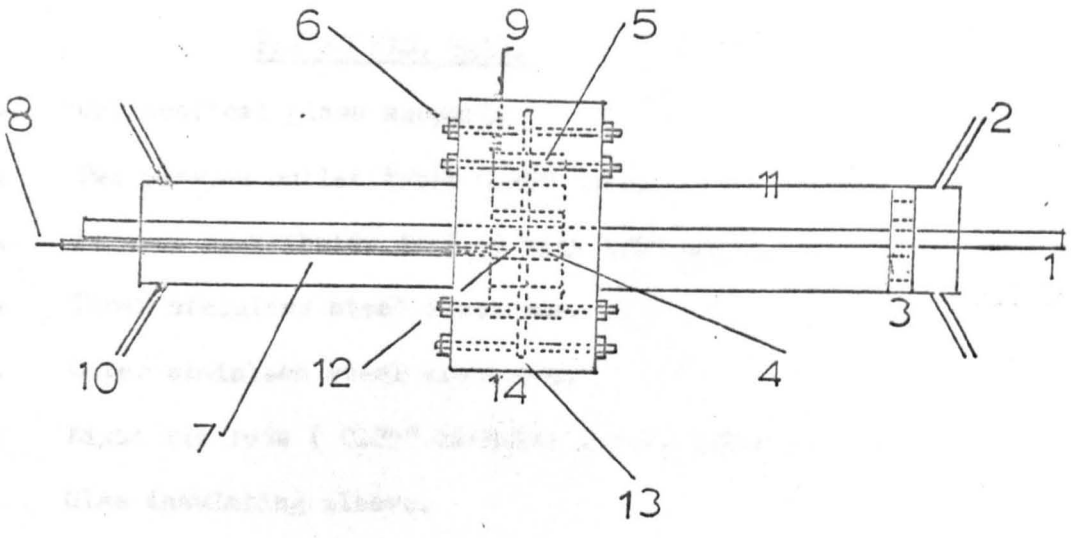


FIG 51a

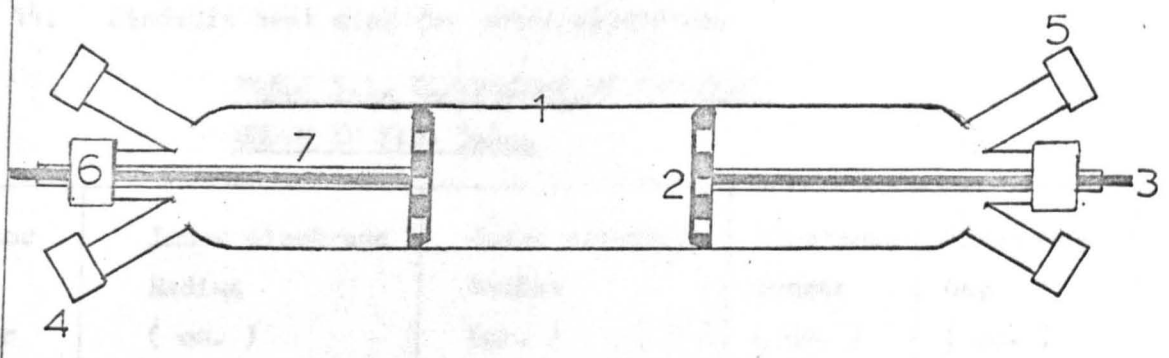


FIG 51b

FIG 51

KEY TO FIG. 5.1a.

1. Cylindrical glass support.
2. Two perspex outlet tubes 0.25" bore.
3. Perspex distributor drilled with 1/6" holes.
4. Inner stainless steel electrode.
5. Outer stainless steel electrode.
6. Eight tie rods (0.25" diameter B.S.F. bolts).
7. Glas insulating sleeve.
8. Stainless steel conductor attached to inner electrode.
9. Stainless steel conductor attached to outer electrode.
10. Two perspex inlet tubes 0.25" bore.
11. Perspex tube araldited to Sindania heat sink (14).
12. Sindania bush heat sink for inner electrode.
13. High temperature silicon 'O' ring.
14. Sindania heat sink for outer electrode.

TABLE 5.1. DIMENSIONS OF REACTORS
SHOWN IN FIG. 5.1a.

Reactor Test Number	Inner electrode Radius (cm.)	Outer electrode Radius (cm.)	Electrode Length (cm.)	Electrode Gap (cm.)
1.	2.54	3.34	3.0	0.8
2.	1.27	1.67	1.5	0.4
3.	0.635	0.835	0.75	0.2

KEY TO FIG. 5.1b.

1. Quartz tube (2.0 mm wall thickness).
2. Interchangeable perforated aluminium electrode.
3. Stainless steel conductor.
4. Two quickfit screw joint SQ4/13 inlets.
5. Two quickfit screw joint SQ4/13 outlets.
6. Quickfit screw joint SQ4/18.
7. Glass sleeve insulator.

Compressed stainless steel gauze (0.25" thick) was also used for electrodes in these reactors.

TABLE 5.2. DIMENSIONS OF REACTORS SHOWN IN FIG. 5.1b.

Reactor Test Number	Reactor Tube Diameter (cm.)	Electrode Diameter (cm.)	Electrode Gap (cm.)	Perforation Diameter (ins.)
4.	0.8	0.795	1.625	1/32, 1/16
5.	1.6	1.590	3.25	1/16, 1/8

Because of the difficulty in machining fine holes ($1/32''$, $1/64''$ diameter) through stainless steel, electrodes of this material were not tested. Although it would have been feasible to machine $1/16''$ holes through stainless steel, as experiments using aluminium electrodes had indicated that with this perforation size non-uniform discharges were inevitable, this was not tested. When the diameter of the aluminium electrodes was increased by a factor of 2 a diffuse discharge could no longer be maintained.

Applying the principle of porous electrodes with very small pores, a reactor using push-fit electrodes of compressed stainless steel gauze ($0.25''$ thickness) was tested at the optimum conditions determined previously. No significant improvements were detected and a diffuse discharge which decreased in uniformity as the electrode diameter was scaled-up, was observed.

Continuing with this design of electrode a reactor with an increased ratio of tube diameter to electrode diameter was examined. At increased electrode diameters and small inter-electrode distances this gave a uniform discharge, however because of significant by-passing this approach was discontinued.

With all the reactor (electrode) designs tested, if nitrogen gas was used in place of ammonia a much more uniform discharge was obtained, strongly suggesting that the nature of ammonia gas was a significant factor contributing to the discharge constriction.

At the time of this study similar constriction phenomena were being encountered using pulsed dc discharges(Thornton et al (1970)). These workers found that uniform discharges could be obtained using highly polished parallel, spherical, stainless steel electrodes

with a cross flow arrangement. At higher flows however the discharge was pushed onto the gas exit ports causing gas by-passing and consequently this design was not considered.

The next type of unit tested consisted of a cylindrical tube with parallel ' branched ' electrodes (see Fig. 5.2) resulting in a number of point discharges. Again however only partial uniformity which decreased with scale-up resulted. Because of this, a cross flow design which had been developed to remove the ' by-passing ' associated with the parallel flow reactor was not progressed.

Finally, a reactor which was designed to eliminate the effects of flow variation was tested. Highly polished stainless steel electrodes profiled to remove edge effects were used in this unit. The profile consisted of a flat central area to provide a uniform field guarded by a curved edge (resulting in a surface over which the electric field is lower than in the central region).

A uniform diffuse discharge was obtained over a wide range of experimental conditions of flow, pressure etc. even when the electrode diameter (of 0.794 cms.) was increased fourfold (and the inter-electrode distance increased by the same ratio). Above this diameter irrespective of operating conditions discharge contraction occurred. Increasing power input (current density) merely intensified the glow of the constricted discharge suggesting that a transition from a glow discharge to a glow-to-arc or arc type discharge was occurring. This design of reactor was used in all of the preceding experimental work and has been described in detail in 4.1.3.

FIG 5.2

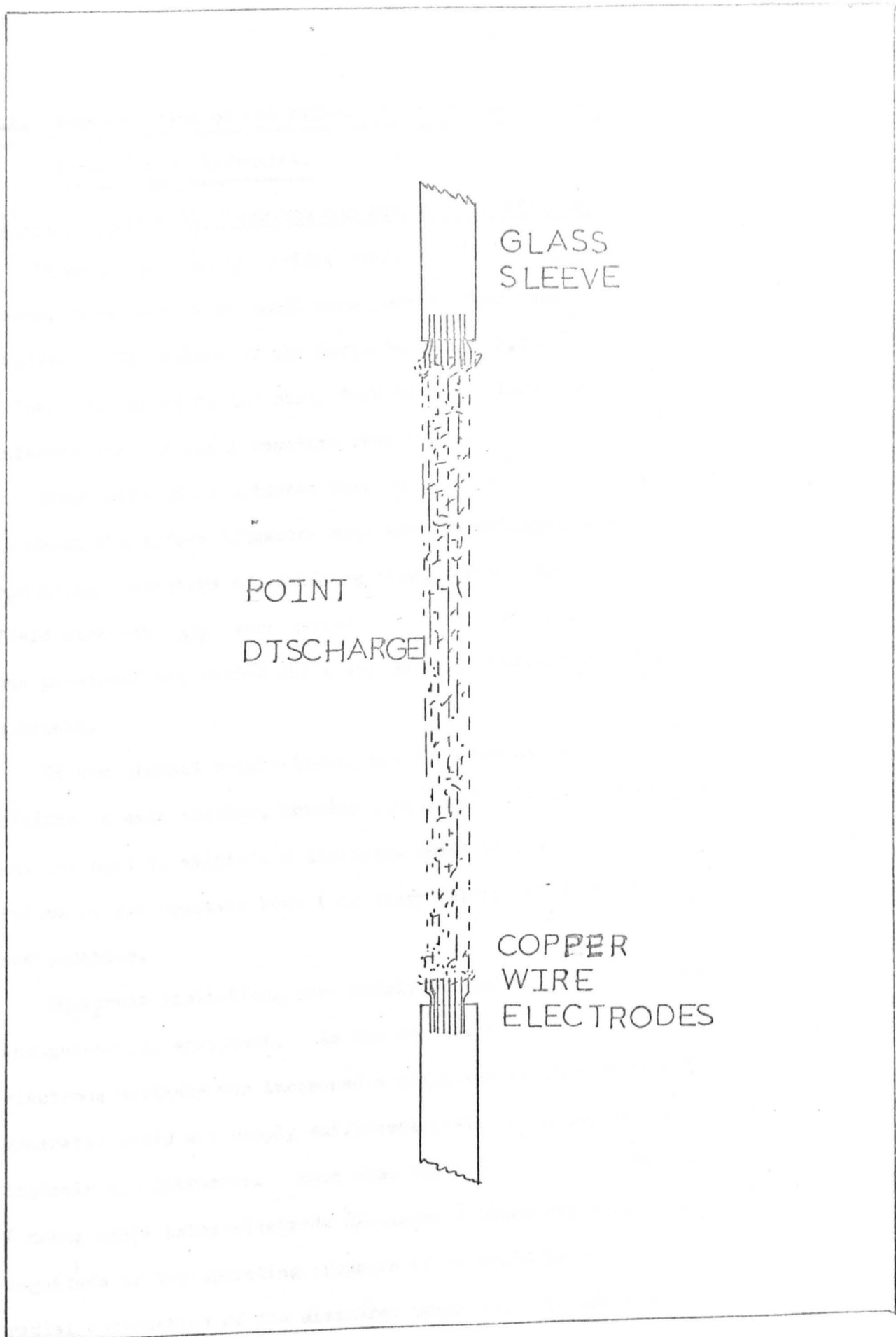


FIG 5.2

5.2. Investigation of the effect of reactor size on the nett rate of formation of hydrazine.

5.2.1. Experimental programme and operating conditions.

Three geometrically similar reactor units of different size designated large, intermediate and small were used in this part of the experimental studies. The volume of the large reactor (50.7 cm³ (i.e. reaction zone volume)), was eight and sixty four times as large as that of the intermediate and small reactors respectively.

Three sets of experiments were carried out in each reactor in which the effect of reactor size was investigated when the operating parameters of residence time, current density, and reduced field strength (E/p) were varied. In each set of experiments one parameter was varied while the other parameters were held constant.

It was planned originally to use the same range of operating conditions in each reactor, however because of equipment limitations and the need to maintain a discharge which occupied the entire volume of the reaction zone (in every experiment) this was not possible.

Equipment limitations were mainly associated with the pumping and generating equipment. As the product of pressure and inter-electrode distance was increased a point was reached where the generator could not supply sufficient power for breakdown to occur and initiate the discharge. Even when the discharge could be initiated (using small inter-electrode distances) there was a limit to the magnitude of the operating pressure which could be used above which radial contraction of the discharge occurred. In addition pumping capacity and pressure drop through the apparatus controlled the range over which flow and pressure could be varied.

As mentioned previously three sets of experiments were carried out in each reactor. The range of operating conditions used in these experiments is detailed in Table 5.3.

TABLE 5.3.

Series	Operating Parameter	Range of investigation		
		Small Reactor	Intermediate Reactor	Large Reactor
1.	Flow ($\text{cm}^3 \text{sec}^{-1}$)	0.4 - 3.4	0.7 - 5.7	1.8 - 15.2
	Pressure (mmHg)	9.5	9.5	9.5
	Current (Milliamps)	~27.5	~43.0	~103
2.	Current	17.5-68.0	23-145	87-208
	Pressure	9.5	9.5	9.5
	Flow	1.6	3.8	5.8
3.	Reduced field strength (volts $\text{cm}^{-1} \text{mmHg}^{-1}$). (positive column)	3 - 5.2	3.7-6.6	2.0-9.2
	Current	~27	~36	~145
	Flow	1.6	2.4	10.3

In the first set of experiments residence time was varied (in the context of this study residence time is defined as the ratio of the volume of the discharge reaction zone to the volumetric ammonia gas flow rate (measured at operating pressure)) by varying the flow rate of ammonia gas. The range of residence time which could be investigated using the large reactor was limited at the low end by the maximum flow rate which could be obtained at the operating pressure used. For the intermediate and small reactors the smallest obtainable residence time was governed by constriction of the discharge with

increasing flow. Increases in residence time for all the reactors was limited by the minimum flow rate which could be measured with the equipment (rotameters) used.

Each reactor was operated at the minimum power input required to sustain a diffuse discharge (occupying the entire discharge volume) over the range of flow investigated. Unfortunately however it was not possible to maintain the reduced field strength at a constant value over the entire range of conditions investigated. This was especially difficult in the experiments carried out in the large reactor where a variation in E/p of up to $\pm 6\%$ from the desired value was obtained. For the intermediate and small reactors the variation of E/p was much smaller and within the limits of experimental error.

In the second series of experiments in which current density was varied this was achieved by varying the discharge current. The range of current density investigated was limited for each reactor at the upper limit by cathode overheating (with subsequent discharge constriction and formation of an arc discharge) and at the low limit by instability and constriction of the discharge.

Originally it was believed that cathode overheating would severely restrict the range of current densities which could be investigated. As the discharge was found to stabilise within a few seconds however it was possible to limit the experimental runs to 2 - 4 minutes duration. Over this period of time only very slight cathode heating occurred this being most pronounced in the small reactor. Nevertheless even for this reactor under the most severe conditions used no fluctuation of the discharge pressure or current was observed.

In the final series of experiments the reduced electric field strength was varied by varying the pressure in the discharge reaction zone. In all of the experiments in this series a higher running voltage was required (at constant power input) with increased pressure.

The range of (E/p) investigated was limited in each reactor at the lower end by the pumping capacity at the flow rate used and at the high end by constriction of the discharge.

As will be shown later it was found that the results from these three sets of experiments were correlated by an equation which was derived using the technique of dimensional analysis.

In order to test the validity of this correlation a number of additional experimental runs were carried out in each reactor over a wide range of operating conditions.

The influence of ' packing ' (a reactor) on the nett rate of hydrazine.

In order to investigate the effect of wall reactions on the formation and degradation of hydrazine the positive columns of the large and intermediate reactors were packed with quartz wool. By weighing the wool and measuring the fibre diameter, using a travelling microscope, it was possible to determine the weight of wool (surface area) which needed to be packed into the intermediate and large reactors, so that the surface area to volume ratio (of the positive column) in these reactors, was identical to that of the unpacked small reactor.

Four experimental runs covering a range of operating conditions were carried out in both the intermediate and large reactors (packed). In the experiments using the intermediate reactor the discharge contracted into a thin pencil beam, zig-zagging its way through the packing and considerable reactant gas by-passing was observed. The discharge

in the large reactor (packed) although occupying the entire reaction zone appeared more intense (striated) in various parts of the reaction tube.

Four experimental runs were also carried out in the small reactor (packed) however as with the intermediate reactor discharge constriction occurred and considerable reactant gas by-passing was noted.

5.2.2. Presentation of Experimental results.

The most widely used parameter for the correlation of chemical discharge experimental data has been W/F the ratio of power to flow rate. This parameter was first introduced by Kobozov, Vasile'ev and Eremin in 1936 and has since been used to correlate experimental data obtained under different conditions of current, power, flow rate and reactor geometry.

Sergio in 1968 carried out an analysis similar to that presented by Deckers (1966) in which a region of an electrical discharge was considered where the electrical variables field strength, current density, and electron concentration were uniform. (This hypothesis corresponds very closely to the conditions of the positive column of a dc discharge).

An equation was developed in which the energy received by the electrons from the field was related to the energy dissipated in elastic and inelastic collisions of the electrons with the species in the discharge and on collisions with the wall.

Solution of this equation showed that the nett rate of formation of stable products in a discharge is proportional to W/F whenever the rate of formation of these products is controlled by elementary steps

involving inelastic collisions with electrons, thus giving some theoretical justification to the use of W/F .

Savage (1970) used W/F to correlate experimental data obtained from the dc glow discharge synthesis of hydrazine. Over the range of power and flow rate investigated Savage reported that a very poor correlation was obtained. Skorokhodov et al (1961) noted that the parameter W/F had always been used to correlate data obtained in constant pressure experiments. These workers preferred the more general parameter WP/F to correlate their experimental data obtained for the synthesis of hydrazine. Carbaugh (1967B) however reported that the parameter $I\tau$ (discharge current x gas residence time) gave a better correlation of experimental data than WP/F while Thornton et al (1969) and Savage (1970) preferred a combination of the parameters π/P and τ .

In 1968 Waller carried out an analysis of the discharge system in which the parameter W/FP was developed and used to correlate experimental data obtained from a methane discharge system. It is interesting to note that this parameter may be rearranged to give:

$$W/FP = E/P \times \tau \times J$$

where E/P = the ratio of the electric field strength to pressure,

τ = reactant gas residence time,

J = current density,

this is important in that the primary activation of a molecule in a discharge depends upon the energy imparted during an inelastic collision (i.e. primary activation depends upon E/P) and the frequency with which collisions occur (i.e. depends upon J, τ) and thus is a function of the dimensionless combination W/FP .

To the author's knowledge this parameter has never been used to correlate data obtained in the glow discharge synthesis of hydrazine. It is unlikely however that this parameter alone could describe the chemical processes occurring in this discharge system because of the importance of secondary processes and of the discharge surface.

Confirmation of this has in fact been obtained in the present study in which WP/F (where W is the power in the positive column) failed to correlate the experimental data satisfactorily.

It follows from above that the active surface area of the discharge must be considered in any analysis of the glow discharge synthesis of hydrazine. If the active surface area is defined as the ratio of the surface area of the positive column to the volume of the positive column, then in a glow discharge reactor of fixed geometry, the nett rate of formation of hydrazine will depend upon the variables -

Ammonia gas flow rate: F

Pressure (in the positive column): P

Ammonia gas concentration (in the positive column): C

Discharge current: I

Potential across the positive column: V_p

Length of the positive column: L

Diameter of the reaction tube: D

Inspection of these variables reveals that even if sufficient time was available to determine the effect of each individual variable on the nett rate of hydrazine formation by empirical means (i.e. the empirical method of obtaining an equation relating these variables to

the nett rate of hydrazine formation would require that the effect of each separate variable be determined in turn by systematically varying that variable while keeping all others constant) this would not be possible as all of these variables can not be varied independently.

Fortunately however, a method which is intermediate between formal mathematical development and a completely empirical study exists, which can be used in order to develop an equation relating these variables to the nett rate of hydrazine formation. This method is often referred to as dimensional analysis and is based upon the fact that, if a theoretical equation does exist among the variables affecting a physical process that equation must be dimensionally homogeneous. Because of this requirement it is possible to group many factors into a smaller number of dimensionless groups of variables which are often independent of each other even when the individual variables in the groups are interdependent.

Application of dimensional analysis to the present investigation yielded the following relationship:-

$$\left(\frac{rD^3}{FC}\right) \propto \left(\frac{WD^4}{F^3C}\right)^a \left(\frac{D^4P}{F^2C}\right)^b \left(\frac{L}{D}\right)^c \quad (5-1)$$

which has been used to correlate the experimental results obtained in this study. Derivation of this equation is outlined in Appendix 5.0.

The validity of this analysis depends solely upon whether or not all of the relevant variables which effect the nett rate of hydrazine formation in an electrical discharge were included in the dimensional analysis. The fact that this equation (as will be shown later) has been found to give a very good correlation of the experimental data is indicative that this requirement was probably satisfied.

As noted in chapter 2.0 hydrazine is formed only in the positive column of a dc discharge. Therefore it would seem logical that the experimental conditions in this part of the discharge should be used in the correlation of experimental data.

To the best of the author's knowledge, with the exception of a single study by Devins and Burton (1954), no correlation of experimental data using parameters based upon the positive column of the discharge has been reported in the literature. Without doubt this is due to the difficulties and time consuming calibration experiments associated with the measurement of conditions in the positive column of a discharge. In this respect the present investigation is no exception as the time scale for experimental work made the measurement of the operating conditions in the positive column impracticable.

Fortunately however, detailed measurements of the cathode fall of potential and the length of the cathode dark space, for a glow discharge in ammonia, have been recorded by Ouchi (1953) for a wide range of operating conditions of current and pressure. Inspection of this data has revealed that equations can be developed from which the potential difference across the positive column and the length of the positive column may be estimated for the range of experimental conditions used in the present study. The derivation of these equations is detailed in Appendix 6.0.

Essentially an equation was developed from which the cathode fall of potential (V_c) could be estimated and consequently the potential across the positive column could be determined from the relationship -

$$V_p = V - V_c - V_a \text{ (volts)}$$

where V = potential across discharge, V_c = the abnormal cathode fall of potential, V_c = the potential across the positive column, and V_a = the anode fall of potential.

Similarly a relationship was developed between the length of the cathode dark space, discharge operating pressure, and the abnormal cathode fall of potential facilitating estimation of the former. From the length of the cathode dark space the distance (dn) between the cathode and the leading edge of the positive column could be estimated and thus the length of the positive column could be determined simply by subtraction of (dn) from the inter-electrode distance.

5.2.3. Results and Discussion

The results of the experimental runs in which flowrate, discharge current, and (E/p) were varied are recorded in tables A4.1, A4.4, and A4.7 respectively for the large reactor, A4.2, A4.5 and A4.8 respectively for the intermediate reactor and A4.3, A4.6 and A4.9 respectively for the small reactor.

Substitution of these results into equation (5 - 1) shows that for each size reactor a number of experiments were carried out in which -

- 1) The parameter $\frac{(V_p I D^4)}{(F^3 C)}$ was varied at constant values of the parameters

$$\frac{(D^4 P)}{(F^3 C)} \text{ and } \frac{(L)}{(D)}$$

- 2) The parameter $\frac{(D^4 P)}{(F^3 C)}$ was varied at constant value of the parameter $\left(\frac{L}{D} \right)$

The first set of results have been used to evaluate the relationship between $\frac{(rD^3)}{(FC)}$ and $\frac{(VID^4)}{(F^3C)}$ which was found to be of the form $\frac{(rD^3)}{(FC)} \propto \frac{(VID^4)^a}{(F^3C)}$

where the mean value for the three reactors of the index

a was -0.27. Plots of $\ln \frac{(rD^3)}{(FC)}$ vs $\ln \frac{(VID^4)}{(F^3C)}$ for the large, intermediate

and small reactors are shown in Figs. 5.3, 5.4 and 5.5 respectively. The corresponding results for these plots are located in tables A4.2, A4.5 and A4.8 respectively.

The second set of results (with $\frac{rD^3}{FC}$ corrected for variation of $\frac{(VID)^4}{(F^3C)}$) were used to evaluate the relationship between $\frac{(rD^3)}{(FC)}$ and $\frac{(D^4P)}{(F^2C)}$.

This was found to be of the form $\frac{(rD^3)}{(FC)} \propto \left(\frac{D^4P}{F^2C} \right)^b$ where the mean

value for the three reactors of the index b was 0.71. Plots of $\ln \left(\frac{(rD^3)}{(FC)} \frac{(VID)^4}{(F^3C)} \right)^{0.27}$ vs $\ln \left(\frac{D^4P}{(F^2C)} \right)$ are shown in Figs. 5.6, 5.7 and 5.8 for the large, intermediate and small reactors respectively. The results for these plots are located in tables A4.1, A4.4 and A4.7 respectively.

Finally, the relationship between $\frac{(rD^3)}{(FC)}$ and $\frac{(L)}{(D)}$ (with the former corrected for variation in $\frac{(VID)^4}{(F^3C)}$ and $\frac{(D^4P)}{(F^2C)}$) was determined to be of the form $\frac{(rD^3)}{(FC)} \propto \left(\frac{L}{(D)} \right)^c$ where the mean value for the three reactors for the index c was - 0.59.

Plots of $\ln \left(\frac{(rD^3)}{(FC)} \frac{(VID)^4}{(F^3C)} \left(\frac{D^4P}{(F^2C)} \right)^{-0.71} \right)$ vs $\ln \left(\frac{L}{(D)} \right)$ are shown for the large, intermediate and small reactors in Figs. 5.9, 5.10 and 5.11 respectively. The results for these plots are located in tables A4.3, A4.6 and A4.9 respectively.

All of the experimental results (tables A4.1 - A4.12) were substituted in the equation -

$$\frac{(rD^3)}{(FC)} \propto \frac{(VID)^4}{(F^3C)} \left(\frac{D^4P}{(F^2C)} \right)^{0.71} \left(\frac{L}{(D)} \right)^{-0.59} \quad (5 - 2)$$

Figs. 5.12, 5.13 and 5.14 show plots of $\ln \left(\frac{(rD^3)}{(FC)} \right)$ vs $\ln \left(\frac{(VID)^4}{(F^3C)} \right)^{-0.27}$

$\left(\frac{D^4P}{(F^2C)} \right)^{0.71} \left(\frac{L}{(D)} \right)^{-0.59}$ for the large, intermediate and small reactors respectively.

Regression analysis of these plots showed that within the limits of experimental error equation (5-2) correlates the results obtained in the three reactors of different size and varying in volume by a factor of up to 64.1. The correlation coefficients obtained for these three plots were 0.99, 0.97, 0.98, for Figs. 5.12, 5.13, and 5.14. respectively.

All of the experimental results (tables A4.1 - A4.12) are plotted in the form of the equation (5-2) in Fig. 5.15. Inspection of this plot confirms that equation (5-2) correlates the experimental data within the limits of experimental error. A correlation coefficient of 0.98 was obtained for this plot.

As mentioned previously a number of additional experiments were carried out in each reactor in order to test the validity of equation (5-2). The results of these experiments are located in tables A4.10, A4.11 and A.4.12 for the large intermediate and small reactors respectively. All of these results are plotted in the form of equation (5-2) in Fig. 5.16. Inspection of Fig. 5.16 confirms that within the limits of experimental error equation (5-2) correlates experimental data obtained from the glow discharge in ammonia gas.

Effect of reactor size.

From equation (5-2) it may be deduced that $r \propto D^{-0.65}$ indicating that as reaction tube diameter (size) is increased the nett rate of formation of hydrazine is decreased. This is not in agreement with the findings of Devins and Burton (1954). It is not correct however to compare directly the findings of these two studies as Devins and Burton reported only the initial rate of formation,

and not the nett rate of formation of hydrazine as is reported in the present study. In chapter 2.0 it was noted that hydrazine was decomposed in an electrical discharge and consequently the initial rate of formation of hydrazine may not always vary in the same manner as the nett rate of formation of hydrazine with changes in operating conditions. Unfortunately it is not possible to determine the nett rate of formation of hydrazine from Devins and Burton's data so that a correct comparison can be made.

Effect of packing reactors.

The results of the experimental runs in which the large and intermediate reactors were packed with quartz wool are recorded in Table A4.13 and in Figs. 5.17 and 5.18. Inspection of these results reveals that -

- 1) the nett rate of formation of hydrazine in the large packed reactor was significantly less than in the unpacked large reactor.
- 2) The nett rate of formation of hydrazine in the intermediate reactor was significantly less than in the unpacked intermediate reactor.

In Table A4.13 and Fig. 5.19 the results of the experiments in which the small reactor was packed are recorded. As with the large and intermediate reactors the nett rate of formation of hydrazine was significantly decreased as a result of packing the reactor.

The decrease in the nett rate of formation of hydrazine as a result of packing the intermediate and small reactors may be attributed to the large amount of by-passing which occurred in these reactors because of discharge constriction. In the large reactor however no constriction was observed (although striations was apparent) and consequently the nett rate of formation of hydrazine

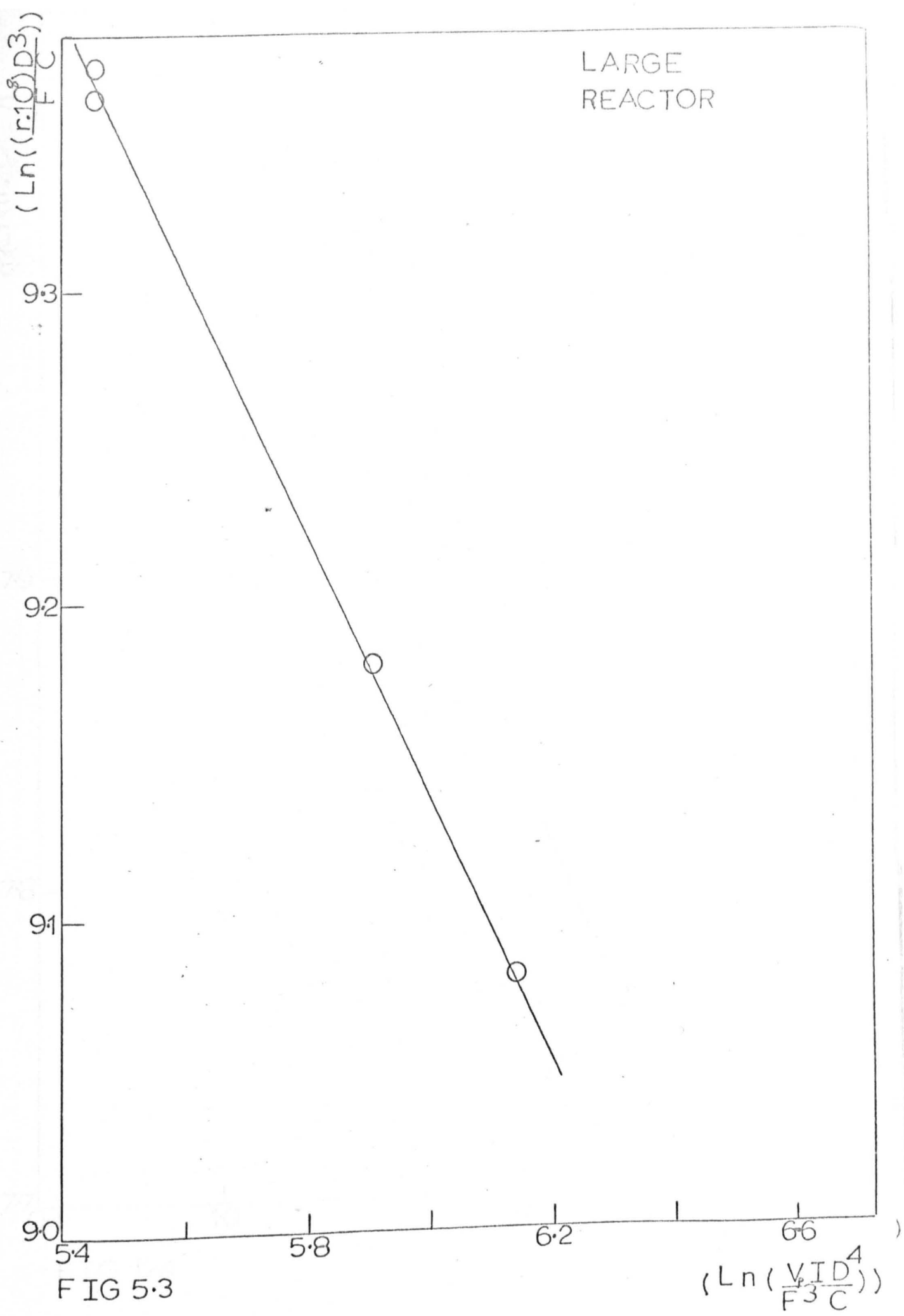


FIG 5.3

$$\left(\ln\left(\frac{V D^4}{F^3 C}\right)\right)$$

INTERMEDIATE REACTOR

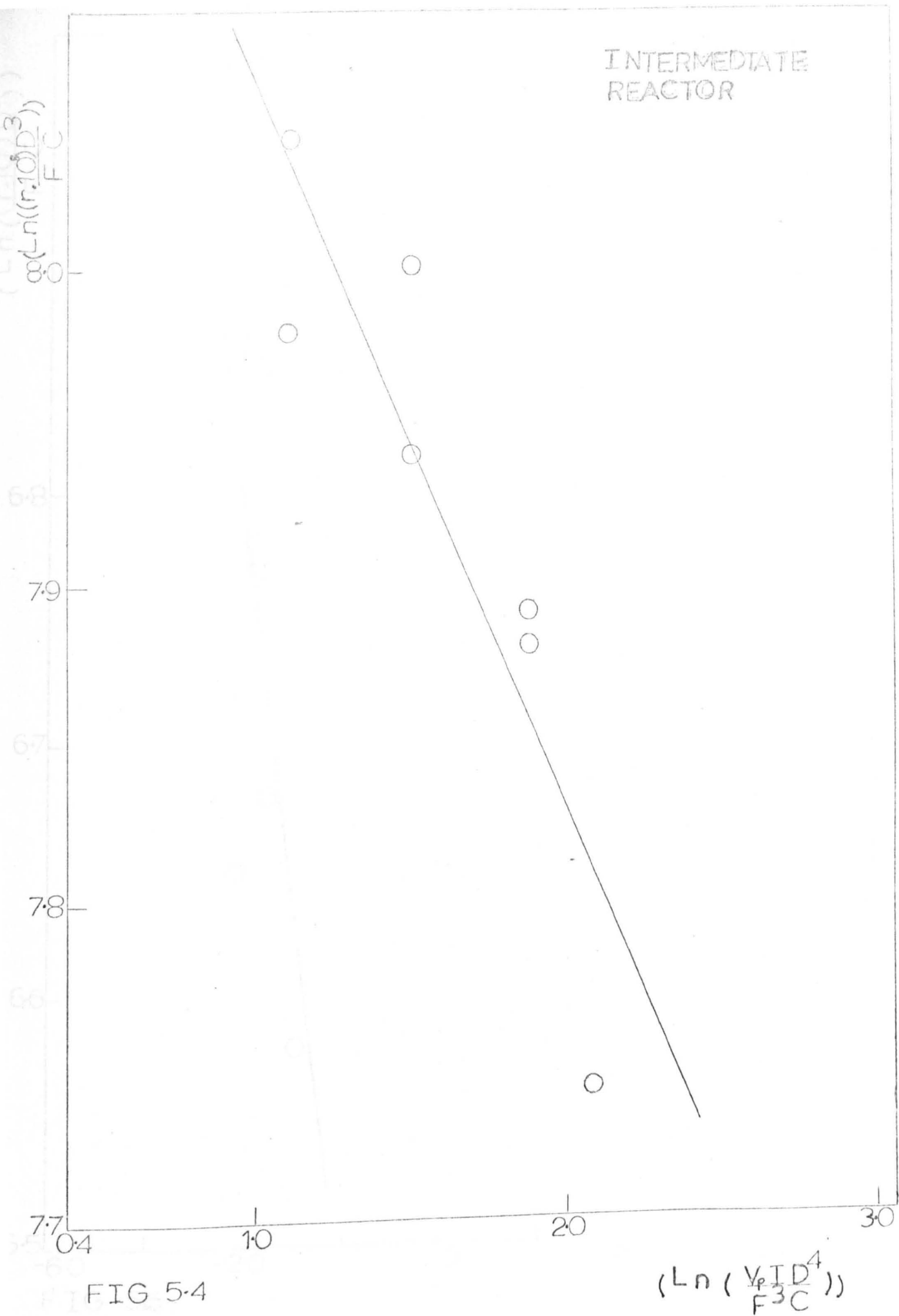


FIG 5-4

$$\ln \left(\frac{V_p I D^4}{F^3 C} \right)$$

SMALL
REACTOR

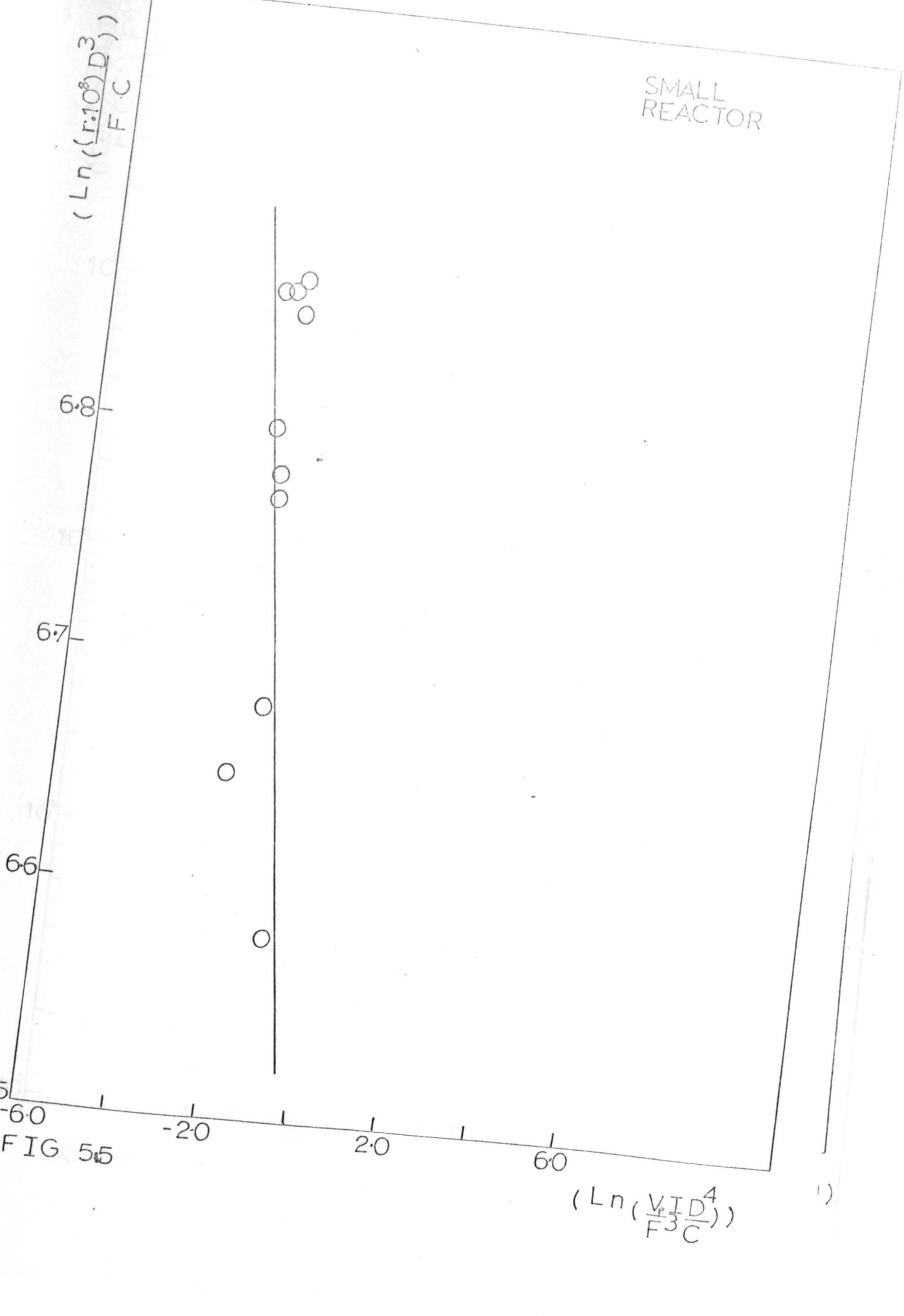


FIG 55

1)

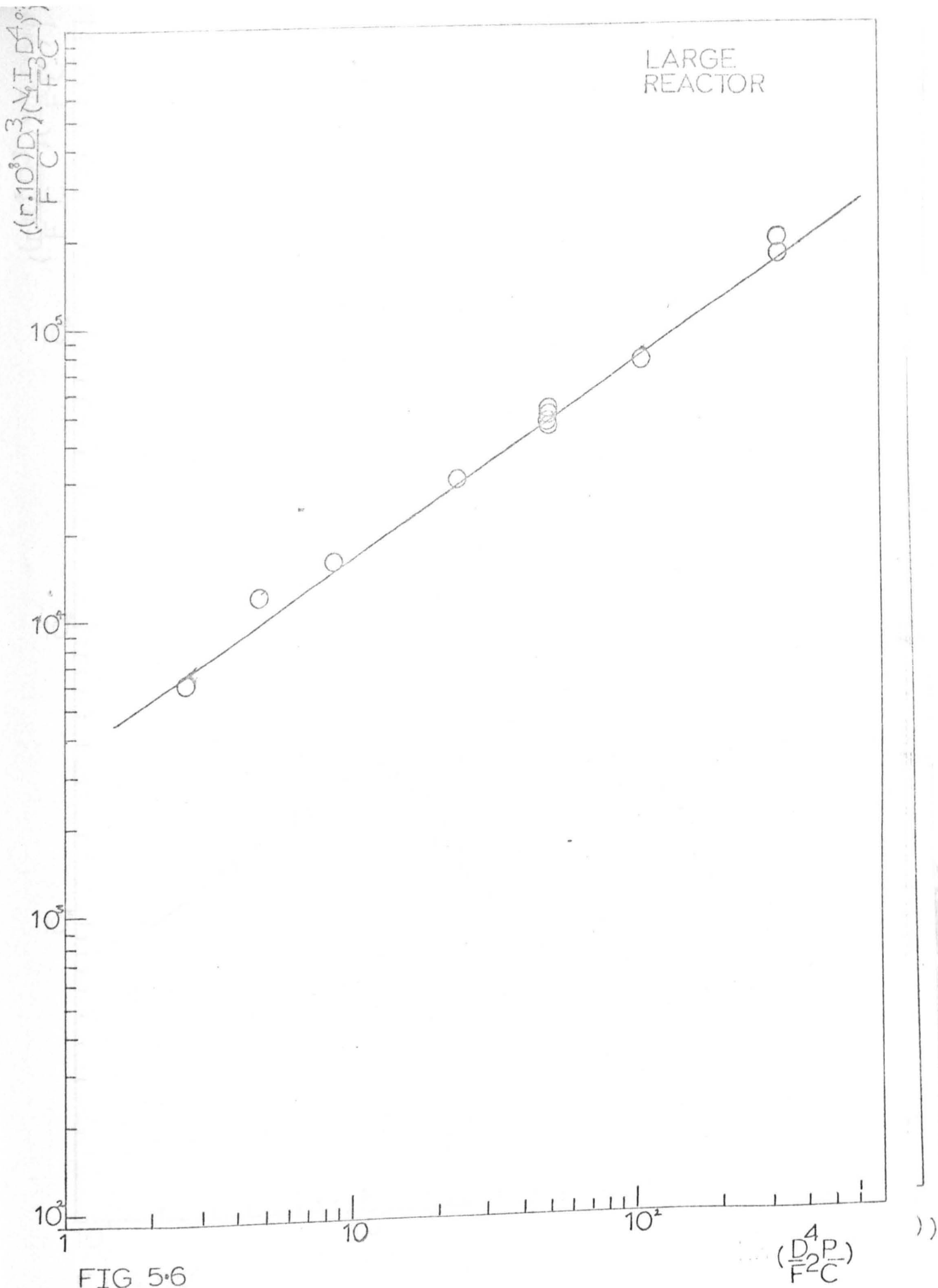


FIG 5.6

$\left(\frac{D^4 P}{F^2 C}\right)$

INTERMEDIATE
REACTOR

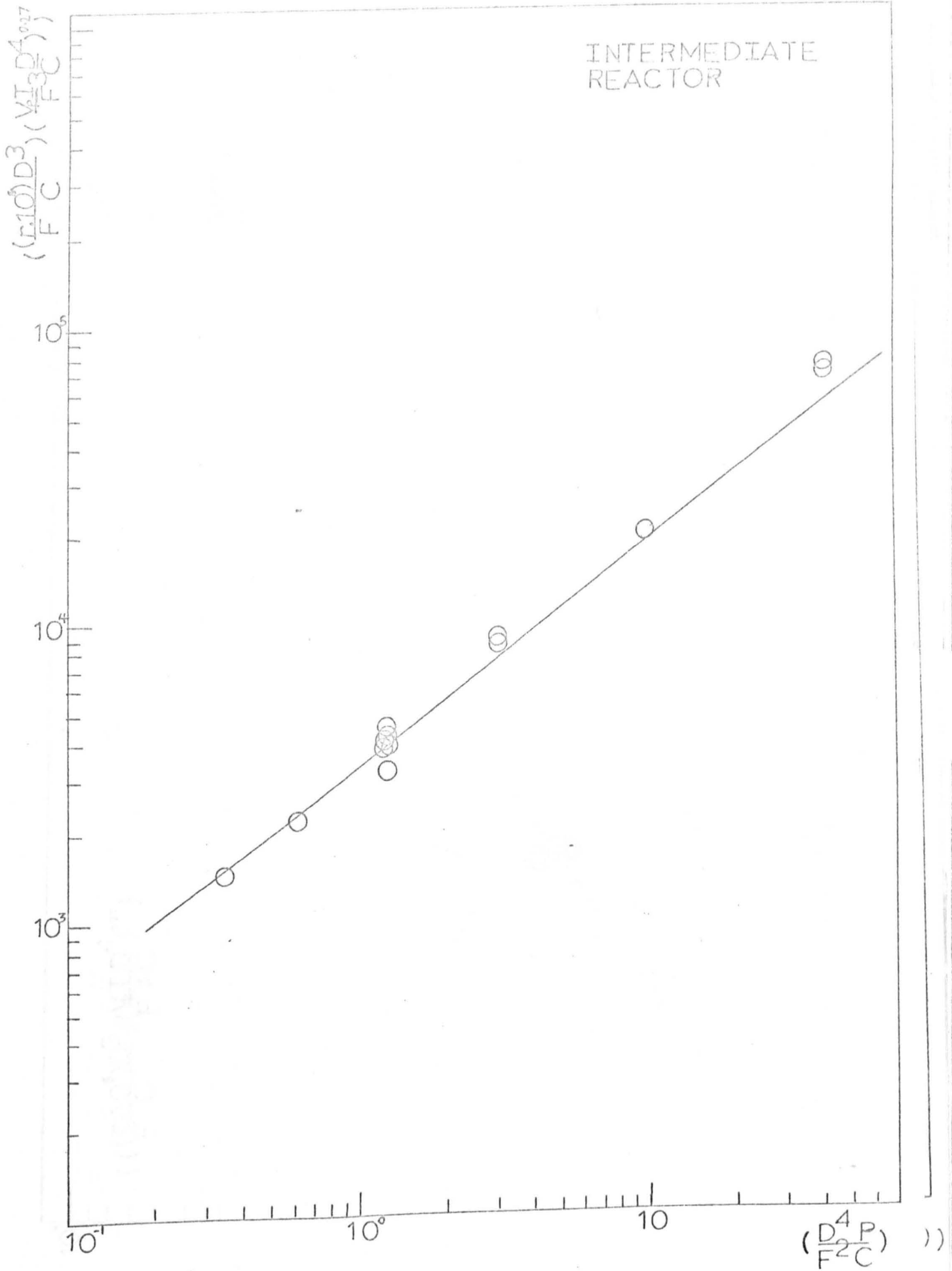


FIG 57

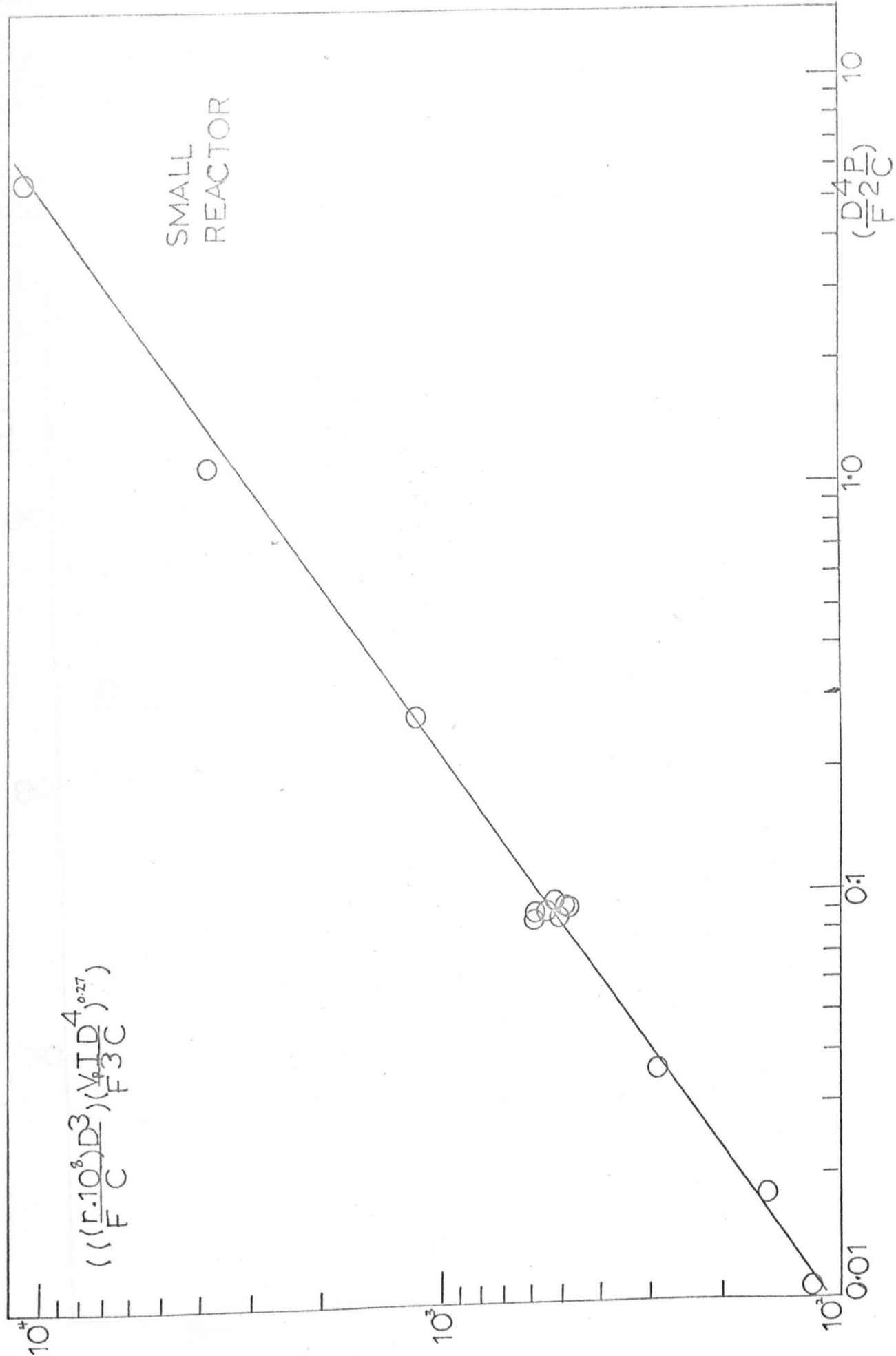


FIG 5.8

LARGE REACTOR

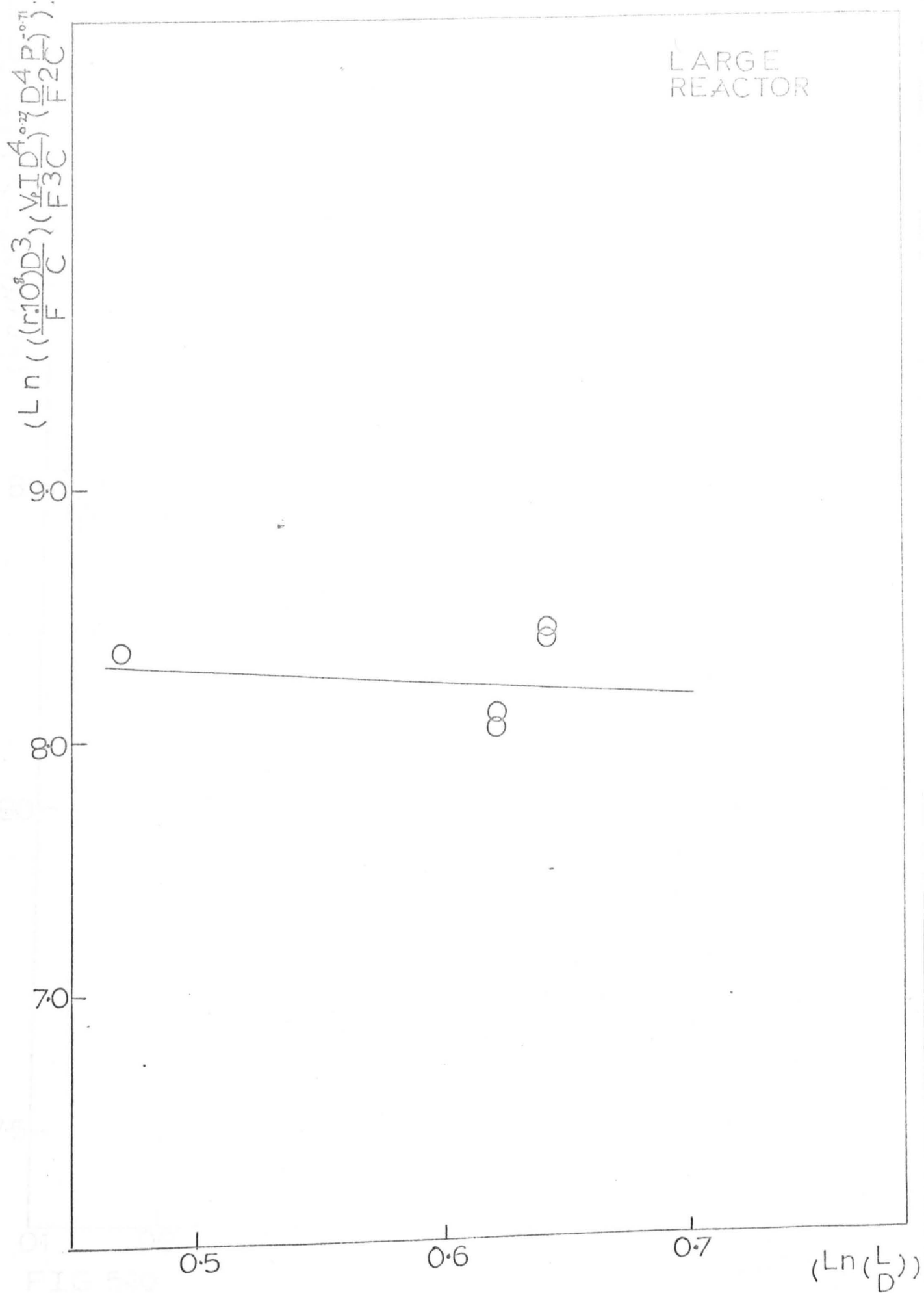


FIG 5.9

INTERMEDIATE
REACTOR

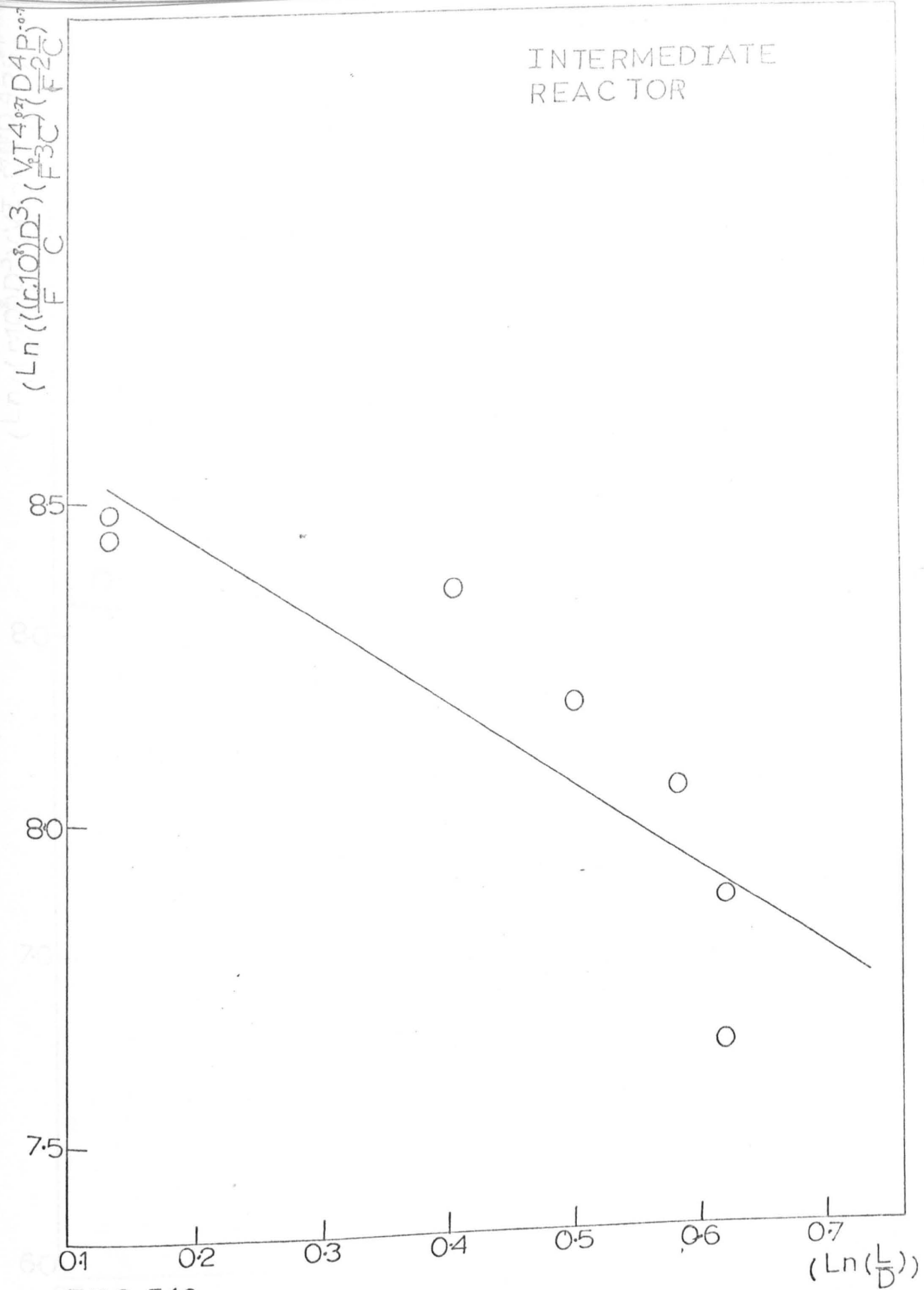


FIG 5.10

SMALL
REACTOR

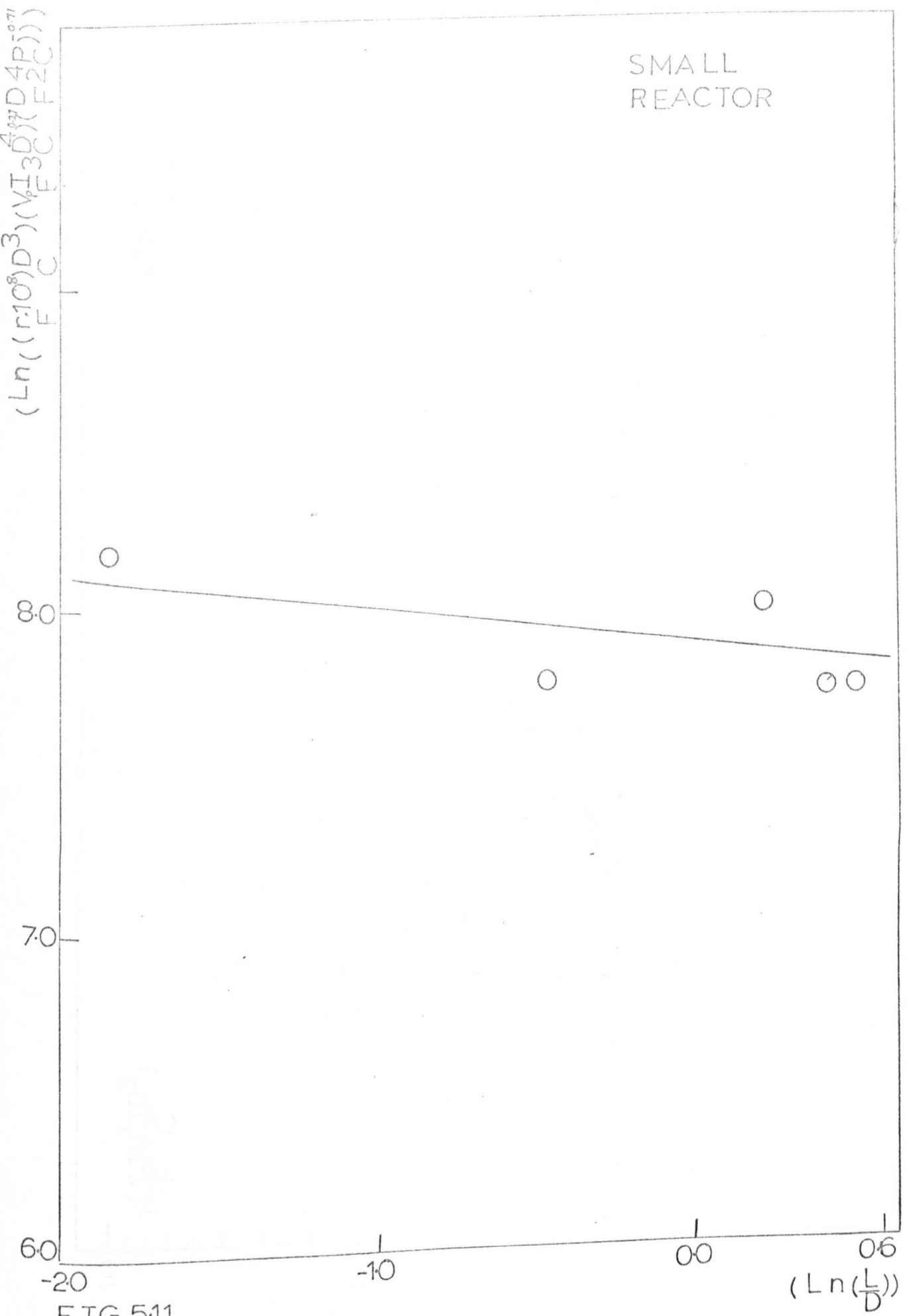


FIG 5.11

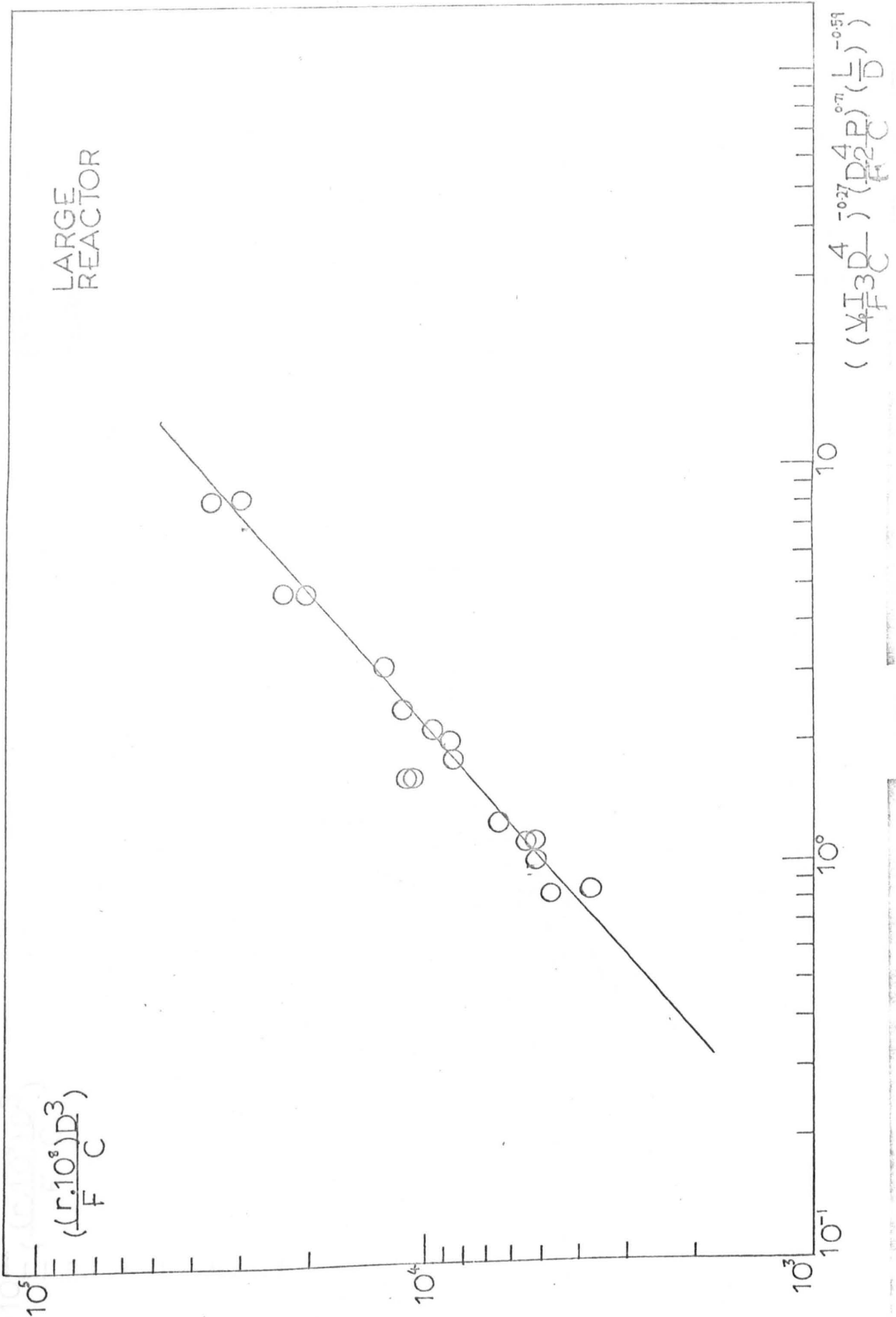


FIG 5.12

FIG 5.13

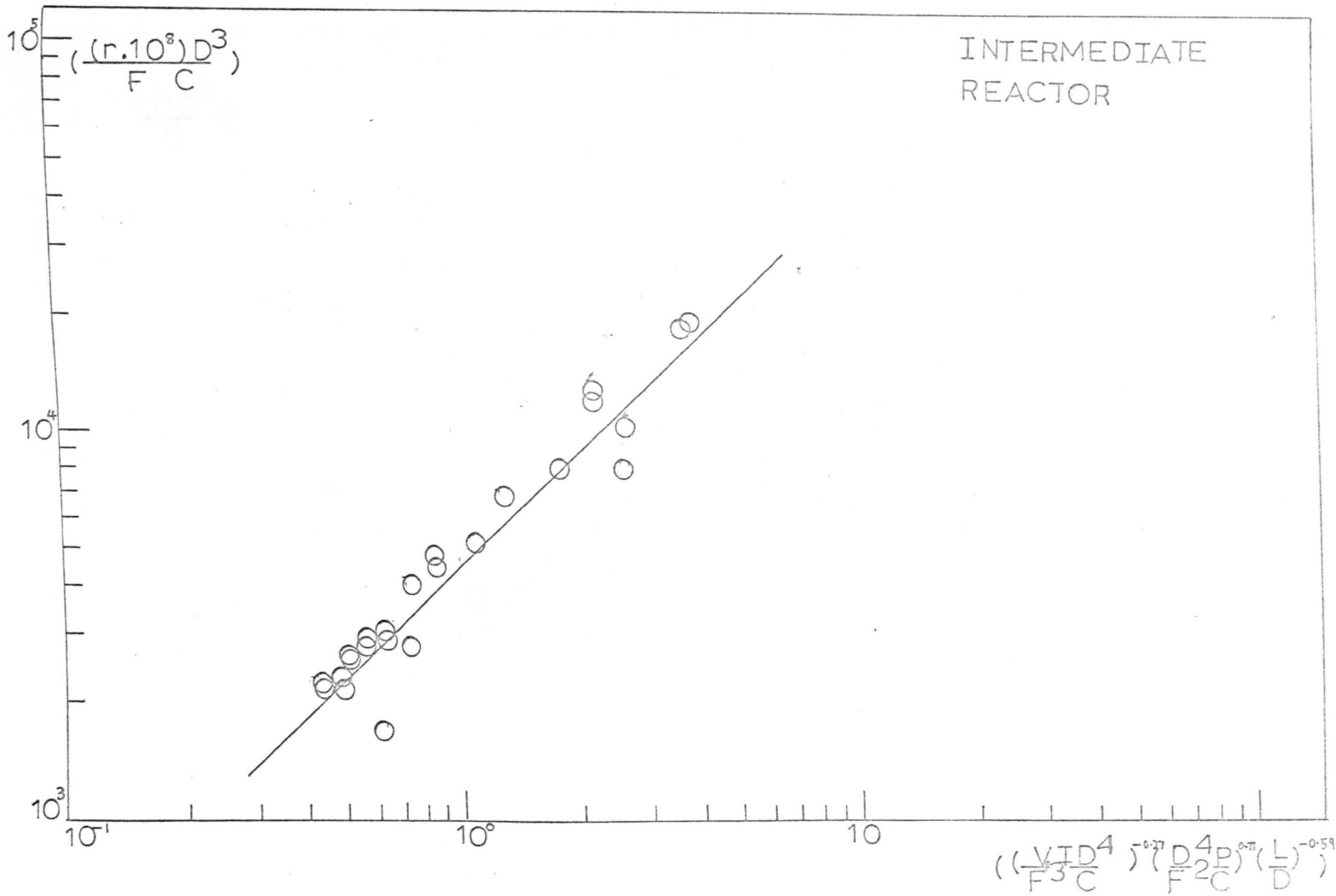
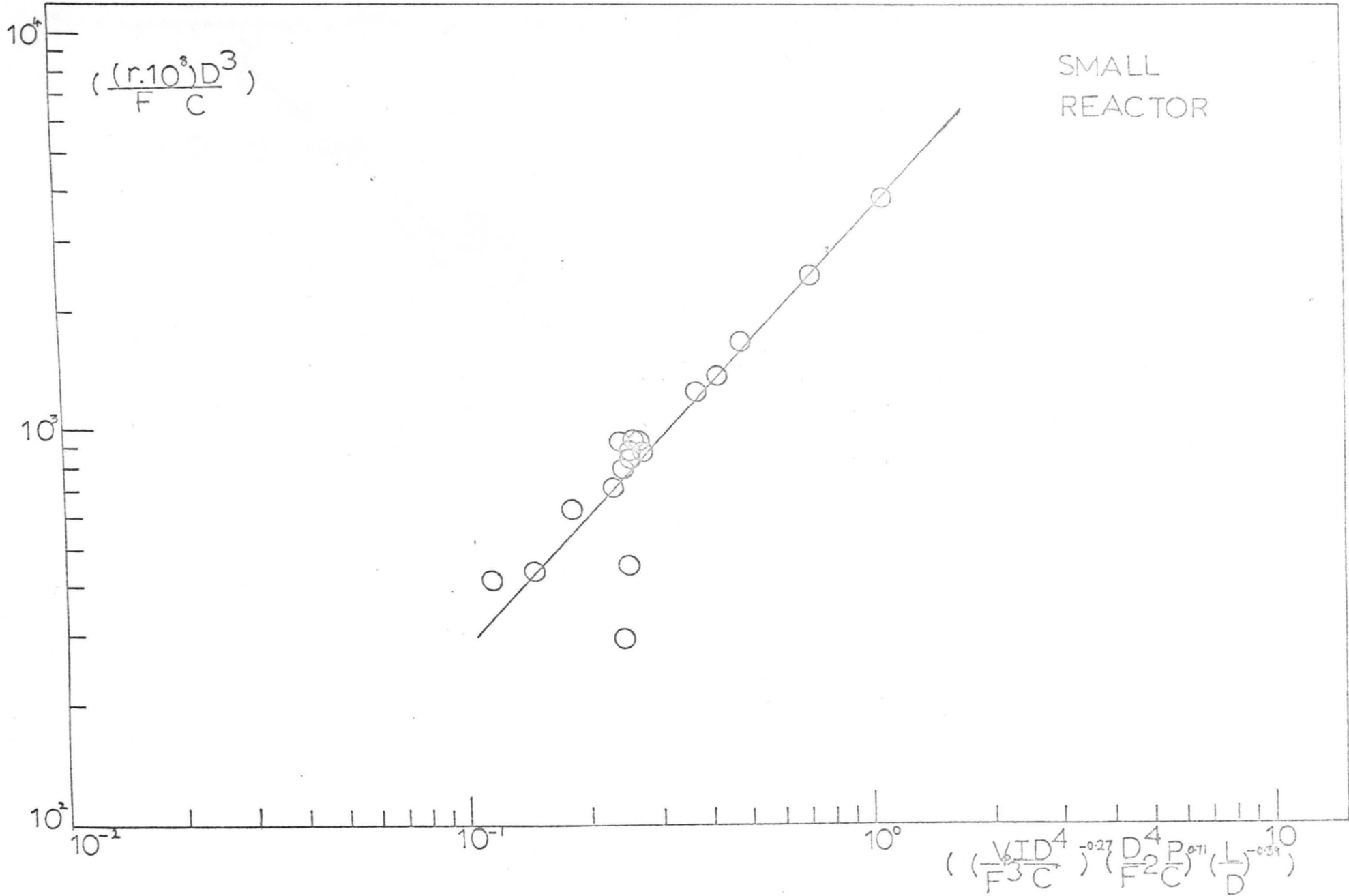


FIG 5.14



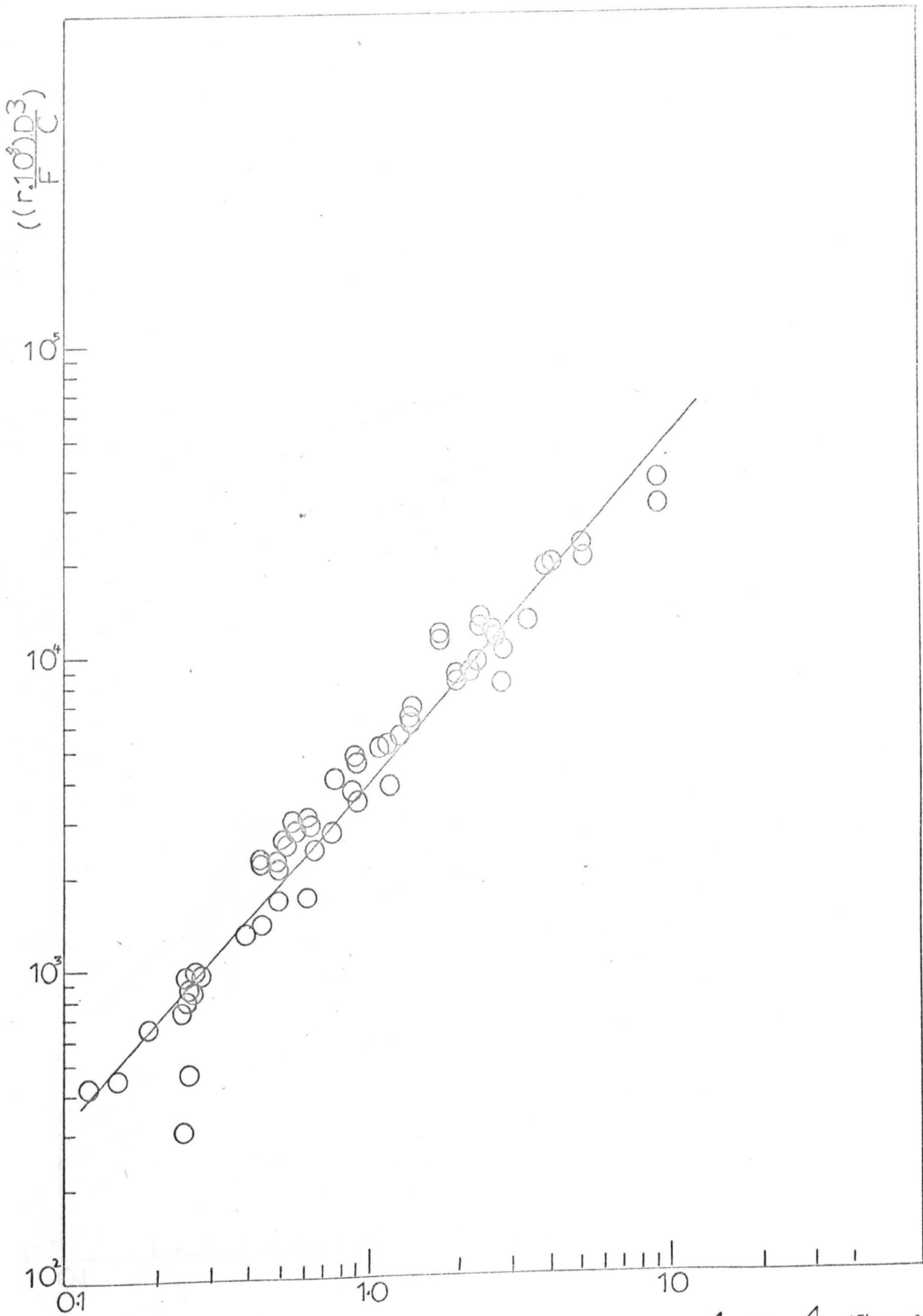


FIG 5.15

$$\left(\left(\frac{V_p ID^4}{F^3 C} \right)^{-0.27} \left(\frac{D^4 P}{F^2 C} \right)^{0.71} \left(\frac{L}{D} \right)^{-0.59} \right)$$

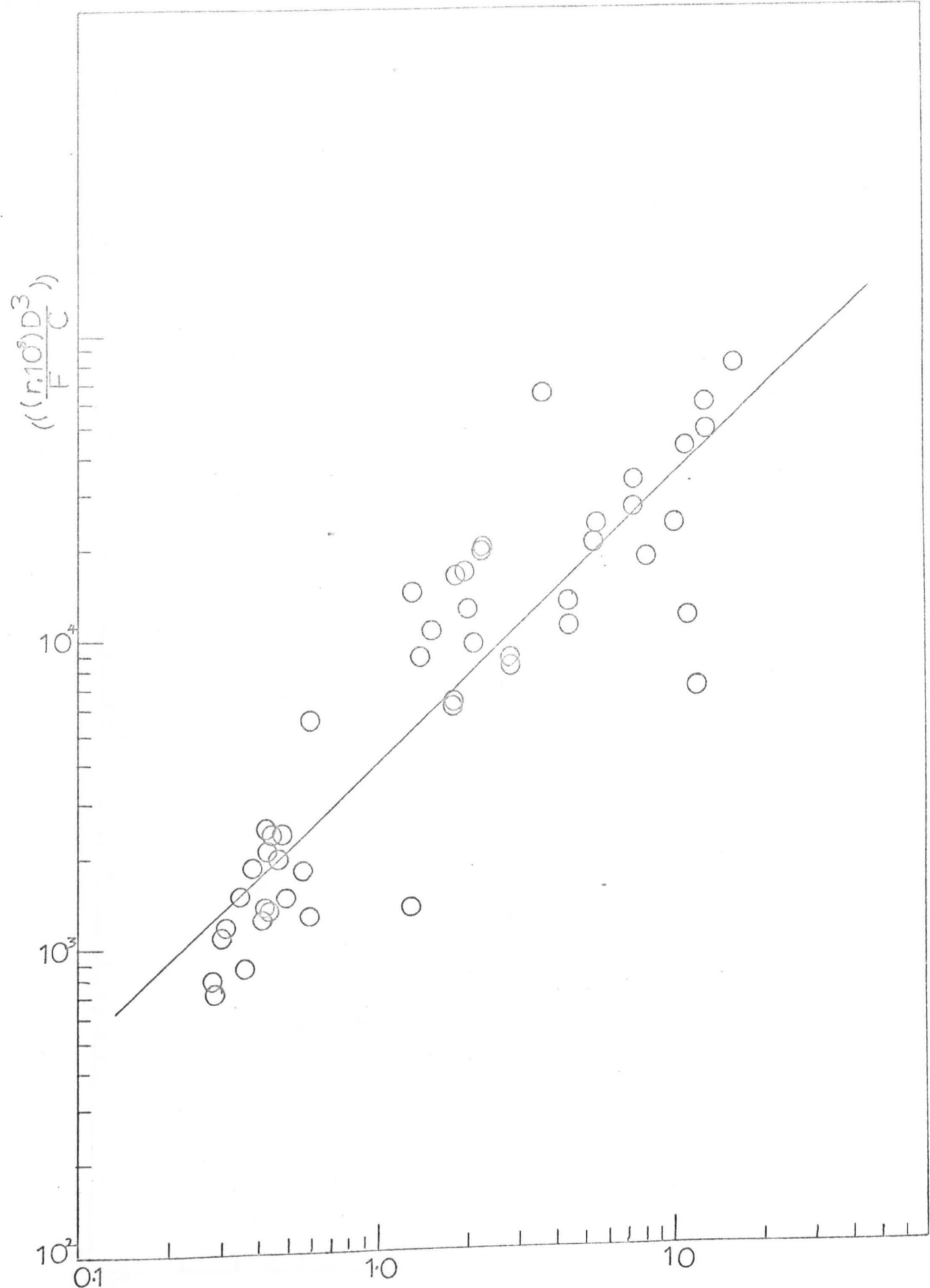


FIG 546

$$((\frac{V_p ID^4}{F^3 C})^{-0.27} (\frac{D^4 P}{F^2 C})^{0.71} (\frac{L}{D})^{-0.59})$$

LARGE
REACTOR

$(\frac{L \cdot 10^3}{F C})$

10^5

10^4

10^3

10^2

10^{-1}

10^0

10

LEGEND

PACKED ○

UNPACKED —

○

—

FIG 5.17

$$\left(\left(\frac{V I D^4}{F^3 C} \right)^{0.71} \left(\frac{D^4 P}{F^2 C} \right)^{0.71} \left(\frac{L}{D} \right)^{-0.59} \right)$$

INTERMEDIATE
REACTOR

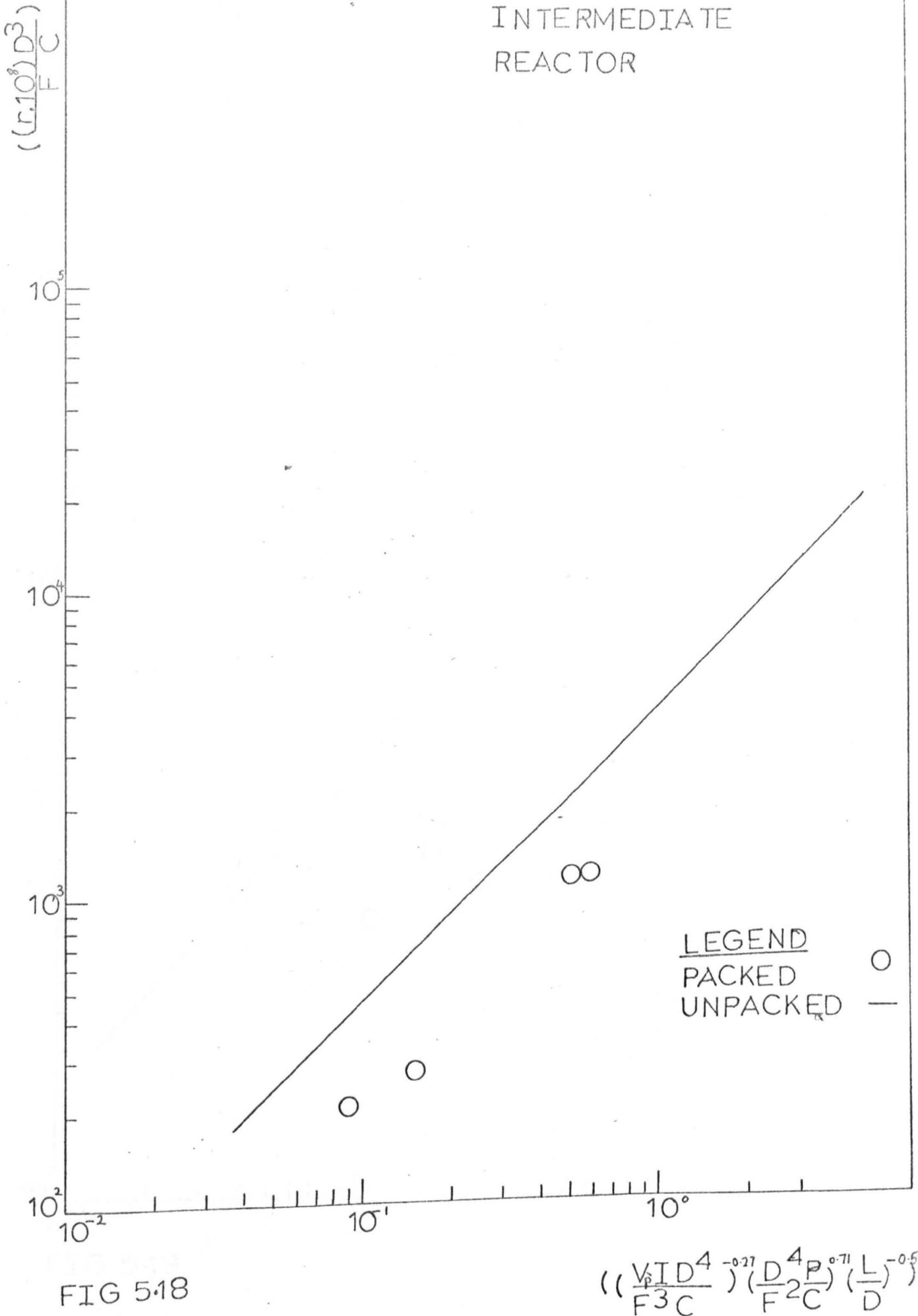


FIG 518

$$\left(\left(\frac{V_p I D^4}{F^3 C}\right)^{0.27} \left(\frac{D^4 P}{F^2 C}\right)^{0.71} \left(\frac{L}{D}\right)^{-0.59}\right)$$

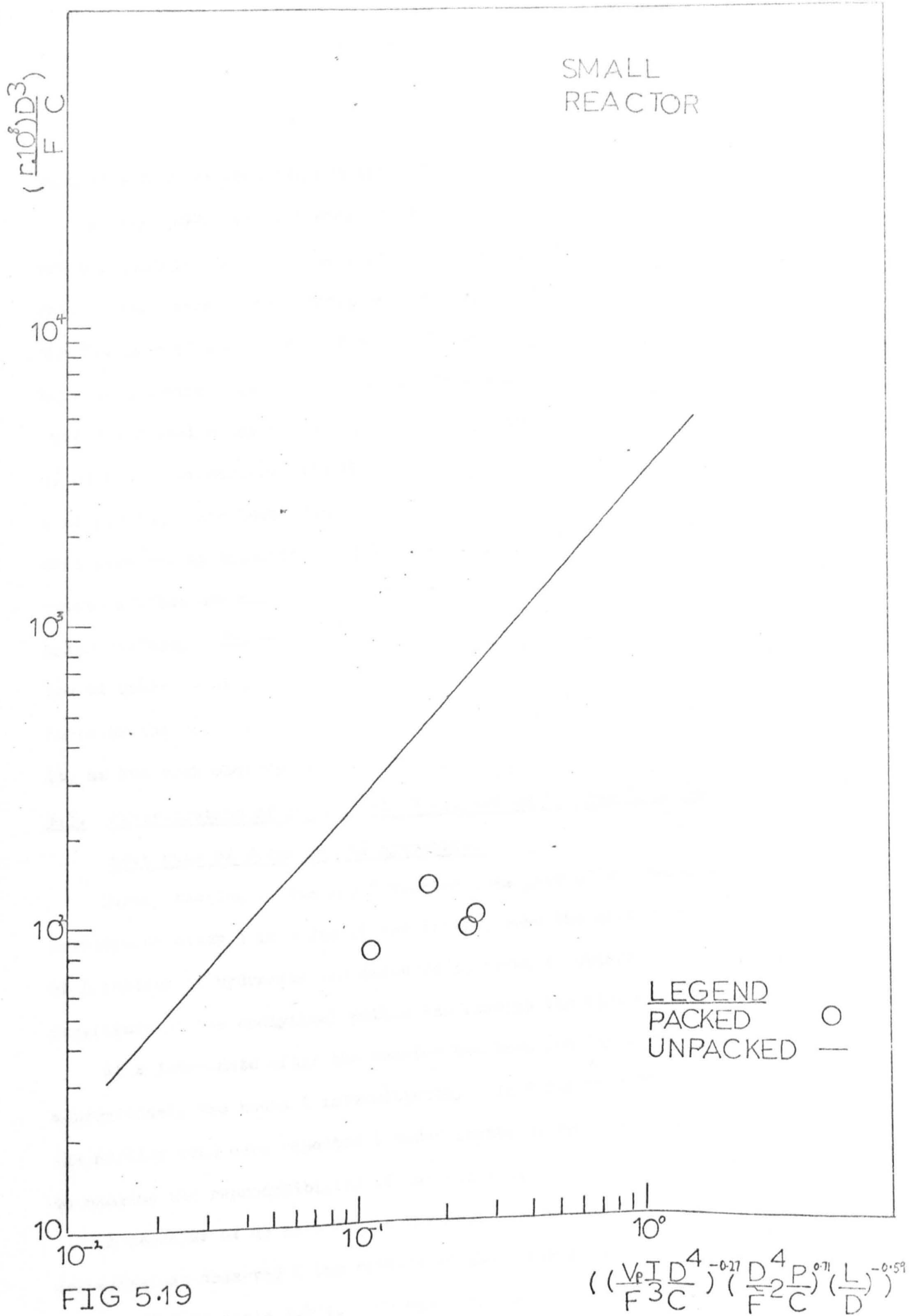


FIG 5.19

must have been reduced for another reason.

Savage (1970) using a similar reactor to the large size reactor employed in this study, observed an increase in the nett rate of formation of hydrazine, on packing, in direct opposition to the findings of the present study. The only significant difference between the experiments of Savage and of the present investigation is that glass wool packing was employed in the former study. Variation of catalytic properties with the nature of the discharge surface (or packing) has been observed by a number of workers, and most recently by Brown and Howarth (1970) who found that a quartz surface was more favourable to hydrazine synthesis than a pyrex surface. The results of these workers suggest that the use of quartz wool packing in comparison to glass wool packing, should increase the nett rate of formation of hydrazine and not decrease it, as has been observed in this study.

5.3. Investigation of the effect of Reactor Unit ' age ' on the nett rate of formation of hydrazine.

During testing of the small reactor (as part of the reactor development study) in a few of the initial runs the nett rate of formation of hydrazine was measured in order to obtain experience of the analytical method and examine its limitations.

At a later date after the reactor had been run for a period of approximately two hours (intermittently) to ' run in ' the electrodes the earlier runs were repeated (under identical operating conditions) to examine the reproducibility of the results.

A decrease of up to $\sim 48\%$ in the nett rate of formation of hydrazine was observed (the results of these two sets of experiments are recorded in table 5.4). On operation of the discharge for a

further ninety minutes it was found that the nett rate of formation of hydrazine remained constant (within the limits of experimental error), indicating that the reactor and electrodes were in a ' steady state ' condition.

In view of these results both the large and intermediate reactors were ' run in ' for a period of approximately three hours until a ' steady state ' condition was achieved, before commencing the experimental study outlined in chapter 5.2. As with the small reactor a decrease in the nett rate of formation of hydrazine with increasing reactor age was observed for both these reactors. On completion of the work detailed in chapter 5.2 a short experimental programme was carried out to investigate the ' ageing ' phenomenon previously described.

As identical operating conditions were used for the two sets of experiments recorded in table 5.4, the most probable explanation for the ageing effect observed was that the reactor unit surface influenced the nett rate of formation of hydrazine in some way, and the degree of this influence varied with reactor age.

As noted in chapter 2.3 Westhaver (1933) reported that with freshly machined electrodes the cathode fall of potential is significantly less than with aged electrodes. Thus for fixed conditions of inter-electrode distance and operating pressure a reduction in the cathode fall of potential should give rise to either a decrease in the inter-electrode voltage or an increase in the potential difference across the positive column (i.e. if the inter-electrode voltage remained constant).

Examination of the results in Table 5.4 shows that the inter-electrode voltage is independent of whether freshly machined or aged

electrodes are used suggesting -

- 1) the cathode fall of potential is independent of electrode age or
- 2) the cathode fall of potential is increased when aged electrodes are used, however the potential difference across the positive column is decreased by a corresponding amount, with the result that the inter-electrode voltage remains constant.

If the first of these alternatives is correct then it would appear that the reaction tube surface and not the electrode surface is responsible for the ageing effects noted (it is unlikely that the electrode surface could have a catalytic influence on the nett rate of formation of hydrazine as the electrodes are relatively distant from the positive column).

If the second alternative is correct, then the nett rate of formation of hydrazine would be expected to increase with increasing electrode age (i.e. as the potential difference across the positive column decreased, then E/p and consequently the mean electron energy should decrease. As will be shown later, over the range of conditions investigated, a decrease in the mean electron energy leads to an increase in the nett rate of formation of hydrazine due to decreased destruction of hydrazine (or its precursor) by both electron and atomic hydrogen attack).

In fact a decrease in the nett rate of formation of hydrazine with increasing reactor age was observed (see Table 5.4) suggesting that electrode age does not influence the nett rate of formation of hydrazine. In order to confirm this an identical reactor (designated the 'new' intermediate reactor) to the intermediate reactor (which will now be referred to as the 'aged' intermediate reactor) was constructed and a series of experiments was carried out.

(using identical operating conditions) in which freshly machined and aged electrodes were used in both these reactors. Results of this work are located in table 5.5.

In both reactors the use of freshly machined electrodes resulted in an increase in the nett rate of formation of hydrazine, (by approximately 4.9% and 4.1% in the new and aged reactors respectively) however the increase was within the limits of experimental error, indicating that electrode age does not significantly effect the nett rate of formation of hydrazine. In agreement with the experimental findings for the small reactor, (reported in table 5.4) no difference in current - voltage characteristics were observed in either of the intermediate reactors, suggesting that reactor age does not influence inter-electrode voltage.

The most significant thing about the results reported in table 5.5. however, is that the nett rate of formation of hydrazine is approximately 51% larger in the aged reactor than in the new reactor, in direct contrast to the results obtained in the small reactor (table. 5.4.).

In view of this a further series of experiments were carried out using the new intermediate reactor (with freshly machined electrodes) operated under identical conditions to the previous series of experiments reported in table 5.5. Fifty four runs of one minute duration were carried out in which the nett rate of formation of hydrazine was measured during every fifth run. A further seventy ' one minute ' experiments were carried out with the nett rate of formation of hydrazine measured for every tenth run. The results of these experiments are located in table 5.6 and Fig. 5.20 which illustrates how the nett rate of formation of hydrazine varies with the reactor age.

Inspection of Fig. 5.20 reveals that the nett rate of formation of hydrazine increases with increasing reactor age. This again is in direct contrast to the trend observed in the experiments using the small reactor. Examination of the results in table 5.5 and 5.6 shows that even after more than two hours operation the nett rate of formation of hydrazine in the new intermediate reactor was less than in the aged intermediate reactor (although the difference between the rates in the two reactors was within the limits of experimental error).



FIG 5.20

INTERMEDIATE
REACTOR(NEW)

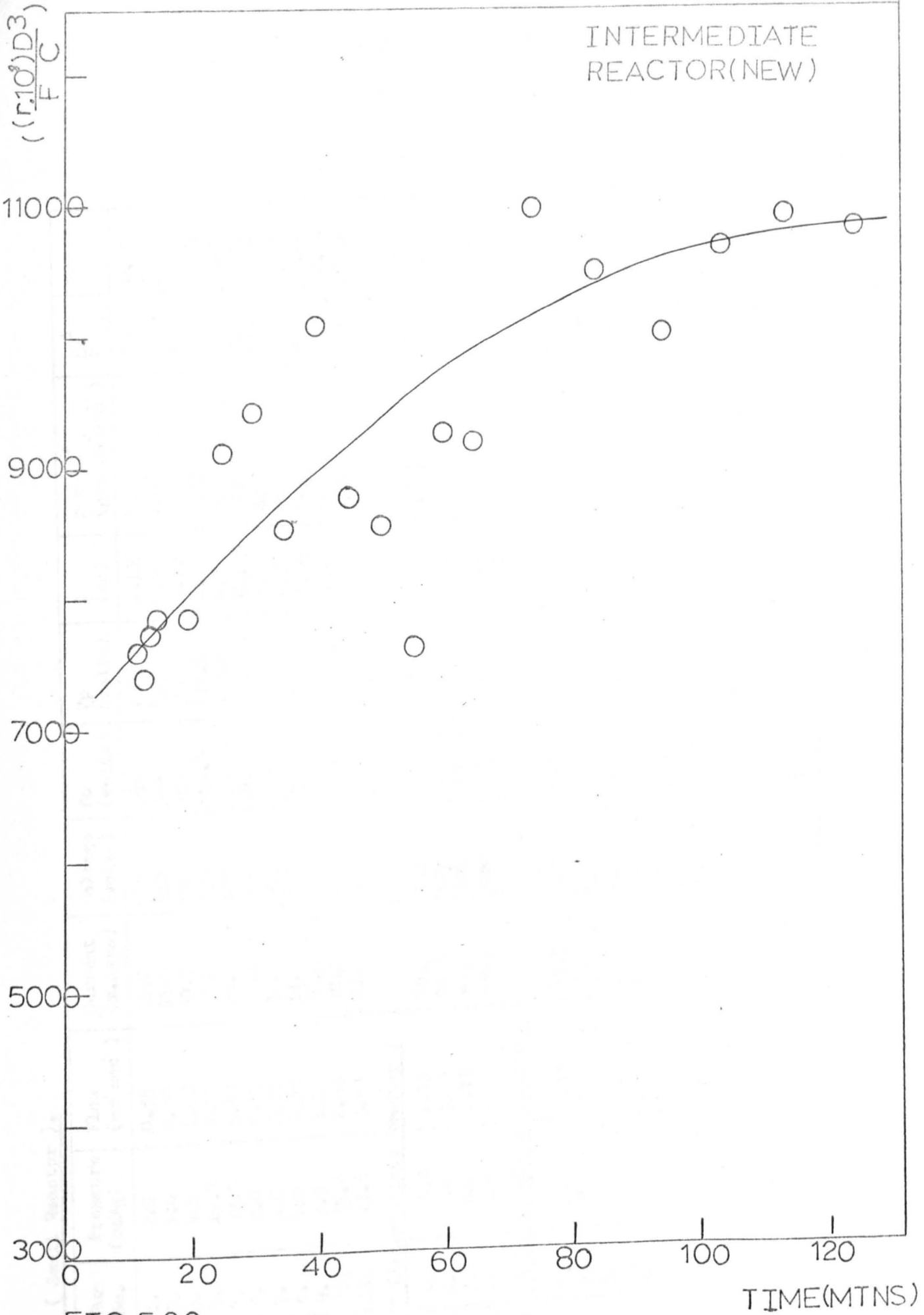


FIG 5.20

TIME(MTNS)

TABLE 5.4. (Small Reactor).

Reactor Age	Run No.	Pressure (mmHg)	Flow (cm ³ sec ⁻¹)	Current (m.amps)	Voltage (volts)	Vc (volts)	Vp (volts)	L (cm)	r x 10 ² (gms cm ⁻² sec ⁻¹)	rD ³ /FC	Z
New	1.	2.0	0.35	26.0	680	668	1.0	0.125	654	596	0.35
	2.	5.0	0.88	31.5	560	544	5.0	0.50	1165	1700	0.48
	3.	9.5	1.68	30.0	590	489	90.0	0.98	797	1203	0.24
	4.	15.0	2.65	30.0	590	464.5	114.5	1.2	1030	1204	0.25
	5.	19.5	3.41	29.0	610	457	142.0	1.3	992	983	0.26
Aged	6.	2.0	0.35	31.5	560	548	1.0	0.125	341	311	0.33
	7.	5.0	0.88	31.5	560	544	5.0	0.5	820	1197	0.48
	8.	5.0	0.88	31.5	560	544	5.0	0.5	894	1305	0.48
	9.	9.5	1.68	30.0	540	489	90.0	0.98	565	854	0.24
	10.	15.0	2.68	30.0	610	464.5	134.0	1.2	617	721	0.24
	11.	19.5	3.41	29.0	610	457	142.0	1.3	686	680	0.26

TABLE 5.5* (Intermediate Reactor)

Aged (NE)	1.	9.0	1.13	49.5	615	467	137	2.55	45.4	11383	2.12
	(AE) 2.	9.0	1.13	44.5	620	467	142	2.55	43.6	10932	2.11
New (NE)	3.	9.0	1.13	49.5	620	467	142	2.55	30.2	7572	2.11
	(AE) 4.	9.0	1.13	49.5	620	467	142	2.55	28.8	7221	2.11

TABLE 5.6. (Intermediate Reactor)

Time ** (mins)											
1.	9.0	1.13	49.5	620	467	142	2.55	30.28	7592	2.11	
2.	"	"	"	"	"	"	"	29.54	7407	"	
3.	"	"	"	"	"	"	"	31.00	7773	"	
4.	"	"	"	"	"	"	"	31.38	7868	"	
5.	"	"	"	"	"	"	"	"	"	"	
6.	"	"	"	"	"	"	"	36.38	9122	"	
7.	"	"	"	"	"	"	"	37.64	9438	"	
8.	"	"	"	"	"	"	"	33.96	8515	"	
9.	"	"	"	"	"	"	"	40.24	10090	"	
10.	"	"	"	"	"	"	"	34.92	8756	"	
11.	"	"	"	"	"	"	"	33.96	8515	"	
12.	"	"	"	"	"	"	"	30.28	7592	"	

TABLE 5.6. (continued).

Reactor Age	Run No.	Pressure (mmHg)	Flow (cm ³ sec ⁻¹)	Current (m.amps)	Voltage (volts)	Vc (volts)	Vp (volts)	L (cm)	r x 10 ⁸ (gms cm ⁻³ sec ⁻¹)	$\frac{rD^3}{FC}$	Z
	13.	9.0	1.13	49.5	620	467	14.2	2.55	336.92	9257	2.11
	14.	"	"	"	"	"	"	"	336.60	9177	"
	15.	"	"	"	"	"	"	"	43.56	10922	"
	16.	"	"	"	"	"	"	"	41.70	10456	"
	17.	"	"	"	"	"	"	"	39.86	9994	"
	18.	"	"	"	"	"	"	"	42.40	10631	"
	19.	"	"	"	"	"	"	"	43.34	10867	"
	20.	"	"	"	"	"	"	"	42.94	10767	"
	21.	"	"	"	"	"	"	"	42.74	10717	"

* Each result is an arithmetic mean average of three results.

** The discharge had been operated for ten minutes prior to these experiments.

r= Nett rate of formation of hydrazine in positive column.

$$Z = \frac{(V_p I D^4)^{-0.27} (D^4 P)^{0.71} (L)^{-0.51}}{(F^3 C) (F^2 C) (D)}$$

NE= New electrodes.

AE= Aged electrodes.

CHAPTER 6.0.

6.0. Interpretation of Results.

6.1. Discharge Constriction

In the present study it has been shown that there is a limit to the diameter of electrodes which may be employed in a dc discharge reactor, above which discharge constriction occurs. This critical size of electrode is dependent upon a number of different factors, the principal ones being:-

- a) The nature of the gaseous reactant.
- b) Reactor unit geometry.
- c) Electrode profile and material of construction.
- d) Flow pattern of the gaseous reactant (which is dependent upon (b)).
- e) Electrical and operating conditions, of which the most important are electrical current density, operating pressure and gas flow rate.

Constriction phenomena are complex and as yet very poorly understood. Although it is beyond the scope of this investigation to examine such phenomena in detail, a few general observations seem pertinent.

Considering factors (a) to (d) as fixed for a particular reactor unit and reactant gas then operating pressure, electrical current density, and gas flow rate become the independent variables upon which the maximum diameter of electrodes which can be used (without discharge constriction) depend.

The effect of higher pressures will be to hinder the diffusion of electrons and ions that tend to spread the discharge radially thus it might be expected that constriction effects should set in at higher pressures, for gases which have larger ambipolar diffusion coefficients as is observed for helium relative to other rare gases (Massey (1965)).

High current densities on the other hand contribute to the narrowing of the conducting channel in a much more complicated fashion. A summary of some possible reasons given by Phelps(1967) is as follows :-

1) Thermal gradients which result from the flow of heat from the centre of the arc to the wall result in a reduced gas density and higher E/p at the centre of the arc. If the rate coefficient for ionisation increases sufficiently rapidly with E/p then the higher ionisation rate more than compensates for the faster diffusion.

2) Cumulative ionisation. Cumulative ionisation refers to the ionisation of excited atoms or molecules which have been produced by electron impact. Because this process is proportional to the square of current density, this will lead to higher rates of ionisation in the regions of higher current density and tends to contract the discharge.

3) Electron-ion recombination. Some authors (Kenty (1962)) have proposed that the recombination of electrons and ions at large radii leads to constriction of the discharge.

4) Electron - electron interaction. Since collisions among electrons tend to make electron energy distribution functions more Maxwellian and to increase the excitation and ionisation rate coefficient. The ionisation rate near the centre of a discharge will be higher and will tend to constrict the discharge, (Golubovskii (1966)).

The effect of high gas flow rates is to distort the electric field and consequently bring about channelling of the discharge zone.

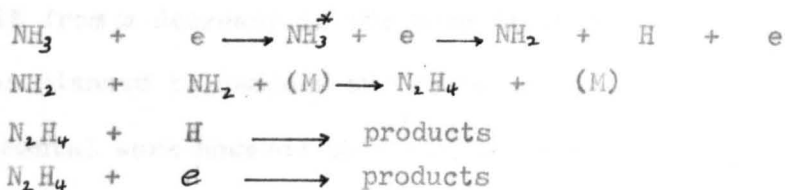
Inspection of equation (1) shows

According to Maier (1934) this effect becomes significant when the gas velocity is comparable to the drift velocity of the ions, i.e. in the range of 40 - 100m per sec. It is usually found that under these conditions the gradient in the positive column becomes non-uniform along its length, and less than the normal value in still gasses, and also shortening of the positive column occurs. Similar effects have also been observed in the case of radio frequency discharges (Romig (1960)). In the present study flow rates exceeding approximately 8m per sec. brought about discharge constriction.

It follows from what has been said that most laboratory size discharge reactors will not be amenable to treatment by conventional scale-up criteria because of discharge constriction. Thus until sufficient knowledge is acquired to prevent constriction during the operation of large scale reactors, it will be necessary to develop novel reactors in which the limitation of constriction is overcome. One possible way in which this might be achieved would be by employing a reactor where a means for moving the discharge relative to the gas stream is provided. In this way scanning of the entire reactor cross-section will result and by-passing of the reactant gas should be minimised (Haji (1972) Thornton (1972)).

6.2. Effect of reaction tube size upon the nett rate of formation of hydrazine.

In chapter 2.3 the following reaction mechanism was put forward:



Inspection of equation (5.2) reveals that the nett rate of

formation of hydrazine decreases as reaction tube diameter is increased.

This may be explained by either -

6.2.1) a decrease in the rate of formation of hydrazine, and/or

6.2.2) an increase in the rate of destruction of hydrazine or its precursor.

6.2.1. Decrease in the rate of formation of hydrazine.

As hydrazine is formed primarily by the combination of two amino radicals, a decrease in the rate of formation of hydrazine must in practice result from a decrease in the concentration of amino radicals available for hydrazine formation. Such a situation could arise from either:-

6.2.1. 1) a decrease in the rate of formation of amino radicals or

6.2.1. 2) an increase in the rate of reaction of amino radicals to form products other than hydrazine.

6.2.2. Increase in the rate of destruction of hydrazine.

As noted in chapter 2.3 an increase in the rate of destruction of hydrazine or its precursor may occur in two ways which are:-

6.2.2. 1) an increase in the rate of electron destruction, and

6.2.2. 2) an increase in the rate of atomic hydrogen destruction.

Each of these alternatives will now be considered to determine which if any are in agreement with the experimental results obtained.

6.2.1. 1. Decrease in the rate of formation of amino radicals.

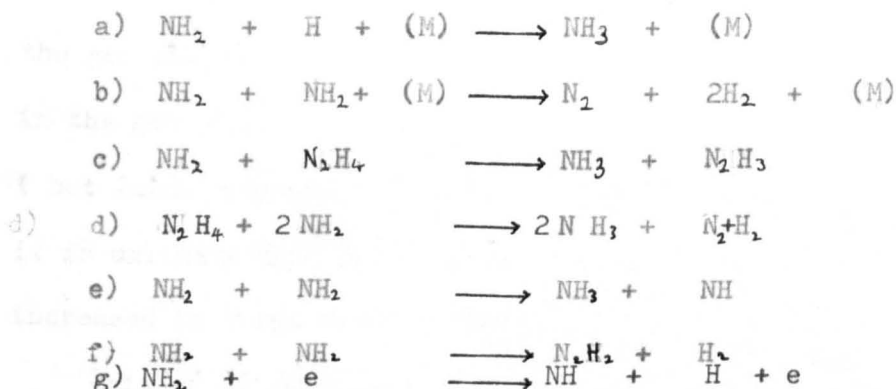
Amino radicals are formed primarily in the decomposition of ammonia and therefore a decrease in the rate of formation of amino radicals must result from a decrease in the rate of decomposition of ammonia.

It was planned to measure the decomposition of ammonia in all of the experimental work however this aim was not achieved as the chromatographic equipment was not functional. Thus it was not possible to measure whether or not the rate of ammonia decomposition

was a function of reaction tube size. From a theoretical point of view however it may be concluded that the rate of ammonia decomposition is independent of reactor size and is primarily a function of the energy of the electrons in the discharge. It follows therefore that a decrease in the nett rate of formation of hydrazine with increasing reactor size is not due to a decrease in the rate of formation of amino radicals.

6.2.1. 2. Reaction of amino radicals to form products other than hydrazine.

A number of reactions of amino radicals to form products other than hydrazine have been suggested. The most important of these are listed below.



An increase in reaction tube diameter should lead to a decrease in the rate of diffusion of amino radicals to the reaction tube surface and conversely to an increase in the concentration of amino radicals in the gas phase. Both reactions (a) and (b) have been shown to occur on the reaction tube surface ((a) Wiig (1937), (b) Swarcz (1949)) and therefore the rate of these reactions should decrease with increasing reaction tube diameter.

If the rate of reactions (c) and (d) increased with increasing reactor size this would account for the experimental results observed in this investigation. It is unlikely however that these

reactions are of any significance in comparison to the reaction of hydrazine with atomic hydrogen atoms.

Since amino radicals and hydrogen atoms are produced at the same rate (from the decomposition of ammonia) and amino radicals can disappear more readily (react more readily) the amino radical steady state concentration should be much smaller than the hydrogen atom steady state concentration. The reaction of hydrazine with amino radicals should therefore be negligible, compared to the reaction of hydrazine with hydrogen atoms.

Increasing the reaction tube diameter will decrease the rate of diffusion of both amino radicals and hydrogen atoms to the tube surface and therefore increase the concentration of both in the gas phase. As atomic hydrogen recombination does not occur in the gas phase over the range of pressure used in this study (but amino radicals can react to form hydrazine and other products) it is unlikely that amino radical destruction of hydrazine will be increased in large size reactors.

Neither of reactions (e) or (f) are known to occur on the surface of the reaction tube and therefore it is feasible that the rate of these reactions would increase as reaction tube size is increased. A considerable amount of evidence has been put forward in chapter 2.3 (for example Haines and Bair (1963)) however suggesting that the most important reaction of amino radicals is in the formation of hydrazine and also that this reaction takes place in the gas phase (Anderson et al (1959) Skorohodov (1961)) and not on the reaction tube surface as suggested by Rathsack (1961). Increasing reaction

tube diameter should lead to an increase in the concentration of amino radicals in the gas phase and in turn an increase in the primary reaction of amino radicals to form hydrazine. Thus it is unlikely that reactions (e) or (f) (or in fact reactions (a) to (g)) are of any significance compared to the reaction of amino radicals to form hydrazine and it is equally unlikely that these reactions become important as reaction tube size is increased.

It will be shown in 6.1.2.1. that the destruction of amino radicals (and thus hydrazine) with electrons (reaction (g)) is not significant in comparison to atomic hydrogen destruction of hydrazine. Even if this were not so however the rate of electron decomposition of amino radicals is governed primarily by the energy of the electrons in the discharge. Thus changing the reaction tube diameter should not change the primary conditions which lead to amino radical destruction by this route. Increasing the reaction tube diameter however will lead to a decrease in the rate of diffusion of electrons to the reaction tube surface and therefore to an increase in the concentration of electrons in the discharge reaction zone. As electrons diffuse to the discharge surface much faster than do atomic hydrogen atoms, however it is unlikely that the increase in electron concentration in the gas phase would be significant, compared to the increase in atomic hydrogen atom concentration, in large size reactors.

To summarise it would seem that the experimental results may not be explained by an increase in the rate of reaction of amino radicals to form products other than hydrazine or in more general terms to a decrease in the rate of formation of hydrazine. On the contrary it would appear that increasing reaction tube size should lead to an increase

in the concentration of amino radicals in the gas phase and as a result to an increase in the formation of hydrazine.

As this is not in agreement with the experimental results observed it follows that the rate of destruction of hydrazine must be increased in larger size reactors to such an extent that the nett rate of formation of hydrazine is decreased.

6.2.2.1. Destruction of hydrazine by electron collision.

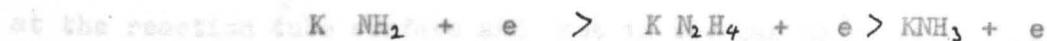
It is relevant at this stage to examine the significance of electron destruction of hydrazine over the range of conditions used in this study.

In chapter (2.3) it was reported that Savage (1970) using a mathematical model of the discharge in ammonia compared the relative importance of hydrazine destruction by electron attack and atomic hydrogen attack. Savage showed that although electron induced decomposition of hydrazine was relatively significant the primary mode of destruction was by atomic hydrogen attack of hydrazine.

The range of reaction conditions i.e. reduced field strength (electron energy) used in Savage's work is very similar to the reaction conditions used in the present study (compare reduced field strength values of ~ 12 volts $\text{cm}^{-1} \text{mmHg}^{-1}$ (Savage) with 10 volts $\text{cm}^{-1} \text{mmHg}^{-1}$ used in the present study) and consequently it may be assumed that Savage's findings are applicable to the present study.

Further evidence of this may be obtained from the work of Barker (1970). Barker reported that in addition to electron induced decomposition of hydrazine, at higher electron densities another electron-induced decomposition reaction comes into play, namely the reaction between electrons and amino radicals - (i.e. reaction (g) in 6.2.1.2.).

This will not only remove amino radicals necessary for hydrazine formation but also produce more hydrogen atoms which will engage in hydrazine degradation reactions. Barker has found that electrons react more efficiently with amino radicals than they do with hydrazine. By assuming a Maxwellian distribution of electron energies and taking the bond dissociation energies as $D(\text{NH}-\text{H}) = 3.8$ e.v. (Altshuller (1954)) $D(\text{H}_2\text{N}-\text{NH}-\text{H}) = 3.3$ e.v. (Foner (1958)) and $D(\text{NH}_2-\text{H}) = 4.5$ e.v. (Altshuller (1954)) he showed that the rate constants for the electron-induced decomposition reaction were in the order -



when Barker's work showed that for a power input of 2.5 to 10 watts the major mechanism of hydrazine destruction is atomic hydrogen attack, but that at 50 watts and above electron-induced decomposition of amino radicals and hydrazine predominates.

The volume of the discharge zone used in Barker's experiments was approximately 3.0 cm^3 (in some of the experiments at higher power and flow the discharge extended outside the volume of the discharge tube cavity*) therefore the power densities corresponding to the power inputs of 10 - 50 watts are approximately 3.33 and 16.66 watts cm^{-3} respectively. In the present study power densities used ranged from 0.43 to 5.11 watts cm^{-3} (positive column) indicating that electron-induced destruction of hydrazine or amino radicals was of little significance.

Furthermore as the rate of electron-induced decomposition

* private communication.

with reactor aging (i.e. similar to the trend observed in other intermediate reactor) which is attributed to other factors.

of hydrazine is governed primarily by the energy of the electrons in the discharge, it should be independent of reaction tube size even under conditions where this mode of destruction would be significant. It may be concluded therefore that another mechanism of destruction of hydrazine is primarily responsible for the experimental results obtained.

6.2.2.2 Destruction of hydrazine by atomic hydrogen attack.

The destruction of hydrazine^{by H} atom attack has been established by a number of workers as reported in chapter 2.3 (for example Manion (1962) Barker (1970)). As atomic hydrogen atom recombination occurs at the reaction tube surface and not in the gas phase it follows that when the diameter of the reaction tube is increased, the rate of diffusion of atomic hydrogen to the reaction tube surface would be decreased. This will lead to an increase in the concentration of atomic hydrogen in the gas phase, which in turn will lead to an increase in the rate of destruction of hydrazine, and consequently a decrease in the nett rate of formation of hydrazine. Such a sequence of events is in agreement with the experimental results obtained in this study.

6.3. Effect of Reactor age on the nett rate of formation of hydrazine.

Variation of reactor surface ' activity ' with ageing has been observed by other workers. Brown and Howarth (1970) reported an ageing effect similar to that observed in the small, intermediate and large reactors i.e. a decrease in the nett rate of hydrazine formation with increasing reactor age. On the other hand Savage (1969) noted an increase in the nett rate of hydrazine formation with reactor ageing (i.e. similar to the trend observed in the new intermediate reactor) which he attributed to either ' surface effects '

or to better analysis techniques.

Details of the methods by which vitreous silicas are manufactured are proprietary but four basic types can be recognised (Hetherington (1962) (1963)) with differences based principally upon hydroxyl and metallic impurity concentration and on methods of fusing. For three of these four types metallic impurity concentrations are in the reverse order of the hydroxyl contents (Hetherington (1965)).

At present very little is known about the effect of high field gradients in the region near the surface of a quartz reactor, however Hetherington (1965) has suggested that inside quartz there are a number of loosely bound species which could migrate under the influence of the field.

As discussed in chapter 6.2 the presence of atomic hydrogen in an electrical discharge results in a decrease in the nett rate of formation of hydrazine. Thus the migration of species which increase or decrease hydrogen atom recombination to or from the discharge surface would increase or decrease the catalytic efficiency of that surface, and consequently increase or decrease the nett rate of formation of hydrazine.

The different types of quartz contain varying amounts of hydroxyl and metallic impurities. As far back as 1922, Wood in his work on the dissociation of hydrogen in a low frequency discharge concluded that water vapour or oxygen reduced the ability of the reaction tube surface to catalyse atomic hydrogen recombination. Recently a large amount of work has been carried out on the catalytic production of atomic hydrogen in a discharge when small amounts of water or oxygen are added. Increases of atomic hydrogen yield

by factors of ten or so when switching from dry hydrogen to hydrogen containing 0.1 - 0.3% water have been noted (Kaufmann (1966)).

Whereas hydroxyl inhibits the recombination of atomic hydrogen many workers (e.g. Eremin et al (1967) (1969)) have demonstrated that the presence of metallic surfaces in an electrical discharge catalyses the recombination of atomic hydrogen. Therefore depending upon the type of quartz used (i.e. the concentration of hydroxyl and metallic impurities) the operation of an electrical discharge could effect the catalytic activity of the reaction tube surface in a number of different ways.

The quartz used for the new intermediate reactor was not from the same batch as that used for the construction of the other reactors (as it was a remnant of previous stock) thus the different surface ageing behaviour observed in the new intermediate reactor compared with the other reactors may be due to the different types of quartz used in the construction of these reactors.

The behaviour of the new intermediate reactor could be explained by assuming that this reactor was made from high hydroxyl content silica. Thus initially the efficiency of the reaction tube surface to catalyse hydrogen atom recombination would be low (compared with a silica surface rich in metallic impurities) however as increasing operations of the discharge promoted migration of hydroxyl ^{impurities} away from the reactor surface (and/or migration of metallic impurities to the reactor surface) so the catalytic efficiency of the surface would increase (with a corresponding increase in the nett rate of formation of hydrazine).

because saturated / reacting in so

Similarly, the behaviour of the other reactors could be explained by assuming that these reactors were constructed from high metallic impurity content silica. Thus initially the efficiency of the reaction tube surface to catalyse atomic hydrogen recombination would be high (compared with a silica surface rich in hydroxyl constituents) however as increasing operation of the discharge promoted migration of metallic impurities away from the reactor surface (and/or migration of hydroxyl impurities to the reactor surface) so the catalytic efficiency of the surface would decrease (with a corresponding decrease in the nett rate of hydrazine formation).

Another possible explanation of the different surfaces properties observed in the various reactors may be connected with the variation of surface adsorption processes over a period of discharge operation. Ammonia discharges in the small, intermediate and large reactors had been operated for a fairly long period of time (during the reactor development study) before commencement of the experimental programme outlined in chapter 5.2. and it is quite probable that the surfaces of these reactors were saturated with ammonia and other discharge gases. This ammonia layer could prevent atomic hydrogen recombination and as the layer gradually thickened this effect would increase with a resultant decrease in the nett rate of formation of hydrazine.

In the new intermediate reactor the walls would be unsaturated and therefore in the earlier runs the rate of adsorption of discharge gases including hydrazine would be high. As discharge operation was continued this adsorption rate would decrease (as the walls became saturated) resulting in an apparent increase in the nett rate

of formation of hydrazine.

Perhaps if the discharge in the new intermediate reactor had been run for a much longer period of time, the reactor walls would have become saturated with discharge gases and then the new intermediate reactor would have displayed identical ageing characteristics to the other reactors.

It is of interest to note that Brown and Howarth (1970) investigated the formation of a molecular layer on the surface of the reaction tube. In their experiments, an aged quartz reaction tube in which the nett rate of formation of hydrazine, had been found to decrease with increasing reactor age, was thoroughly cleansed with hydrofluoric acid in order to remove any molecular layer which might have been formed.

This treatment was found to have no effect upon the nett rate of formation of hydrazine, indicating that either a molecular layer was not formed on the tube surface, or if one was it did not effect the nett rate of formation of hydrazine.

6.4. The influence of quartz wool packing on the nett rate of formation of hydrazine.

In principle adding extra surface area to the positive column of the discharge should lead to an increase in the rate of recombination of atomic hydrogen with a subsequent increase in the nett rate of formation of hydrazine.

One explanation of why the experimental results (for the packing of the large reactor) did not exhibit this trend may be associated with the nature of the packing used. The preparation of quartz wool in a water vapour atmosphere would almost certainly ensure

a high hydroxyl content wool. Thus as noted in 6.3 the presence of this hydroxyl in the discharge would inhibit the recombination of atomic hydrogen, rendering the extra surface area of little use, if any. Whether or not the presence of this hydroxyl in the discharge zone could influence the efficiency of the discharge tube itself to catalyse atomic hydrogen recombination is a matter of conjecture. If this was the case however it would explain the reduced nett rate of formation of hydrazine in the packed large reactor in which no gas by-passing was apparent.

At present surface effects are poorly understood and are open to speculation and until further work is undertaken the role of the surface will remain a 'bottleneck' in the understanding of the discharge chemistry.

CHAPTER 7.0.

7.0. Recommendations for future work.

A comprehensive review of the necessary research into the chemistry and physics of electrical discharges has been given by Spedding (1969). The present investigation has highlighted some of the engineering problems that are associated with the gas phase glow discharge synthesis of hydrazine. There are many areas of study where further research is necessary.

1. Reactor Design

In the present study it has been shown that it is feasible to maintain uniform discharges only over limited electrode areas and under conditions which are not of practical interest. Thus the range of operating conditions over which constriction of the discharge does not occur is located mainly in the low pressure regions with all the attendant engineering difficulties. Certainly more research into the effects of:

- a) reactor unit geometry,
- b) nature of electric power

is required to determine whether or not constriction may be minimised, however, it is probable that the solution of this problem may be found by developing means of overcoming, rather than eliminating discharge constriction. In this respect the development of novel reactors in which a means of moving the discharge relative to the gas stream is provided, may prove to be rewarding. In such reactors scanning of the entire reactor cross-section will ensure that by-passing of the reactant gas will be minimised (Haji (1972) Thornton (1972)).

Chemical Studies.

1. Further work is needed to confirm whether or not increasing

reactor size results in an increase in the concentration of atomic hydrogen in the discharge zone with a resultant increase in the destruction of hydrazine. One way of doing this would be by the use of an atomic hydrogen scavenger (for example an allyl compound i.e. allyl amine, allyl alcohol etc). If an increase in atomic hydrogen concentration does occur in a large size reactor then addition of sufficient scavenger to react with the additional atomic hydrogen formed should yield an increase in the nett rate of formation of hydrazine (i.e. compared with the nett rate of formation of hydrazine obtained when no scavenger is used).

2. Additional information concerning the role of the electrodes in the synthesis of hydrazine is needed. Such information could be obtained by using a reactor with an adjustable size opening between the electrode compartments and the reaction zone of the apparatus. In this way it would be possible to determine the nett rate of formation of hydrazine for a range of hole sizes. Extrapolation to zero hole size could be used to eliminate the effect of the electrodes on the nett rate of formation of hydrazine.

3. The present study has confirmed the importance of the discharge surface and in this respect more information is required concerning:

- a) The catalytic efficiency of different discharge surfaces.
- b) Variation of this efficiency over a period of discharge operation.
- c) Methods of rejuvenating aged discharge surfaces.

Point (c) is of particular importance from the standpoint of industrial application of chemical discharge reactor's as surface

ageing will play an important part in the process economics.

4. Further work under different conditions utilising different packing materials could lead to a much clearer explanation of the changes occurring on packing a reactor.

CHAPTER 8.0.

8.0 Conclusions.

Within the limits of experimental error and in the domain of the experimental conditions investigated, several significant conclusions can be drawn from the present investigation.

A. Reactor Design Studies.

1. One of the major problems of scale-up has been identified. This problem is the constriction of the discharge zone into a narrow beam thereby allowing some of the reactant gas to by-pass this zone completely.

Work in this field has shown that there is a limit to the diameter of electrodes which may be employed. Under dc discharge conditions electrodes of diameter greater than a critical size which is dependent upon a number of interdependent factors give rise to non-uniform constricted discharges.

The principal factors are:-

- a) The nature of the reactant gas.
- b) Reactor unit geometry.
- c) Electrode material and electrode profile.
- d) The flow pattern of the gaseous reactant (which is dependent on (b) and (c).
- e) Electrical and operating conditions - of which the most important are electric current density, operating pressure and gas flow rate.

B. Electrical Studies.

1. The continuous dc glow discharge operated in the abnormal glow region where an increase in current is accompanied by a slight increase in voltage.
2. Equations have been developed from the data of Ouchi (1952) which may be used to estimate the cathode fall in potential and the length of the positive column for a discharge in ammonia gas operating in the abnormal glow region. These equations are of the form -

$$V_c = m (J P^{-2}) + c_1$$

and

$$L = l - c_2 (c_3 - c_4 V_c) P^{-1}$$

where V_c , J , P , L and l represent cathode fall in potential, current density, pressure, length of the positive column and inter-electrode distance respectively and m and c are constants.

C. Chemical Studies.

1. The application of the similarity principle to electrical discharges in which chemical reactions occur has been examined. While the discharge processes depending on single electron impact activation follow the similarity principle the relationship does not hold for chemical reaction where secondary processes are of primary importance. Thus it may be concluded that if two discharges are physically similar this does not mean that the chemistry of these discharges will follow suit.

2. An equation of the form -

$$\left(\frac{rD^3}{FC} \right) \propto \left(\frac{V_p I D}{F^2 C} \right)^{4-0.29} \left(\frac{D^4 P}{F^2 C} \right)^{0.71} \left(\frac{L}{D} \right)^{-0.59}$$

developed using the technique of dimensional analysis has been found to correlate the experimental results obtained over a wide range of the operating parameters, reduced electric field strength, current density and gaseous reactant residence time.

3. Evidence has been provided which suggests that hydrazine is degraded in the discharge primarily by atomic hydrogen attack rather than by electron - induced destruction.
4. The nett rate of formation of hydrazine has been found to be inversely proportional to reactor size.
5. Evidence has been provided which suggests that changing the reaction tube size results in a change in the concentration of atomic hydrogen in the reaction zone. As the reaction tube diameter is increased ~~the~~

the rate of diffusion of atomic hydrogen to the reaction tube surface is decreased. This results in a decrease in the rate of recombination of atomic hydrogen at the reaction tube surface and consequently an increase in the concentration of atomic hydrogen in the reaction zone. In turn this leads to an increase in the rate of destruction of hydrazine by atomic hydrogen attack and as a result a decrease in the nett rate of formation of hydrazine.

6. Attempts to minimise the concentration of atomic hydrogen in large scale reactors by packing the reactors with a quartz surface (wool) failed due to field distortion with subsequent discharge constriction and also due to the catalytic nature of the quartz surface employed.

7. The important effects of the discharge surface on the nett rate of formation of hydrazine have been noted. It has been observed that not only does the nett rate of formation of hydrazine depend upon the material of construction of the discharge surface but also upon the ' age ' of the discharge surface. It has been found that as the discharge surface ages the nett rate of formation of hydrazine may be increased or decreased as a result of changes in the reaction tube surface and not due to changes in the electrode surface as was previously believed.

8. A number of explanations of this ageing phenomenon have been advanced, namely -

(1) the action of the electric field on the surface of the quartz reaction tube is to promote the migration of metallic impurities (which catalyse the recombination of atomic hydrogen atoms) and or hydroxyl ions (which inhibit the recombination of atomic hydrogen atoms) to, or away from the reaction tube surface, with the result that the ability of the surface to catalyse the recombination of atomic hydrogen atoms (and consequently the nett rate of formation of hydrazine) increases

or decreases with increased operation of the discharge (i.e. reactor age).

(2) In a new reaction tube the rate of adsorption of hydrazine onto the reaction tube surface decreases with increasing discharge operation (i.e. increasing reactor age) resulting in an increase in the nett rate of formation of hydrazine. Once the reaction tube surface is saturated with gases however a layer of gas molecules (predominately ammonia gas) is formed on the surface inhibiting the recombination of atomic hydrogen atoms on this surface. As this layer thickens with increasing discharge operation (increasing reactor age) the rate of recombination of atomic hydrogen progressively decreases and as a result the nett rate of formation of hydrazine also decreases.

CHAPTER 9.0.

9.0. Nomenclature.

- A. Area.
- A. Constant (equation 4 - 2).
- a. Constant.
- a. Constant (equation 5 - 1).
- B. Constant (equation 4 - 1).
- b. Constant (equation 5 - 1).
- C. Ammonia gas concentration.
- C. Constant.
- C. Constant (equation 4 - 1).
- c. Constant (equation 5 - 1).
- D. Reaction tube diameter.
- d. Width of cathode dark space.
- d. Inter-electrode distance.
- dn. Distance between cathode and leading edge of the positive column.
- E. Electric field strength.
- F. Ammonia gas flow rate.
- I. Discharge current.
- J. Current density.
- K. Rate constant.
- L. Length.
- L. Length of the positive column (equation 5 - 1).
- l. Inter-electrode distance.
- M. Mass.
- m. Constant.

Nomenclature (continued).

- N. Viscous influence number.
- N. Concentration of charged particles.
- n. Concentration of gas molecules.
- P,p. Gas pressure.
- Q. Electric charge.
- Q. Collision cross-section.
- R. Gas constant.
- R,r. Radially measured distance.
- r. Nett rate of formation of hydrazine.
- T. Temperature.
- T. Time.
- t. Time.
- V. Potential difference across an electrical discharge.
- Va. The anode fall of potential.
- Vp. Potential difference across the positive column of a discharge.
- Vs. Breakdown potential.
- V. Gas volume.
- Vol. Volume of gas collection vessel.
- \tilde{v} Electron drift velocity.
- W. Discharge power input.
- α Ppm hydrazine.
- α Rate coefficient for electron-ion recombination.

Nomenclature (continued)

ρ	Density.
ρ	Space charge density.
γ	Rate coefficient for electron emission.
δ	Secondary rate coefficient of electron emission.
λ	Electron mean free path.
μ	Gas viscosity.
μ_0	Permeability of free space.
ϵ_0	Permittivity of free space.
σ	Surface charge density.
τ	Lifetime of excited species.
τ	Gas residence time.
π	Power density.
Ω	Ohms.

CHAPTER 10.0.

10. O. Literature References.

1. Altschuller, A. (1954) J. Chem. Phys. 22 1947.
2. Anderson et al (1959) Ind. Eng. Chem. 51 527.
3. Bamford, C. (1939) Trans. Farad. Soc. 35 568.
4. Barker, R. (1970) Electricity Council Research Centre, Report No. 276.
5. Bayes, K. et al (1963) Z. Naturforsch 17A 676.
6. Bailey, V. Duncanson, L. (1930) Phil. Mag. 505 144.
7. Becker, H. (1920) Wiss Veroffentl Siemens-Konzern 1 76.
8. Becker, K. Welge, K. (1963) Naturforsch 18A 600.
9. Birse and Melville (1940) Proc. Roy. Soc. London 175A 164, 187.
10. Birse and Melville (1938) Nature 142 1080.
11. Brown, B. Howarth, C. (1970) University of Newcastle-upon-Tyne, Private Communication.
12. Bruche, E. (1927) Ann Physik 1 93.
13. Bruche, E. (1929) Ann Physik 83 1065.
14. Brewer, K. Westhaver, J. (1929) J. Phys. Chem. 33 883.
15. Brewer, K. Westhaver, J. (1930) J. Phys. Chem. 34 153, 1280, 2348.
16. Bruce, F. (1949) J. Inst. Elec. Engrs. 94 Part 2 138.
17. Carbaugh, D. et al (1967A) J. Chem. Phys. 47 5211.
18. Carbaugh, D. (1967B) Phd Thesis Univ. of Maryland.
19. Cassano et al (1967) I.E.C. 59 18.
20. Dallenbach, W. (1925) Phys. Z 26 483.
21. Deckers et al (1966) Canadian J. Chem. 44 2981.
22. Devins, J. Burton, M. (1954) J. Am. Chem. Soc. 76 2618.
23. De La Rue, W. Muller H.W. (1880) Phil. Trans. Roy. Soc. 171 109.

24. Diessen, R. (1963) J. Chem. Phys. 39 2121.
25. Dixon, J. (1932) J. Am. Chem. Soc. 54 4262.
26. Dixon, J. Steiner, W. (1932) Physik Chem. B17 327.
27. Elgin, J. Taylor, H. (1929) J. Am. Chem. Soc. 51 2059.
28. Engel, A. Steenback, M. (1939) See Loeb, L.B. Fundamental Processes of Electrical Discharges in Gases CH. XL. Wiley.
29. Eremin et al (1965) Z Hur. Prik. Chem. 38 11 2479.
30. Eremin et al (1966) Russ. J. Phys. Chem. 40 1671.
31. Eremin et al (1968) Russ. J. Phys. Chem. 42 536.
32. Fenn, J. (1961) U.S. Patent 3 1005 762.
33. Foner, S. Hudson, R. (1958) J. Chem. Phys. 29 442.
34. Francis, G. (1956) Encyclopedia of Physics (by S. Flugge) 22 80.
35. Francis, G. (1960) Ionisation Phenomena in Gases London. Butterworths.
36. Gedye, G. Allibone, (1932) Proc. Roy. Soc. A 130 346.
37. Gedye, G. Rideal, G. (1932) J. Chem. Soc. 135 1160.
38. Goshō, Y. (1969) Scientific Papers of the Institute of Physical and Chemical Research. Vol. 63 No. 1 P7.
39. Gray, P. Thynne J. (1964) Trans. Farad. Soc. 60 1047
40. Golubovski, Y. et al (1966) Opt. Spectr. (USSR.) 20 317.
41. Haines, M. Bair, E. (1963) J. Chem. Phys. 38 672.
42. Haji, F. (1972) Phd Thesis University of Newcastle-upon-Tyne.
43. Hetherington et al (1962) Phys. Chem. Glasses 3 129.
44. Hetherington et al (1963) Quarzglas und Quarzglas; Ullmans Encyclopedie der Technischen Chemie 14 511 Urban and Schwarzenberg Minchen Berlin.

45. Hetherinton et al (1965) Physics and Chemistry of Glasses
Vol. 6 No. 1 p6,16.
46. Holm, R. (1924) Z. Phys. 25 497 26 412.
47. Hussain, D. Norrish, R. (1963) Proc. Roy. Soc. 273A 145.
48. I.C.I. Ltd. (1964A) Brit. Patents 948772, 958776, 958777,
958778.
49. I.C.I. Ltd. (1964B) Brit. Patent 966406.
50. Jones, R. Lossing, F. (1969) Can. J. Chem. 47 1391.
51. Kaufmann, F. (1969) Advance Chem series 80 29.
52. Kenty, C. (1962) Phys. Rev. 126 1235.
53. Kobozev et al (1936) Z Hur. F12. Chim. 7 619.
54. Koenig, A. Wagner, A. (1929) Z. Physik Chem A144 213.
55. Lampe et al (1963) Industrial uses of Large Radiation
Sources Proc. 1. J.A.E.A. Vienna 41.
56. Lampe et al (1967) U.S. Patent 3,322,660.
57. Lind, S. Glockler, G. (1927) Trans. Am. Electrochem. Soc. 52 37.
58. Lind, S. Glockler, G. (1929) J. Am. Chem. Soc. 50 1767, 1928,
51 2811, 3655.
59. Lind, S. Glockler, G. (1930) J. Am. Chem. Soc. 52 4450.
60. Lind, S. (1928) Trans. Am. Electro. Chem. Soc. 53 25.
61. Llewellyn-Jones, F. (1966) * Ionisation and Breakdown in Gases
Methuent Co. Ltd., London.
62. Logan, F. (1968) Phd Thesis Univ. of Maryland.
63. Logan, F. Marchello, J. (1968) J. Chem. Phys. 49 3029.
64. Logan, F. Marchello, J. (1969) J. Chem. Phys. 50 2724.

65. Lunt, R. Mills, J. (1925) Trans. Farad. Soc. 31 786.
66. Lunt, R. Meek, C. (1936) Proc. Roy. Soc. London A157 146.
67. Maier, E. (1934) Z. Physik 93 65.
68. Manion, P. (1958) U.S. Patents 2849356, 3020, 223.
69. Mantei, K. Bair, E. (1968) J. Chem. Phys. 49 3248.
70. Massey, J. Cannon S. (1965) J. Appl. Phys. 36 361.
71. Massey, J. Cannon S. (1965) J. Appl. Phys. 36 373.
72. McCarthy, J. Robinson, G. (1959) J. Chem. Phys. 30 999.
73. McDonald et al (1954) J. Chem. Phys. 22 908.
74. McDonald, C. Gunning, H. (1955) J. Chem. Phys. 23 532.
75. McEachron, K. George, R. (1922) Bull Purdue Univ. 6 1.
76. Ouchi, K. (1949) J. Electro. Chem. Soc. Japan 17 285.
77. Ouchi, K. (1952) J. Electro. Chem. Soc. Japan 20 164, 168, 378.
78. Ouchi, K. (1952) Sci. Rept. Res. Inst. Tshoka Univ. A4 203.
79. Paschen, F. (1889) Weid Ann 37 69.
80. Pearson, J. Harrison, J. (1969) Brit. J. Appl. Phys. (JPHYS.D.)
Ser. 2 vol. 2 77.
81. Phelps, A. (1967) Advan. Chem. Ser. 80 18.
82. Ramsay, D. (1953) J. Phys. Chem. 57 415.
83. Rathsack (1957) Z. Physik Chem. (LEIPZIG) 206 285.
84. Rathsack (1960) Z. Physik Chem. (LEIPZIG) 214 101.
85. Rathsack (1961) Z. Physik Chem. (LEIPZIG) 216 246.
86. Romig, M. (1960) Phys. of Fluids 3 (1) 129.
87. Rouy, A. et al (1961) U.S. Patent 3,003,939.
88. Rummel, T. (1940) British Patent 527,899.
89. Savage, D. (1970) Phd Thesis Univ. of Newcastle-upon-Tyne.

- 112.
90. Schiavello, M. Volpi, G. (1962) J. Chem. Phys. 37 1510
91. Schnepf, O. Dressler, K. (1960) J. Chem. Phys. 32 1632.
92. Schueller, H. (1959) German Patent 1, 116,638.
93. Sergio, R. (1968) Phd Thesis Univ. of Newcastle-upon-Tyne
Table 3.1 P63.
94. Shastri, Jogaro (1959) J. Sci. Ind. Res. (India) 18B 38.
95. Skorokhodov et al (1961) Russ. J. Phys. Chem. 35 503
96. Spedding, P. (1968) Industrial Research Fellow Report No. 4,
Inst. of Chem. Eng.
97. Srikantan, S. (1935) Ind. Chem. Soc. 13 79
98. Steenbeck, M. (1932) Wiss Veroff Siemens 11 (2).
99. Stief De Carlo (1965) Nature 205 889.
100. Stief De Carlo (1966) J. Chem. Phys. 44 4638.
101. Stief De Carlo (1967A) J. Chem. Phys. 46 592.
102. Stief De Carlo (1967B) J. Chem. Phys. 71 2350.
103. Stief De Carlo (1968) J. Chem. Phys. 49 100.
104. Swarzc, M. (1949) Proc. Roy. Soc. 198A 267, 285.
105. Takashi, S. (1960) Bull Chem. Soc. Japan 33 1350.
106. Thornton, J. (1966) Chem. Proc. Supplement 56.
107. Thornton, J. Spedding, P. (1967A) Nature 713 1118.
108. Thornton et al (1967B) Am. Chem. Soc. Div. Fuel. Chem
Preprints 11 (2) 129.
109. Thornton et al (1969) Adv. Chem. Ser. 80 175.
110. Thornton et al (1970) Univ. of Newcastle-upon-Tyne. Private Communication.
111. Thornton, J. Haji F. (1972) Electrochemical Engineering
Symposium Univ. of Newcastle-Upon-Tyne.

112. Townsend, J. (1915) ' Electricity in Gases ' Oxford: Clarendon Press.
113. Von Engel et al (1932) ' Elektrische Gas ent la Dungen ' Berlin Springer.
114. Von Engel, A. (1955) ' Ionised Gases ' Oxford Clarendon Press.
115. Von Engel, A. (1956) Handbuch Der Physik Vo. 21 Heid Elberg: Springer
116. Von Engel et al (1959)
117. Wallar, D. (1968) Phd Thesis Univ. of Newcastle-Upon-Tyne.
118. Watt, G. Chrisp J. (1952) Analytical Chemistry 24 2006.
119. Westhaver (1933) J. Phys. Chem. 37 897.
120. Wiig (1935) J. Am. Chem. Soc. 57 1559.
121. Wiig (1937) J. Am. Chem. Soc. 59 827.
122. Williams, H. (1967) U.S. Patent 3,342,713.
123. Wood, R. (1922) Phil. Mag. 44 538.
124. Woolsey, G. (1970A) ' Discharges in Electronegative Gases ' P.70-76 (Taylor and Francis Ltd. London).
125. Woolsey et al (1970B) *ibid* P125-139.

APPENDIX 1.0.

Appendix 1.

Description of the Chromatograph.

The complete chromatograph was housed in a screened metal case which contained a thermostatically controlled oven and the detector device. The carrier gas which was supplied from an external cylinder, was maintained at constant pressure by two pressure regulators, one at the external source and one within the instrument. After leaving the pressure regulator in the instrument the gas fed the reference chamber of a thermal conductivity detector before passing on to the sample injection system. Gaseous samples were introduced into the system through a special gas sampling valve. The combined carrier gas and sample mixture then passed through the analytical column, where the components of the sample were separated according to their affinities for the material with which the column was filled. Those components having little affinity for the column material passed through the column rapidly, while those with greater affinities were retained in the column for longer periods. After leaving the column the separated components were swept one by one into the sensing chamber of the thermal conductivity detector. Heated platinum wires or thermistor beads in both the reference and sensing chambers were connected into a balanced bridge circuit. Heat was lost from these elements by conduction through the gases and when both chambers were filled with pure carrier gas the bridge was balanced. When a sample component entered the sensing chamber the difference in thermal conductivity modified the heat losses, causing a change in the wire or thermistor temperature. This resulted in a resistance change, which unbalanced the bridge, generating a signal that was proportional

to the thermal conductivity. This signal drove the pen of a standard strip chart recorder (Kent Recorder) to produce in graphic form a qualitative and quantitative description of the sample. The detector sensitivity could be varied by means of a range control which attenuated the signal fed to the recorder by successive factors of two so that each sensitivity setting was half that of the previous setting.

Choice of Carrier Gas.

The choice of carrier gas depended to a large extent on the best sensitivity and linearity achieved with the thermal conductivity detectors. In this respect, the best carrier gas was one whose thermal conductivity was very different to that of the sample. Both argon and helium although expensive were suitable because of ' their chemical inertness '. Helium has a high thermal conductivity (34.8×10^{-5} Cal/Cm/Sec/ $^{\circ}$ C) with respect to argon (3.98×10^{-5} Cal/Cm/Sec/ $^{\circ}$ C) ensuring a better detector sensitivity. However, helium has the disadvantage that it gives a poor response to hydrogen in comparison with nitrogen.

Chromatography Column.

The separating ability of a column depends upon many factors, the length and diameter of the column, the particle size and structure of the material with which the column is filled, the uniformity of packing, the operating temperature, the properties of the components in the sample mixture and the flow rate and pressure of the carrier gas.

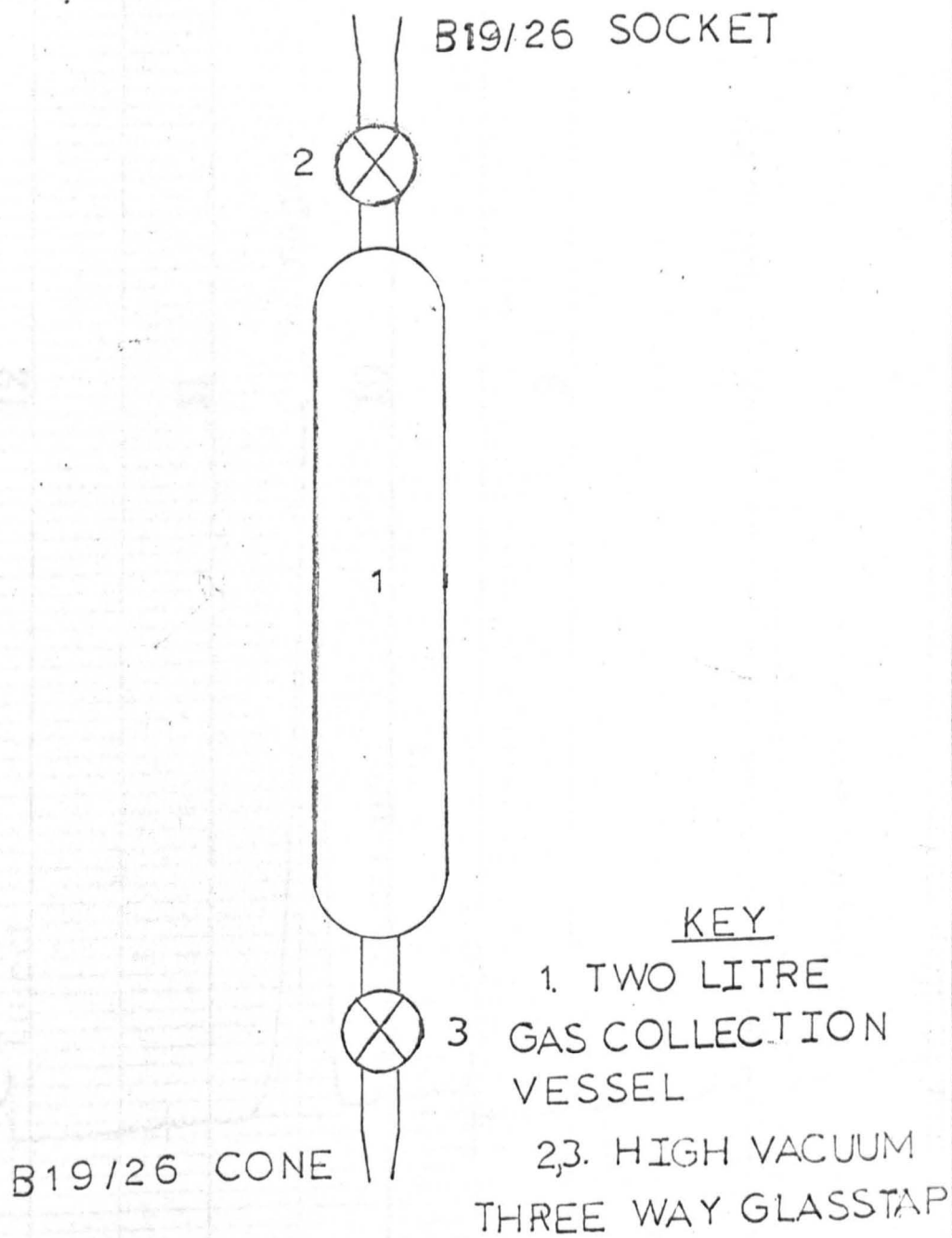
An 18ft. column packed with molecular sieve 5A and operated at the following conditions was found to be suitable for analysing

nitrogen and hydrogen in a sample mixture at 6.0 mmHg pressure.

Oven Temperature = 30°C.
Carrier Gas pressure (internal) = 10 lb. in⁻²
Carrier Gas pressure (external) = 28.0 lb. in⁻²
Detector sensitivity setting. = 8.0.
Injection block temperature. = 0°C.
Sample injection pressure = 6.0 mmHg.

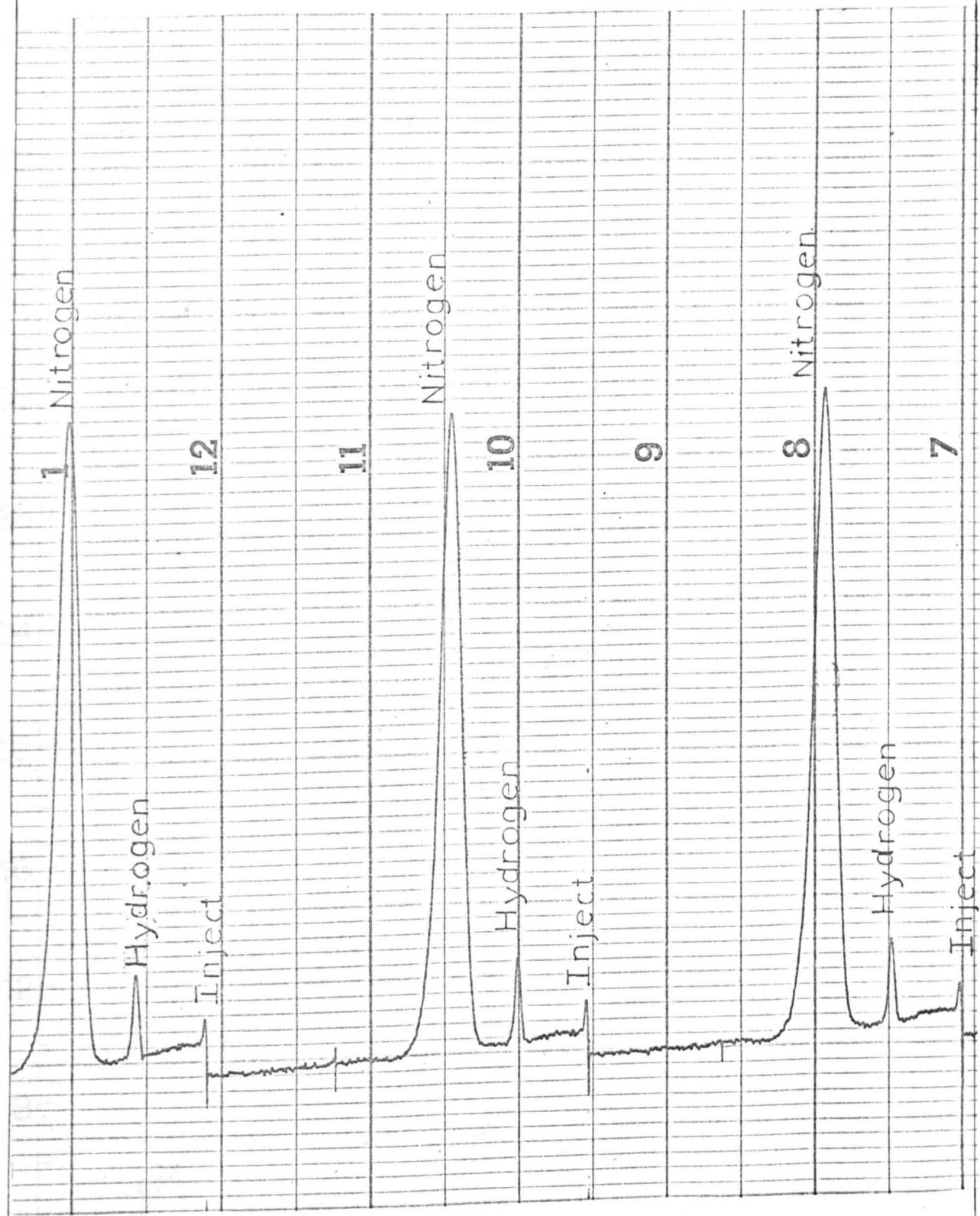
TABLE A1.1 % Hydrogen and Nitrogen in
Calibration mixtures and corresponding
peak heights.

Sample injection Pressure. (mmHg)	% Nitrogen.	Nitrogen Peak Height.	% Hydrogen.	Hydrogen Peak Height.
6.0	1.884	5.05	2.51	1.0
6.0	2.130	5.6	2.513	1.0
6.0	2.200	5.6	4.95	1.65
6.0	5.54	13.1	9.58	3.2
6.0	10.00	26.7	9.8	3.06
6.0	13.04	35.6	12.84	4.35
6.0	15.92	41.3	16.81	5.6
6.0	19.68	52.9	20.08	6.8



FIGA11 GAS COLLECTION VESSEL

PEAK HEIGHT (CMS)



FIGA12

FIGA13

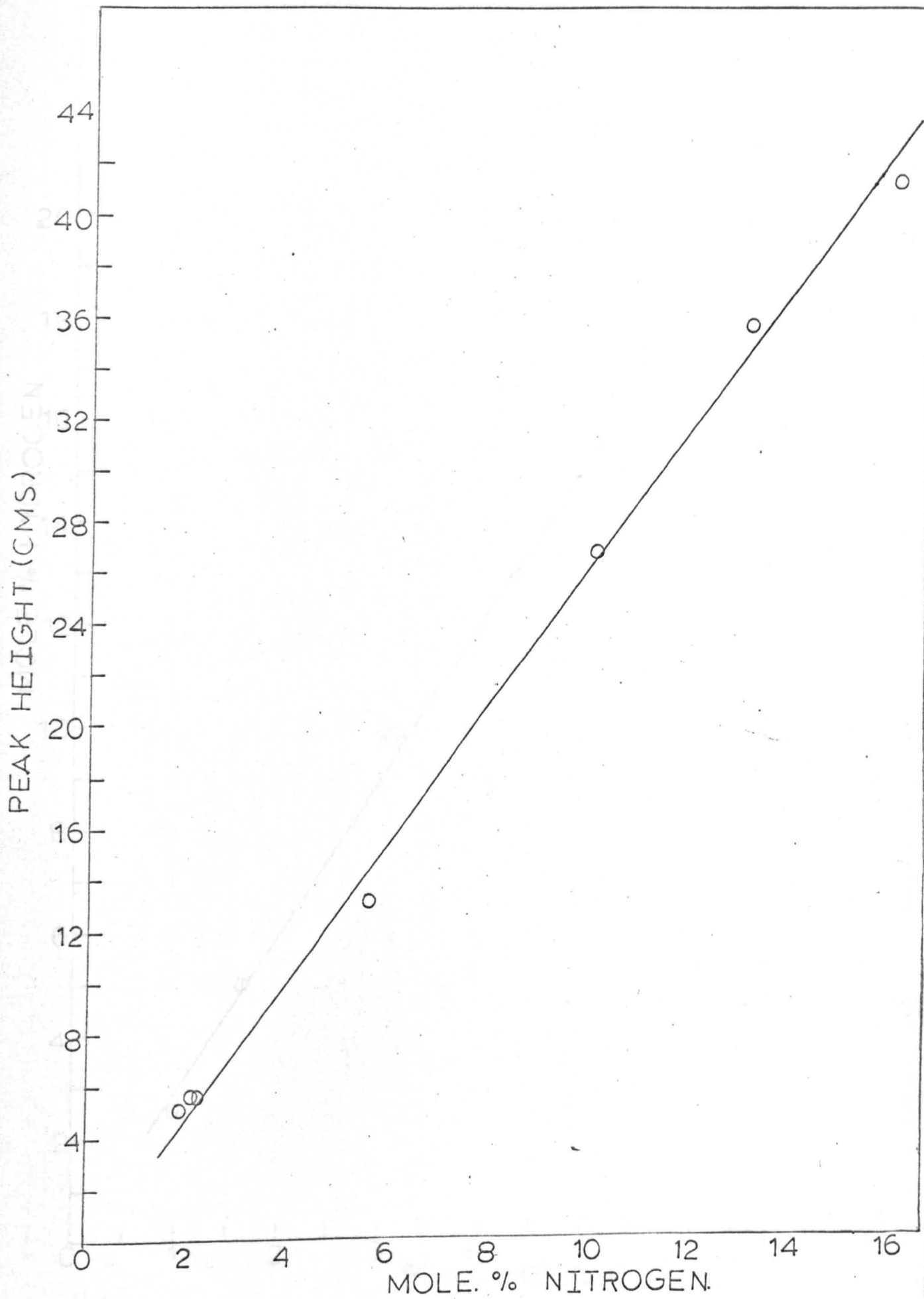


FIG. A13

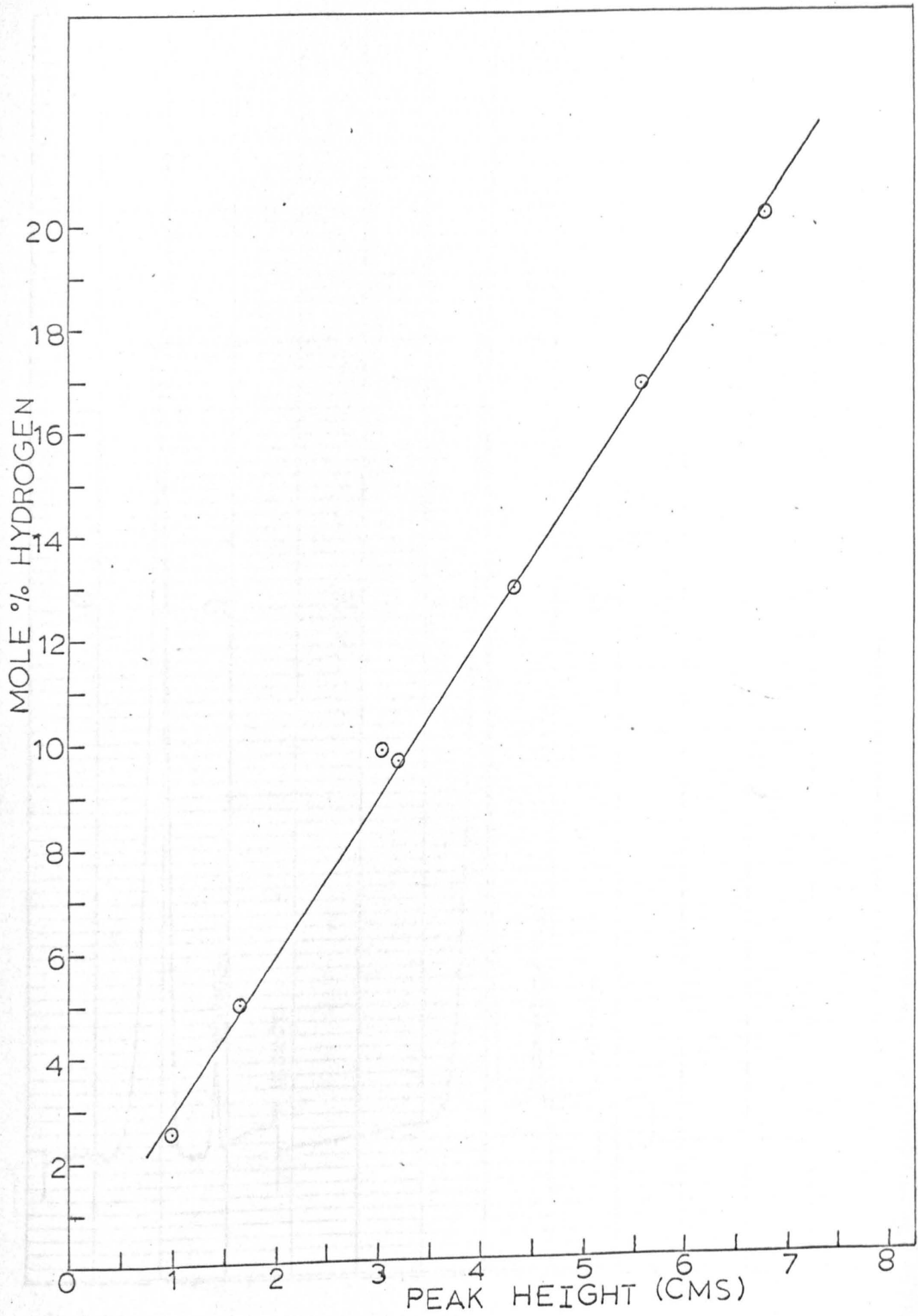


FIG A1.4



FI GA15

APPENDIX 2.0

APPENDIX 2.0

APPENDIX 2.0

APPENDIX 2.0

APPENDIX 2.0

APPENDIX 2.0

APPENDIX 2.0

APPENDIX 2.0

APPENDIX 2.0

APPENDIX 2.0

APPENDIX 2.0

APPENDIX 2.0

APPENDIX 2.0

APPENDIX 2.0

APPENDIX 2.0

APPENDIX 2.0

APPENDIX 2.0

APPENDIX 2.0

APPENDIX 2.0

APPENDIX 2.0

APPENDIX 2.0

APPENDIX 2.0

APPENDIX 2.0

APPENDIX 2.0

APPENDIX 2.0

APPENDIX 2.0

APPENDIX 2.0

APPENDIX 2.0.

Appendix 2.

Hydrazine Analysis.

Discussion of Colorimetric method employed.

Methods for the determination of hydrazine depend upon its basic character or reducing properties, and are thus subject to interference owing to the presence of other substances having similar properties. The method of analysis described by Watt and Chrisp(1952) was used for all the experimental results.

This method uses the yellow colour developed upon the addition of p - dimethyl amino benzaldehyde to solutions of hydrazine in dilute hydrochloric acid as the basis of an spectrophotometric method of hydrazine determination. This system is characterised by a transmittancy minimum at 458 μ . The calibration curve for this method in which absorptancy (100 - % transmittancy) at 458 μ is plotted against log concentration of hydrazine in parts per million exhibits maximum slope at about 63% absorptancy; in agreement with Beers Law and thus has a maximum accuracy corresponding to 2.7% relative analysis error per 10% absolute photometric error or about 1.2% relative error for a precision of 0.4% in making the measurements. To attain this precision it is necessary to ensure that cross contamination of solutions via transfer pipettes does not occur. In order to keep the relative analysis error within 1.0% the hydrazine concentration must be within the limits 0.06 to 0.47 ppm.

At room temperature the yellow colour develops immediately and is stable after a period of ten minutes. For a given concentration of hydrazine the per cent transmittancy is unchanged if the hydrochloric

acid concentration is less than 1M. but increases at acid concentrations greater than 1M. Thus for a hydrazine concentration of 0.13 ppm, the relative transmittancy is increased 1.6% if the acid concentration is 2M. and 4.5% if the acid concentration is 3M.

Coloured solutions containing different quantities of hydrazine have been found to show no measurable change in transmittancy in twelve hours. Also for a colour developed sample containing hydrazine at a concentration of 0.2 ppm, the effect of temperature over the range 20°C to 40°C has been found to amount to 0.14% absolute transmittancy per 1°C; this effect is completely reversible. Over the hydrazine concentration range 0.1 to 0.3 ppm, samples having the same hydrazine concentration gave an average deviation of 0.1% absolute transmittancy.

Materials.

Hydrazine dihydrochloride, ethylene glycol, p. dimethyl amino benzaldehyde were BDH reagent grade chemicals used without further purification.

Potassium Iodate - analar reagent grade chemical.

Conc. Hydrochloric Acid - BDH reagent grade chemical.

Chloroform - BDH reagent grade chemical.

Industrial Ethanol.

Distilled Water.

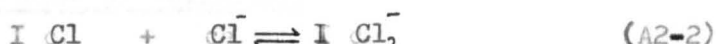
Preparation of standard hydrazine solutions for use in calibration procedure.

Potassium iodate KIO_3 is a stronger oxidising agent than iodine. The reaction of potassium iodate and reducing agents, such as potassium iodide or arsenious oxide, in fairly acidic solutions say 0.1 - 2.0M HCl stops at the stage when the iodate is reduced to iodine.

In 1903 L.W. Andrews showed that in the presence of a high concentration of hydrochloric acid (3 - 9 M) iodate is reduced ultimately to iodine monochloride.



In hydrochloric acid solution, iodine monochloride forms a stable complex ion with the chloride ion:

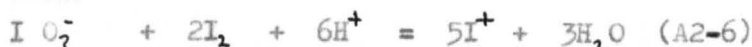
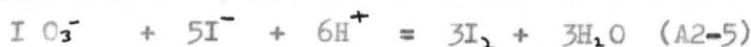


the overall half cell reaction may therefore be written as:

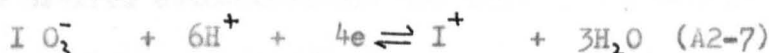


The reduction potential is 1.23 volts, hence under these conditions potassium iodate acts as a very powerful oxidising agent. Furthermore under these particular conditions the equivalent weight of potassium iodate is one fourth the molecular weight $\text{KIO}_3/4$.

Oxidation by iodate ion in a strong hydrochloric acid medium (3 - 9 M) proceeds through several stages.



In the initial stage of the reaction free iodine is liberated as more titrant is added, oxidation proceeds to iodine monochloride and the dark colour of the solution gradually disappears. The overall reaction may be written as:



Detection of end point.

Starch cannot be used because the characteristic blue colour of the starch iodine complex is not formed at high acid concentrations - a few ml's of an immiscible solvent e.g. chloroform is used. If all

the required acid is added initially, the pink colour of the iodine chloroform layer does not appear at the beginning of the titration. The end point is marked by the disappearance of the last trace of violet colour due to iodine from the solvent. The immiscible solvent may be replaced by certain dyes e.g. amaranth (B.C.I. No.184).

Preparation of Solutions.

An approximate 0.4N hydrazine dihydrochloride solution was prepared and standardised by titration with standard potassium iodate solution as follows. A mixture consisting of 10.0 ml of the hydrazine solution, 20 ml of concentrated hydrochloric acid, and 15 ml of chloroform was prepared in an iodine bottle and cooled to about 10°C in an ice bath. After addition of approximately one half of the quantity of potassium iodate solution required in the complete titration, additional concentrated hydrochloric acid was added to give a total acid concentration within the range 3 to 6 M, and the titration was then carried to completion.

The susceptibility of hydrazine to catalytic oxidation and/or decomposition necessitated that the hydrazine solutions should be analysed as soon as possible after preparation.

Appropriate aliquots of the hydrazine stock solution were diluted to the desired concentrations and used in the colour development.

Colour development.

The colour reagent employed had the following composition.
p. dimethylamino benzaldehyde, 0.2 gm, ethanol, 10 ml, concentrated hydrochloric acid, 1.88 ml, distilled water 5.0 ml, and ethylene glycol 5.0. ml. 20 ml of this reagent was added to aliquots of

the standard hydrazine solution selected so that the final hydrazine concentration would be within the range 0.02 to 1.0 ppm, the resulting mixture was 1M with respect to HCl. The blank consisted of the above solution (not including the hydrazine) and was made 1M with respect to hydrochloric acid.

From the results a calibration curve of % absorpency vs log hydrazine concentration in ppm was plotted (Fig. A2.1).

Analysis routine for experimental results.

At the end of an experiment the ethylene glycol in the absorption traps was thoroughly mixed then 2 mls. were pipetted (from a pipette which had been rinsed with this glycol) into a glass bottle with a ground glass stopper. If dilution was necessary distilled water was added, then 20 mls. of standard colour reagent was added and the mixture thoroughly shaken and then allowed to stand for 10 minutes to develop the colour. One unicam cell was washed out then filled with the standard colour reagent while the other was rinsed then filled with the analysis mixture. The two cells were then placed in the spectrophotometer and analysed for hydrazine.

Preparation of calibration curve for the determination of hydrazine.

Determination of hydrazine.

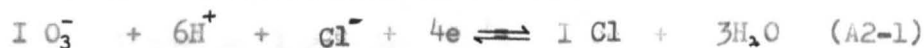
Hydrazine reacts with potassium iodate under the usual Andrews condition thus:



thus $KIO_3 = N_2H_4$

or 1ml of 0.025 M $KIO_3 = 0.0008013$ gm $N_2 H_4$

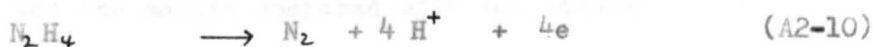
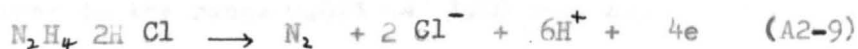
Preparation of standard KIO₃ Solution.



∴ 1.3375 gm of KIO₃ in 250 ml of distilled water gives a
0.025 M or 0.1N solution.

weight of beaker + iodate	95.8755
weight of beaker	<u>94.5380</u>
weight of KIO ₃	1.3375 gm.

An approximate 0.4N solution of hydrazine HCl was prepared:



∴ equivalent weight of N₂H₄H₂Cl₂ = Mwt/4 = 104.97/4

The hydrazine solution was titrated against the 0.025 M KIO₃ (or 0.1N)

	Titration 1.	Titration 2.	Titration 3.
	0.0	0.0	0.0
	<u>39.0</u>	<u>39.0</u>	<u>39.1</u>
KIO ₃	39.0 cc	39.0 cc	39.1 cc

∴ average volume of KIO₃ used = 39.033 cc.

Now $V_1 N_1 = V_2 N_2$ (vol. x normality)

$$\therefore 39.033 \times 0.1 = 10 \times N_2$$

$$N_2 = 0.39033$$

$$\text{hence grams hydrazine} = 0.39033 \times \frac{32}{4}$$

$$= 3.12264 \text{ gm.}$$

Alternative method of calculation.

$$1 \text{ ml of } 0.025 \text{ M KIO}_3 \equiv 0.0008013 \text{ gm } N_2H_4$$

$$\begin{aligned} \therefore 39.033 \text{ ml of KIO}_3 &\equiv 39.033 \times 0.0008013 \\ &= 0.031277 \text{ gm } N_2H_4 \text{ in } 10 \text{ cm}^3 \text{ solution} \end{aligned}$$

∴ in 1 litre of N₂H₄ solution there are
3.1277 gms of hydrazine.

Preparation of diluted hydrazine solutions.

$$1 \text{ ppm} \equiv 1 \text{ gm in } 10^6 \text{ cm}$$

$$\therefore 3.1277 \text{ gms in } 10^3 \text{ cm}$$

$$\text{is } 3.1277 \times \frac{10^6}{10^3} \text{ ppm}$$

$$\text{i.e. } 3127.7 \text{ ppm.}$$

The standard solution was then diluted to give a number of solutions in the range 0.021 - 1.00 ppm, colour reagent was added and the sample compared with the standard blank solution. From the results a table of % absorpency and corresponding hydrazine concentration was constructed (table A2.1).

0.10	10.0
0.20	20.0
0.30	30.0
0.40	40.0
0.50	50.0
0.60	60.0
0.80	80.0
1.00	100.0

TABLE A2.1.

Hydrazine Concentration ppm.	% Absorpancy (100-% Transmittancy).	Average % Absorpancy).
0.021	9.75 10.25 10.75	10.25
0.042	19.0 19.75 19.5 19.75 20.0 20.5	19.75
0.062	28.0 27.75	27.875
0.083	35.0 36.0 35.5	35.5
0.104	41.5 40.5	41.0
0.125	48.25 48.5 48.0	47.125
0.20	62.95 61.75	62.35
0.40	87.5 87.5	87.5
0.60	94.25 94.75 94.5	94.5
0.801	98.5 98.5 98.5	98.5
1.00	99.5 99.5	99.5



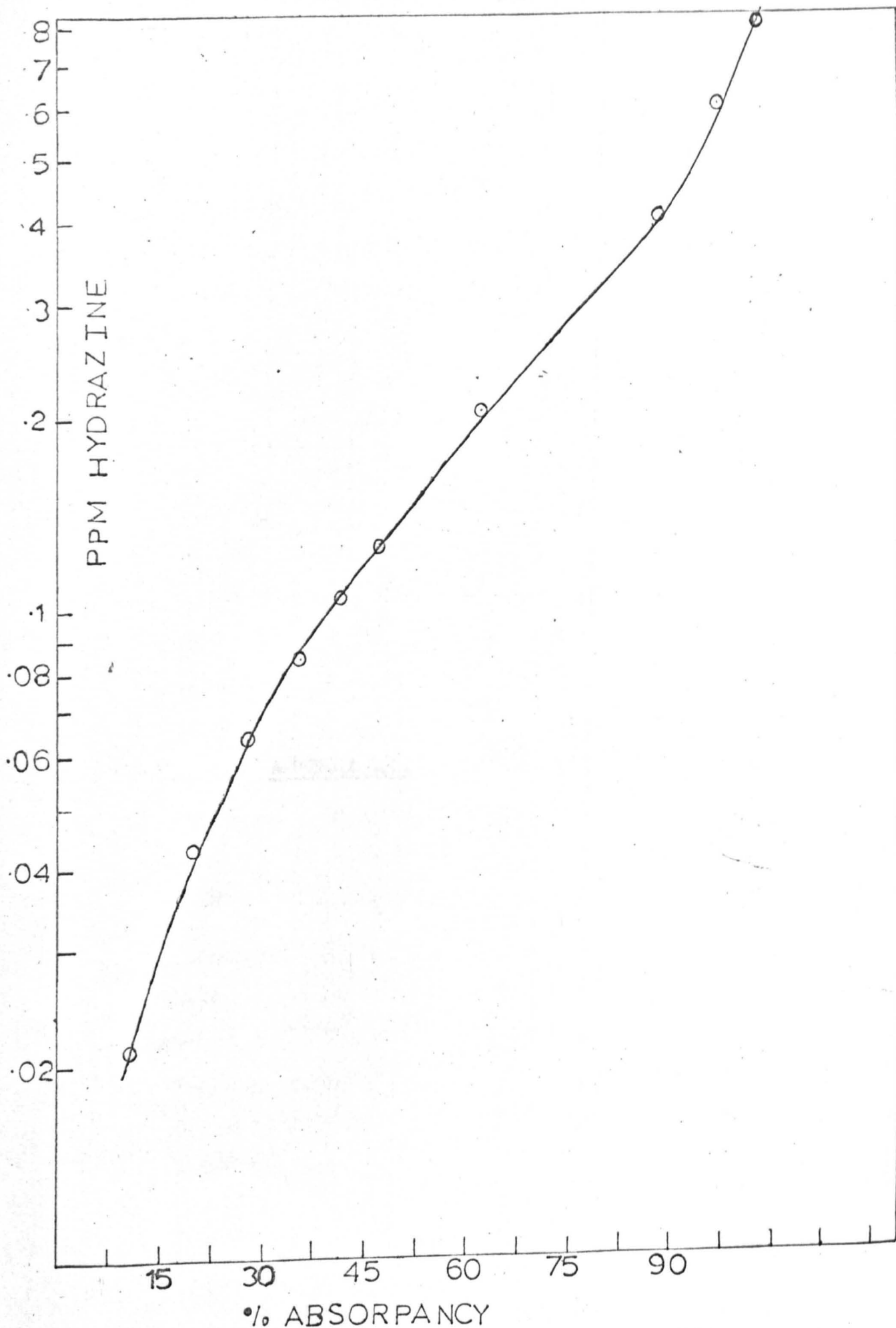


FIG. 2. CALIBRATION CURVE FOR HYDRAZINE

APPENDIX 3.0.

Appendix 3.

Flowmeter calibration results.

Table A3.1 Calibration values for FP -1/16 - G - 5/84 flowmeter
(Tantalum float (density = 16.6 gm cm⁻³))

A = 143, B = 13.6, N = 1599, $\mu_{opt} = 0.00975$, $\rho_{opt} = 0.000716$			
Scale Reading	C value at N = 1599	Flow at 762 mmHg and 15.6 °C (gm min. ⁻¹)	Flow at 762 mmHg and 15.6 °C (cm ³ sec. ⁻¹)
1.	0.0063	0.009341	0.21744
2.	0.0140	0.02076	0.48320
3.	0.0290	0.0430	1.00090
4.	0.0450	0.06672	1.55300
5.	0.0680	0.10080	2.34600
6.	0.0920	0.13640	3.17510
7.	0.1155	0.17125	3.98630
8.	0.1390	0.20610	4.79750
9.	0.1615	0.23950	5.57500
10.	0.184	0.27810	6.35000
11.	0.208	0.30839	7.17850
12.	0.232	0.34398	8.00700
13.	0.2625	0.38920	9.0600
14.	0.2930	0.434418	10.11220
15.	0.3240	0.480381	11.18210
16.	0.3550	0.52634	12.2520

Table A3.2 Calibration values for FP - 1/16 - 10 - G - 5/84

flow meter. (Stainless steel float. (density 8.02 gm cm⁻³))

A = 143, B = 13.6, N = 1111.4, $\mu_{opt} = 0.00975$, $\beta_{opt} = 0.000716$

Scale Reading	C value at N = 1111.4	Flow at 762 mmHg and 15.6°C (gm. min. ⁻¹)	Flow at 762 mmHg and 15.6°C (cm ³ sec. ⁻¹)
3.	0.0044	0.004534	0.106
4.	0.0170	0.017520	0.408
5.	0.0290	0.029890	0.696
6.	0.0470	0.048440	1.128
7.	0.0680	0.070100	1.632
8.	0.0920	0.094800	2.207
9.	0.1170	0.120600	2.807
10.	0.1420	0.146340	3.406

Example of flowrate calibration

FP - 1 - 10 - G - 5/84

stainless steel float density 8.02 gm cm⁻³

from table 7, page 12, flowmeter constant

for tube diameter 1/16" x 1/2", s = 2.00

$\mu_{opt} = 0.00975$ coefficient

from table 6, page 11, $\beta_{opt} = 0.000716$

flow coefficient = 0.00975

flow rate = 0.00975 x (0.004534)

Table A3.3. Calibration values for FP - $\frac{1}{8}$ - 20 - G - 5/84 flowmeter
(Stainless steel float. (density 8.02 gm cm⁻³))

A = 404, B = 76.8, N = 3140.0, μ_{opt} = 0.00975, β_{opt} = 0.000716			
Scale Reading	C value at N = 3140.0	Flow at 762 mmHg and 15.6°C (gm min ⁻¹)	Flow at 762 mmHg and 15.6°C (cm ³ sec ⁻¹)
6.	0.098	0.5703	13.28
7.	0.121	0.7040	16.39
8.	0.143	0.8320	19.37
9.	0.171	0.9950	23.16
10.	0.200	1.1640	27.10
11.	0.226	1.3150	30.61
12.	0.252	1.4670	34.15
13.	0.279	1.6240	37.80
14.	0.306	1.7810	41.46
15.	0.330	1.9210	44.72
16.	0.365	2.1240	49.44
17.	0.395	2.2990	53.52
18.	0.425	2.4730	57.57
19.	0.456	2.6540	61.78
20.	0.486	2.8280	65.83

Example of flowrate calibration procedure.

FP - $\frac{1}{8}$ - 20 - G - 5/84.

Stainless steel float density 8.02 gm. cm⁻³

From table 7, page 12, Fischer & Porter Handbook 10A9010

For tube diameter $\frac{1}{8}$ " A = 404, B = 76.8

$$\mu_{opt} = \mu_{STP} + (\text{temp. coefficient}) (T - 70)$$

from table 6, page 9, F & P Handbook

$$\text{Temp. coefficient} = 0.000019$$

$$\therefore \mu_{opt} = 0.00994 + (0.000019) (60-70)$$

$$M_{opt} = 0.00975$$

$$\rho_{opt} = 0.000716 \text{ (762 mmHg and } 60^\circ\text{F)}$$

$$N = \frac{A}{M_{opt}} (\rho_f \rho_{opt} \rho_{opt})^{\frac{1}{2}} \text{ @ 762 mmHg and } 15.6^\circ\text{C.}$$

$$N = \frac{404}{0.00975} ((8.02 - 0.000716) 0.000716)^{\frac{1}{2}}$$

$$N = 3139.846$$

Using the float characteristic curve (Fig. 10, P 13, F&P Handbook) for $\frac{1}{8}$ " - 20 values of C can be read off at $N = 3140$ and tabulated in column 2 of table A3.2.

From equation 7.31

$$F = C.B (\rho_f \rho_{opt} \rho_{opt})^{\frac{1}{2}}$$

values of F (gm mins⁻¹) can be calculated and are tabulated in column 3 of table A3.2.

For C = 0.098

$$F = 0.098 \times 76.8 ((8.02 - 0.000716) 0.000716)^{\frac{1}{2}}$$

$$F = 0.5703 \text{ gm min}^{-1}$$

Converting F to cm³ sec⁻¹

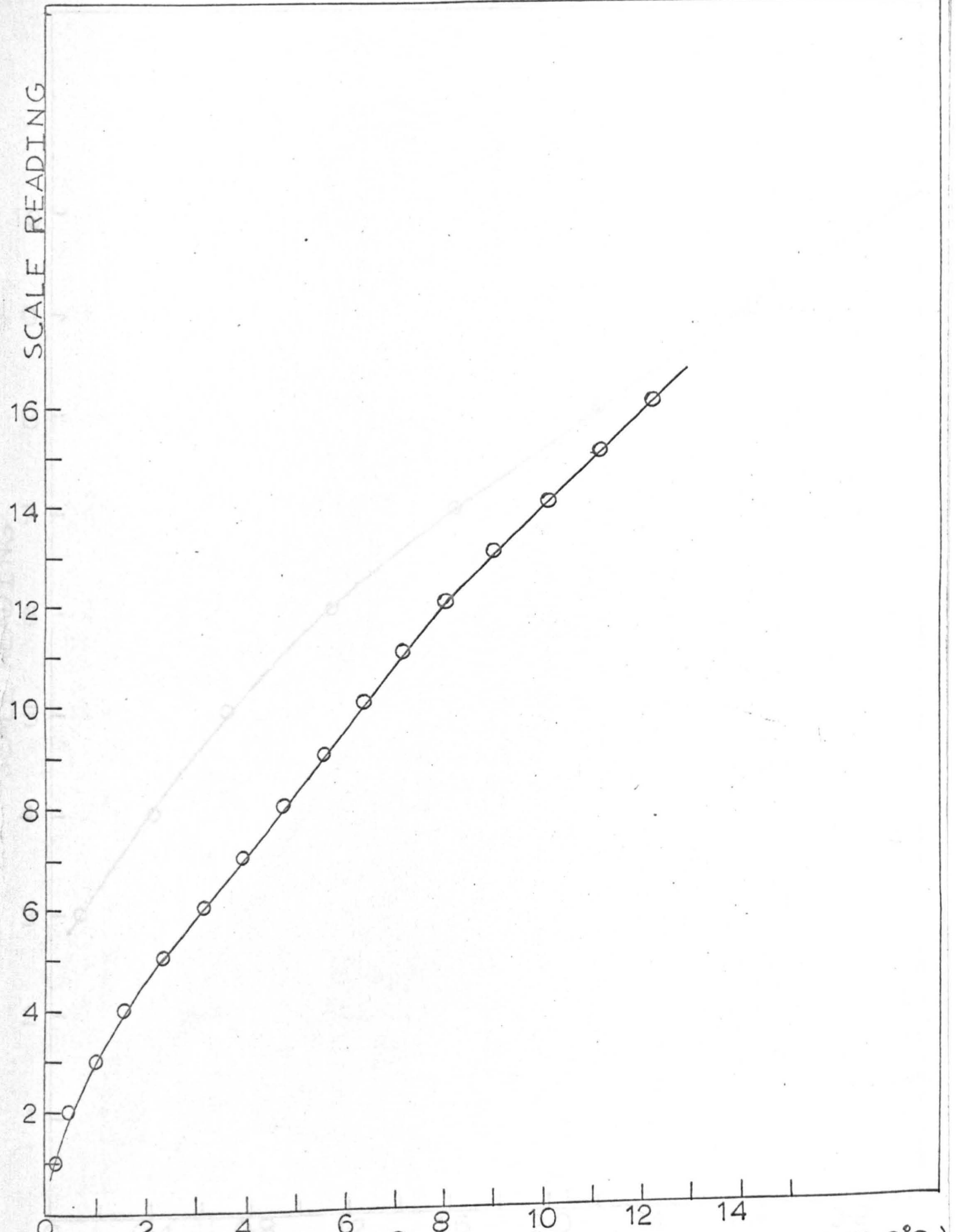
$$F \times \frac{1}{60 \times \rho} = \frac{0.5703}{60 \times 0.000716} = 13.29 \text{ cm}^3 \text{ sec}^{-1}$$

Table A3.4 Calibration values of FP - $\frac{1}{8}$ - 20 - G -5/84 using Soap Bubble Manometer.

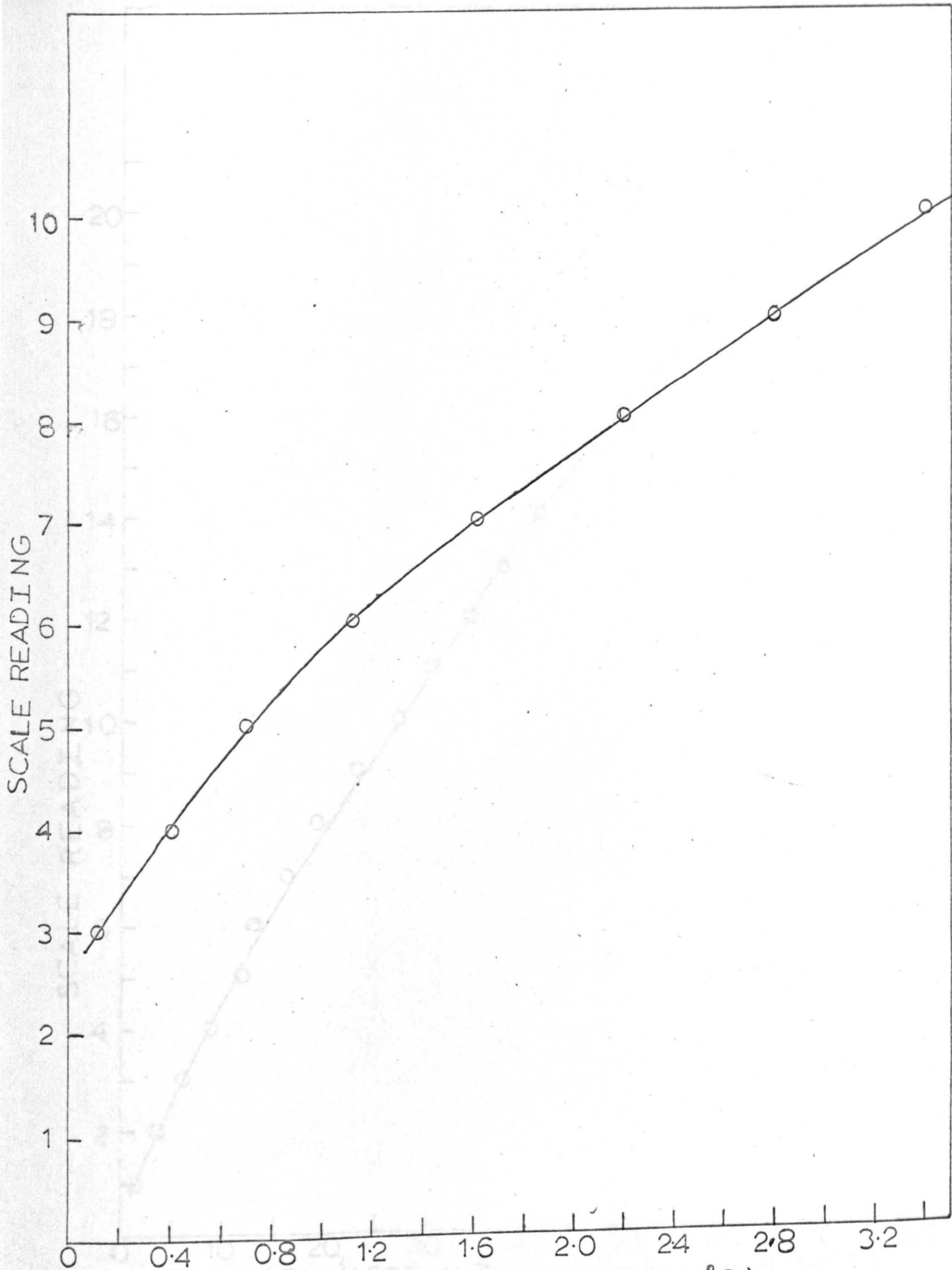
Scale Reading	Pressure (mmHg.)	Volume (cm. ³)	Time (sec.)	Flow at 762 mmHg and 15.6°C (cm ³ sec. ⁻¹)
7.3	802	200	11.7	18.1
13.5	940	300	9.0	41.1
18.0	975	450	10.0	57.5

FLOW (CM³/SEC at 762 mmHg and 15.6°C)

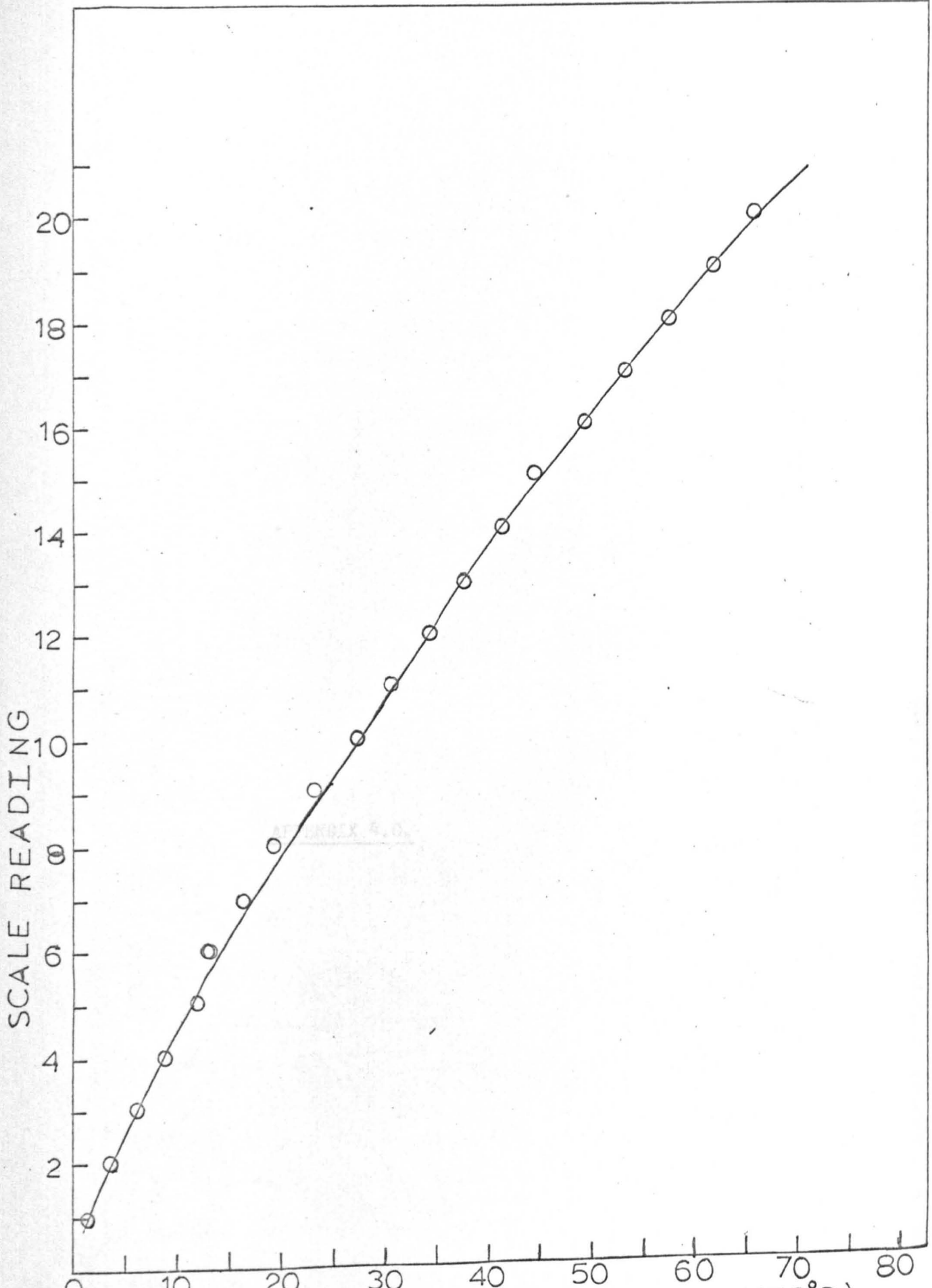
FIGA 34 CALIBRATION CURVE FOR FP - $\frac{1}{8}$ - 20 - G -5/84



FLOW (CM³/ SEC at 762 mm. Hg. Press. and 15.6°C)
 FIG.A 31 CALIBRATION CURVE FOR (FP-1/16-16-G-5/84)



FLOW (CM³ at 762 mm Hg Press and 15.6°C)
 FIGA32 CALIBRATION CURVE FOR (FP-116-10-G-5/84)



FIGA33 CALIBRATION CURVE (FOR FP-18-20-G-5/84)

Appendix 4.0.

Related Entities

Number	File Number	Type	Method	Notes
2015-001	15-001
2015-002	15-002

APPENDIX 4.0.

Tabulated Results.

Reactor	Run No.	Press (mmHg)	Flow (cm ³ sec ⁻¹)	Current (m.amps)	Voltage (volts)	Vc (volts)	Vp (volts)	L (cm)	r x 10 ⁸ (gms cm sec ⁻¹)	$\frac{(r \times 10^8) D^3}{FC}$	Z
<u>Table A4.1</u>											
Large	1.	9.5	1.84	109	650	457	181.4	5.82	4.07	29644	8.76
	2.	9.5	1.84	109	650	457	181.4	5.82	4.88	35589	8.76
	3.	9.5	3.11	108	660	457	192	5.83	9.08	23205	5.0
	4.	9.5	3.11	108	660	457	192	5.83	7.92	20240	5.0
	5.	9.5	4.50	103	690	457	222	5.83	10.60	12894	3.25
	6.	9.5	7.37	100	710	457	242	5.83	18.90	8594	1.92
	7.	9.5	10.24	99	720	457	253	5.83	27.40	6469	1.32
	8.	9.5	12.53	98	725	457	258.3	5.83	32.90	5179	1.06
	9.	9.5	15.18	97	730	457	263	5.83	35.20	3780	0.87
<u>Table A4.4</u>											
Large	10.	9.5	5.75	87	710	455	244	5.83	15.70	11734	2.56
	11.	9.5	5.75	87	710	455	244	5.83	15.50	11625	2.56
	12.	9.5	5.75	152	690	461	218	5.83	12.80	9482	2.25
	13.	9.5	5.75	208	680	466	203	5.83	10.55	8800	2.12

Vc = abnormal cathode fall of potential

Vp = potential difference across positive column.

r = nett rate of formation of hydrazine in positive column.

$$Z = \frac{(Vc)^4}{(F^3 C)^{0.27}} \frac{(D^4 P)^{0.71}}{(F^2 C)} \left(\frac{L}{D} \right)^{-0.54}$$

Table A4.7.

Reactor	Run No.	Press (mmHg).	Flow (cm ³ sec ⁻¹).	Current (m.amps)	Voltage (volts)	Vc (volts)	Vp (volts)	L (cm)	r x 10 ⁸ (gms cm ⁻³ sec ⁻¹)	(rx10 ⁸)D ³ / FC	Z
Large	14.	7.0	10.32	149	670	472	181	5.04	32.58	4818	0.87
	15.	9.5	10.32	140	710	460	239	5.83	23.82	5540	1.19
	16.	9.5	10.32	140	710	460	239	5.83	22.66	5261	1.19
	17.	12.0	10.32	138	720	507	202	6.0	37.35	11271	1.72
	18.	12.0	10.32	138	720	507	202	6.0	36.61	11048	1.72
Table A4.2											
Inter-mediate.	20.	9.5	0.70	44	615	463	141	2.58	27.3	19079	3.82
	21.	9.5	0.70	44	615	463	141	2.58	27.7	19342	3.94
	22.	9.5	1.17	43	620	463	146	2.58	52.3	13092	2.27
	23.	9.5	1.17	43	620	463	146	2.58	49.3	12337	2.27
	24.	9.5	1.89	43	625	463	151	2.58	72.9	6983	1.35
	25.	9.5	2.81	44	630	463	156	2.58	104.7	4539	0.88
	26.	9.5	2.81	43	630	463	156	2.58	110.6	4796	0.88
	27.	9.5	3.73	42	635	463	161	2.58	118.2	2908	0.65
	28.	9.5	4.73	42	640	463	167	2.58	139.1	2128	0.50
	29.	9.5	5.74	41	650	462	177	2.58	163.6	1700	0.61

Vc = abnormal fall of potential

Vp = potential difference across positive column

r = nett rate of formation of hydrazine in positive column

$$r = \left(\frac{VLD^4}{P^2C} \right)^{-0.17} \left(\frac{D^4P}{P^2C} \right)^{-0.71} \left(\frac{L}{D} \right)^{-0.54}$$

Table A4.5

Reactor	Run No.	Press (mmHg)	Flow (cm ³ sec ⁻¹)	Current (m.amps)	Voltage (volts)	Vc (volts)	Vp (volts)	L (cm)	r x 10 ⁸ (gms cm ⁻³ sec ⁻¹)	$\frac{(r \times 10^8) D^3}{FC}$	Z
Inter-mediate.	30.	9.5	3.77	23	635	456	168	2.58	117.4	2821	0.75
	31.	9.5	3.77	44	640	463	166	2.58	128.8	3104	0.63
	32.	9.5	3.77	63	650	470	169	2.59	116.2	2807	0.57
	33.	9.5	3.77	63	650	470	169	2.59	123.1	2971	0.57
	34.	9.5	3.77	106	640	485	144	2.60	110.4	2680	0.51
	35.	9.5	3.77	106	640	485	144	2.60	108.4	2631	0.52
	36.	9.5	3.77	145	640	499	131	2.60	94.3	2289	0.49
Table A4.8											
Inter-mediate.	37.	4.0	2.36	39	610	524	75	1.80	122.1	2200	0.44
	38.	4.0	2.36	39	610	524	75	1.80	127.7	2300	0.44
	39.	7.0	2.36	38	620	472	137	2.36	99.1	4092	0.76
	40.	9.5	2.36	37	630	472	147	2.59	85.8	5291	1.12
	41.	15.0	2.36	35	670	453	206	2.82	77.3	8195	1.88
	42.	20.0	2.36	35	680	451	213	2.93	69.3	10161	2.72
	43.	20.0	2.36	35	680	451	213	2.93	54.6	8012	2.69

Vc = abnormal cathode fall of potential

Vp = potential difference across positive column

r = nett rate of formation of hydrazine in positive column

$$Z = \frac{(Vc/D^4)^{-0.27} (D^4 P)^{0.71} (L)^{-0.54}}{(F^3 C) (F^2 C) (D)}$$

Table A4.3

Reactor	Run No	Press. (mmHg)	Flow (cm ³ sec ⁻¹)	Current (m. amps)	Voltage (volts)	Vc (volts)	Vp (volts)	L (cm)	r x 10 ⁸ (gms cm ⁻³ sec ⁻¹)	$\frac{(r \times 10^8) D^3}{FC}$	Z
Small.	44.	9.5	0.41	28.0	570	486	73	0.98	153.1	3853	1.16
	45.	9.5	0.70	28.0	580	486	83	0.98	287.0	2478	0.65
	46.	9.5	1.13	28.0	580	486	83	0.98	388.0	1285	0.39
	47.	9.5	1.63	27.0	580	486	84	0.98	549.3	875	0.26
	48.	9.5	1.63	27.0	590	485	94	0.98	594.0	946	0.25
	49.	9.5	1.63	27.0	580	485	84	0.98	542.3	864	0.26
	50.	9.5	2.21	28.0	580	486	83	0.98	745.0	645	0.19
	51.	9.5	2.81	28.0	580	486	83	0.98	830.7	445	0.15
	52.	9.5	3.41	28.0	580	486	83	0.98	1153.5	420	0.12
Table A4.6											
Small	53.	9.5	1.63	17.5	570	454	105	0.95	552.5	900	0.28
	54.	9.5	1.63	17.5	570	454	105	0.95	531.3	950	0.28
	55.	9.5	1.63	21.0	580	477	92	0.97	606.9	956	0.27
	56.	9.5	1.63	29.0	580	488	81	0.98	603.4	961	0.27
	57.	9.5	1.63	50.5	590	517	62	1.01	439.7	722	0.24
	58.	9.5	1.63	68.0	590	541	38	1.03	476.9	798	0.25

Vc = abnormal cathode fall of potential

Vp = potential difference across positive column

r = nett rate of formation of hydrazine in positive column

$$Z = \left(\frac{V_c D^4}{F^2 C} \right)^{-0.27} \left(\frac{D^4 P}{F^2 C} \right)^{-0.71} \left(\frac{L}{D} \right)^{-0.54}$$

Table A4.9.

Reactor	Run No.	Press. (mmHg)	Flow (cm ³ sec ⁻¹)	Current (m.amps)	Voltage (volts)	Vc (volts)	Vp (volts)	L (cm)	r x 10 ⁸ (gms cm ⁻³ sec ⁻¹)	$\frac{(rx10^8)^2}{FC}$	Z
Small.	59.	3.0	1.63	28.0	560	548	1.0	0.125	4629	97	0.25
	60.	5.0	1.63	28.0	560	544	5.0	0.50	1078	460	0.26
	61.	9.5	1.63	27.0	580	485	84	0.98	535.6	853	0.26
	62.	15.0	1.63	27.0	580	463	106	1.20	454.2	1398	0.44
	63.	20.0	1.63	26.5	590	456	123	1.31	377.5	1691	0.50

Table A4.10.

Large.	64.	5.0	1.13	96.5	620	478.3	130.5	5.3	3.5	32490	7.14
	65.	5.0	1.13	96.5	620	478.3	130.5	5.3	2.87	26558	7.14
	66.	5.0	4.35	21.0	620	514.2	94.6	5.3	17.22	10776	4.35
	67.	5.0	4.35	21.0	620	514.2	94.6	5.3	17.48	13113	4.35
	68.	5.0	3.11	97	630	478.5	140.3	5.3	18.05	22086	5.32
	69.	5.0	3.11	97	630	478.5	140.3	5.3	19.13	23400	5.32
	70.	9.0	1.69	138	650	461.3	177.5	5.8	6.83	55701	12.22
	71.	9.5	3.68	156	650	461.5	177.3	5.8	12.9	23472	9.84
	72.	9.5	5.75	136.5	700	459.8	229	5.85	24.24	18210	7.97
	73.	10.0	1.69	177	645	461.8	172	5.87	5.06	46440	12.68
74.	10.0	1.69	93.0	660	455.2	193.6	5.86	8.48	77630	15.2	

Table A4.10. (continued).

Reactor	Run No.	Press. (mmHg)	Flow (cm ³ sec ⁻¹)	Current (m.amps)	Voltage (volts)	Vc (volts)	Vp (volts)	L (cm)	r x 10 ⁸ (gms. cm ⁻³ sec ⁻¹)	(rx10 ⁸)D ³ / FC	Z
Large	75.	10.0	2.9	138.5	660	455.8	190	5.86	13.53	42117	10.59
Intermediate	76.	15.0	14.0	118	730	452	266.8	6.07	55.98	11618	10.86
	77.	17.0	20.0	116.5	740	451	277.8	6.12	59.55	6917	11.46
Table A4.11.											
Intermediate.	78.	5.0	1.13	99.5	600	573.4	15.4	2.17	89.28	10587	1.59
	79.	5.0	0.88	58.5	600	521.9	67	2.08	76.15	14274	1.29
	80.	8.0	1.13	61.5	625	478.2	135.6	2.47	74.45	16514	1.77
	81.	8.0	2.21	62	620	478.4	130.4	2.47	155.17	8760	1.46
	82.	9.0	1.13	95	630	484.8	134	2.57	66.15	16844	1.87
	83	9.0	1.13	49.5	620	467.1	141.7	2.55	79.08	19836	2.2
	84.	9.0	1.13	49.5	620	467.1	141.7	2.55	77.17	19359	2.2
	85.	9.5	0.41	45	615	463.6	140.2	2.58	30.69	62453	3.45
	86.	9.5	1.88	47	630	464.3	154.5	2.58	127.29	12320	1.98
	87.	10.0	2.50	35.5	635	459	164.8	2.61	170.65	9945	2.04
	88.	10.0	3.77	38	640	460	168.8	2.61	248.17	6361.5	1.75
	89.	10.0	3.77	38	640	460	168.8	2.61	237.19	6081	1.75
	90.	15.0	377	38.5	680	453	215.5	2.82	212.19	8855	2.7

Table A4.11. (continued).

Reactor	Run No	Press. (mmHg)	Flow (cm ³ sec ⁻¹)	Current (m.amps)	Voltage (volts)	V _c (volts)	V _p (volts)	L (cm)	r x 10 ⁸ (gms cm ⁻³ sec ⁻¹)	$\frac{(r \times 10^8) D^3}{FC}$	z
Inter-mediate	91.	15.0	3.77	38.5	680	453	215.5	2.82	205.9	8555	2.7
	92.	17.0	20.05	135.5	710	462.6	236.2	2.88	796.5	1362	1.27
Table A4.12.											
Small.	93.	5.0	1.13	105	570	553.8	5	0.52	844.3	785	0.28
	94.	5.0	0.88	63	560	543.8	5	0.50	1026.8	1508	0.34
	95.	5.0	0.88	31.5	560	543.8	5	0.50	851.9	1254	0.41
	96.	5.0	0.88	31.5	560	543.8	5	0.50	918.3	1350	0.41
	97.	7.0	1.13	98	570	553.8	5	0.83	642.0	1332	0.42
	98.	8.0	1.13	67.5	570	548.8	10	0.93	766.7	2033	0.46
	99.	8.0	2.21	67.5	570	548.8	10	0.93	1248.3	867	0.36
	100.	9.0	1.13	107	560	543.8	5	1.0	575.9	1851	0.56
	101.	9.0	1.13	53	580	529.1	39.7	0.98	594.8	1874	0.38
	102.	7.5	0.41	48.5	570	514.8	44	1.01	212.95	5540	0.58
	103.	7.5	3.41	14.5	570	467.8	91	0.96	2043.6	731	0.29
	104.	9.5	1.88	50.5	590	517.3	61.5	1.01	961.8	1191	0.31
	105.	9.5	1.13	16.5	590	470.5	108.3	0.97	728.4	2399	0.43
	106.	9.5	1.13	17	570	471.2	87.6	0.97	728.4	2399	0.46

Table A.4.12. (continued)

Reactor	Run No.	Press. (mmHg)	Flow (cm ³ sec ⁻¹)	Current (m.amps)	Voltage (volts)	V _c (volts)	V _p (volts)	L (cm)	r x 10 ⁸ (gms cm ³ sec ⁻¹)	($\frac{r \times 10^8}{FC}$) D ³	Z
Small.	107.	9.5	2.58	27.5	580	485.7	83.1	0.98	1680.0	1073	0.30
	108.	9.5	1.63	12.5	570	464.9	93.9	0.96	1347	2109	0.43
	109.	10.0	1.13	63	580	526.2	42.6	1.05	679.1	2544	0.41
	110.	15.0	2.54	30	590	464.4	114.4	1.2	1156.5	1475	0.49
	111.	15.0	2.54	30	590	464.4	114.4	1.2	1156.5	1475	0.49
	112.	19.5	3.41	29	610	475.3	141.5	1.3	844.4	1260	0.59
Table A4. 13.											
Large	1.	9.5	7.37	100	715	457	207	5.83	11.30	5150	2.0
	2.	9.5	7.37	140	720	460	249	5.83	7.68	3500	1.85
	3.	9.5	15.18	100	730	457	222	5.83	16.76	1800	0.91
	4.	9.5	15.18	140	735	460	264	5.83	6.52	700	0.77
Inter - mediate.	5.	9.5	3.77	63	615	470	134	2.59	48.31	1161.2	0.57
	6.	9.5	3.77	145	620	498.5	110.5	2.61	48.30	1168.0	0.49
	7.	9.5	12.82	63	615	470	134	2.59	130.0	270.0	0.15
	8.	9.5	12.82	145	630	498.5	110.5	2.61	98.0	205.0	0.09

V_c = abnormal cathode fall of potentialV_p = potential difference across positive column

r = nett rate of formation of hydrazine in positive column

$$Z = \left(\frac{V_{cD}^4}{FC} \right)^{0.27} \left(\frac{D^4 P}{FC} \right)^{0.71} \left(\frac{L}{D} \right)^{-0.54}$$

Table A4. 13 (continued)

Reactor	Run No	Press. (mmHg)	Flow (cm ³ sec ⁻¹)	Current (m.amps)	Voltage (volts)	Vc (volts)	Vp (volts)	L (cm)	r x 10 ⁸ (gms cm ⁻³ sec ⁻¹)	$\frac{(r \times 10^8)D^3}{FC}$	Z
small	9.	9.5	1.63	17.5	615	454	150	0.95	70.9	106.0	0.25
	10.	9.5	1.63	27.0	605	485	109	0.98	63.3	97.7	0.24
	11.	9.5	3.41	17.5	615	454	150	0.95	393.6	134.4	0.17
	12.	9.5	3.41	27.0	605	485	109	0.98	231.8	81.7	0.11

Vc = abnormal cathode fall of potential

Vp = potential difference across positive column

r = nett rate of formation of hydrazine in positive column

$$Z = \frac{(VD^4)^{0.27}}{(F^3C)} \frac{(D^4P)^{0.71}}{(F^2G)} \frac{(L)^{0.54}}{(D)}$$

DIFFERENTIAL

DIFFERENTIAL

The following information is provided for the purpose of
clarifying the information contained in the preceding pages.
It is intended to provide a more complete picture of the
situation and to assist in the understanding of the
data presented in the preceding pages.

The information presented in this appendix is intended to
provide a more complete picture of the situation and to
assist in the understanding of the data presented in the
preceding pages. It is intended to provide a more complete
picture of the situation and to assist in the understanding
of the data presented in the preceding pages.

APPENDIX 5.0.

DIFFERENTIAL

The following information is provided for the purpose of
clarifying the information contained in the preceding pages.
It is intended to provide a more complete picture of the
situation and to assist in the understanding of the
data presented in the preceding pages.

The information presented in this appendix is intended to
provide a more complete picture of the situation and to
assist in the understanding of the data presented in the
preceding pages.

Appendix 5.0

Dimensional Analysis

The methods of dimensional analysis are of very wide application and are especially valuable in the study of phenomena which are too complex for complete theoretical treatment. There is little doubt that chemical synthesis in a glow discharge may be classified in this category and thus lends itself ideally to study by dimensional analysis.

Dimensional analysis may be defined as a study of the restrictions placed on the form of an algebraic function by the requirements of dimensional homogeneity. More simply this means that dimensional analysis indicates the possible ways of grouping the magnitude of those physical quantities which the investigator has supposed relevant to the phenomena under study. It is important to note that dimensional analysis cannot tell the investigator whether the quantities he lists are in fact relevant.

Dimensional Formula.

The fundamental magnitudes Mass (M), Length (L), interval of time (T) and electric charge(Q), have been used in this study. The choice of electric charge was purely arbitrary. The magnitudes of magnetic permeability of free space (μ_0), the permittivity of free space (ϵ_0) or electric resistance could equally have been chosen.

In table A5.1 the dimensional formula for the selected discharge parameters are listed.

Table A5.1

Quantity	Symbol	Dimensional Formula
Electric Current	I	(Q T ⁻¹)
Potential difference across the length of the positive column.	Vp	(M L ² T ⁻² Q ⁻¹)
Volumetric flow or reactant gas.	F	(L ³ T ⁻¹)
Pressure in reaction zone.	P	(M L ⁻¹ T ⁻²)
Concentration of reactant gas in positive column	C	(M L ⁻³)
Diameter of reaction tube	D	(L)
Length of positive column	L	(L)
Nett rate of hydrazine formation. in positive column.	r	(M L ⁻³ T ⁻¹)

Analysis

$$r = f ((V_p)^a (I)^b (L)^c (D)^d (F)^e (P)^f (C)^g)$$

substituting dimensional formulae

$$M L^{-3} T^{-1} = f (M L^2 T^{-2} Q^{-1})^a (Q T^{-1})^b (L)^c (L)^d (L^3 T^{-1})^e (M L^{-1} T^{-2})^f (M L^{-3})^g$$

Balancing the exponents of LMT and Q :

Q) 0 = -a + b . . . b = a

M) 1 = a + f + g . . . g = 1 - a - f

L) -3 = 2a + c + d + 3e - f - 3g

t) -1 = -2a - b - e - 2f

Eliminating e gives -

$$-1 = -2a - a - e - 2f$$

$$\therefore e = -3a - 2f + 1$$

eliminating d gives -

$$-3 = 2a + c + d - 9a + 3 - 6f - f - 3g$$

$$\therefore d = 4a + 4f - c - 3$$

$$\text{Thus } r = \frac{F C}{D^3} f \left(\frac{V_p I D^4}{F^3 C}, \frac{L}{D}, \frac{D^4 P}{F^2 C} \right) \quad (\text{A } 5-1)$$

Assuming an exponential relationship

$$\frac{r D^3}{F C} = K \left(\frac{V_p I D^4}{F^3 C} \right)^a \left(\frac{L}{D} \right)^c \left(\frac{D^4 P}{F^2 C} \right)^d \quad (\text{A } 5-2)$$

Although equation (A5-2) has been used to correlate the experimental results obtained in the present study, it should be noted that equation (A5-1) may be rearranged into a number of other equations which might also have been used to correlate the experimental data. Thus for example rearranging equation (A5-1) by replacing $\frac{V_p I D^4}{F^3 C}$ with the quotient of $\frac{V_p I D^4}{F^3 C}$ and $\frac{D^4 P}{F^2 C}$

yields

$$\frac{r D^3}{F C} = f_1 \left(\frac{V_p I}{F P}, \frac{L}{D}, \frac{D^4 P}{F^2 C} \right)$$

It is interesting to examine the possible physical significance of these groups. Thus the group $\frac{r D^3}{F C}$ may be rearranged to give

$$\frac{r D^3}{F C} = \frac{r}{\frac{F C}{D^3}}$$

For the experimental conditions used, the specific volume of ammonia gas (reactant gas) may be assumed to be constant, and it follows therefore that the group $\frac{F C}{D^3}$ is a function of the ammonia space velocity. Thus $\frac{r D^3}{F C}$ is the ratio of the nett rate of formation of hydrazine to the ammonia space velocity.

The primary activation of a molecule (ammonia) in a discharge depends upon the energy imparted during an inelastic collision (i.e. $f \left(\frac{E}{P} \right)$) and the frequency with which collisions occur (i.e. $f (J, \gamma)$). The group $\frac{V_p I}{F P}$ may be rearranged to give

$$\frac{V_p I}{F P} = \frac{E, x J, x \gamma}{P}$$

and thus it follows that the primary activation of a molecule in a discharge is a function of the dimensionless combination $\frac{V_p I}{F P}$.

In the context of this study 'primary activation' refers to the decomposition of ammonia molecules into amine radicals. These amine radicals react in two principal ways, either in the gas phase (to form hydrazine) or at the surface of the reaction tube (to form products other than hydrazine). The dimensionless group $\frac{D^4 P}{F^2 C}$ may be rearranged to yield

$$\frac{D^4 P}{F^2 C} = \frac{P D}{F} \left(\frac{F C}{D^3} \right)^{-1}$$

where the group $\frac{F C}{D^3}$ is a function of the 'translational' space

Velocity of the amine radicals and the group $\frac{P D}{F}$ is a function of the ' diffusional ' space velocity of the amine radicals. More simply the dimensionless group $\frac{D^2 P}{F^2 a C}$ is a function of the ratio of the residence time for the reaction of amine radicals to form hydrazine (in the gas phase) to the residence time for the reaction of amine radicals to form products other than hydrazine (at the surface of the reaction tube).

Finally it was noted in chapter 5.0 that the rate of destruction of hydrazine by atomic hydrogen attack depends upon the concentration of atomic hydrogen in the reaction zone (gas phase). The concentration of atomic hydrogen in the reaction zone will depend upon the rate of diffusion of atomic hydrogen to the reaction tube surface and also upon the (active) area of the reaction tube surface which is available for the recombination of atomic hydrogen (i.e. the surface area of the reaction tube occupied by the positive column of the discharge). Thus it follows that the rate of destruction of hydrazine by atomic hydrogen will be a function of the dimensionless combination $\frac{L}{D}$.

APPENDIX 6.0.

Appendix 6.0.

Method of estimation of the abnormal cathode fall of potential and the length of the positive column.

For a dc glow discharge operated in the abnormal glow region Von Engel (1955) has shown theoretically that -

$V_c = f(J p^{-2})$ and $d = f(V_c)$ where

V_c = the abnormal cathode fall of potential

J = the current density

p = pressure

d = width of cathode dark space.

A number of investigators (including Wolf (1939), Guntherschulze (1930) and Penning (1957)) have shown that over a wide range of current density and pressure for most gases and electrode materials the relationship between V_c and $J p^{-2}$ is of the form -

$V_c = m (J p^{-2}) + C$ where C = a constant

and

$d p = m (V_c) + C_1$, where C_1 = a constant

Estimation of potential difference across the positive column.

For a dc glow discharge operated in the abnormal glow region the total potential across the discharge may be assumed to be the sum of the abnormal cathode fall of potential, the anode fall of potential and the fall of potential across the positive column. Thus assuming the anode fall of potential (which is normally very small) to be of the order of magnitude of the ionisation potential of ammonia i.e. 11.2 volts.

$V = V_c + V_p + V_a$

where V is measured experimentally $V_a = 11.2$ volts and V_c is estimated below.

Thus V_p may be calculated from -

$V_p = V - V_c - V_a$

experimental results are

Estimation of Vc.

In table A6.1 values of Vc and $J p^{-2}$ (for a glow discharge in ammonia gas) obtained from the work of Ouchi (1952) are recorded. These results are plotted in Fig. A6.1 which illustrates that a linear relationship exists between Vc and $J p^{-2}$. Regression analysis of this data yielded the equation -

$$Vc = 61.40 J p^{-2} + 447.90$$

which has been used to calculate Vc for all the experimental results reported.

Estimation of the length of the positive column.

The length of the positive column in an abnormal glow discharge may be estimated as the distance between the electrodes minus the distance from the cathode to the edge of the positive column (cathode end).

In table A6.2 values of Vc and dp (for a glow discharge in ammonia gas) obtained from the work of Ouchi (1952) are recorded.

Fig. A6.2 shows a plot of these results illustrating that a linear relationship of the form -

$$d.p = - 0.0008 Vc + 0.9536$$

exists between dp and Vc. Thus if Vc is known (estimated) then d may be calculated for any pressure.

In an abnormal glow discharge the ratio of the distance between the cathode and the point at which the positive column begins, and the length of the cathode dark space is a constant. Inspection of Ouchi's data shows that the value of this constant is 10.87. Thus the length of the positive column of a discharge operated in the abnormal region may be estimated as -

where $L = \text{Inter-electrode distance (l)} - 10.87 d$
 $d = (0.9536 - 0.0008 Vc) p^{-1}$

This relationship has been used to estimate L for all of the experimental results reported.

Table A6.1

Pressure (mmHg)	Current (milliamps)									
	10		15		20		25		30	
	Jp ⁻² (m.mms) (cm ²)	Vc (volts)	Jp ⁻²	Vc	Jp ⁻²	Vc	Jp ⁻²	Vc	Jp ⁻²	Vc
2	3.18	607	4.78	707	6.37	857	7.96	949	9.55	-
3	1.41	529	2.12	557	2.83	607	3.54	657	4.24	700
4	0.80	471	1.19	514	1.59	546	1.99	586	2.39	614
5	0.61	464	0.76	487	1.02	521	1.27	550	1.53	575
6	0.35	458	0.63	475	0.71	504	0.88	529	1.06	557
7	0.26	450	0.39	464	0.62	479	0.65	507	0.78	529
8	0.20	449	0.30	450	0.40	471	0.50	486	0.60	507
9.5	0.14	440	0.21	445	0.28	452	0.35	473	0.42	487

Table A6.2

Pressure (mmHg)	Current density (milliamps cm ⁻²)							
	12.73		19.10		25.46		31.83	
	dp (cm mmHg)	Vc (volts)	dp	Vc	dp	Vc	dp	Vc
3.13	0.5	527.7	0.47	567.6	0.47	607.5	0.44	647.5
4.20	0.59	492.2	0.55	514.4	0.55	536.5	0.50	558.7
6.30	0.63	467.6	0.57	477.4	0.57	487.3	0.57	497.1
8.0	0.64	460.1	0.64	466.2	0.56	472.3	0.56	478.4
10.0	0.60	455.7	0.60	459.6	0.50	463.5	0.50	467.4

Specimen Calculation.

Run 1. Table A4.1

Potential difference across positive column.

$$\text{Abnormal cathode fall of potential (Vc)} = 61.4 \times \frac{\text{current density}}{(\text{pressure})^2} + 447.9$$

$$\therefore V_c = 61.4 \times \frac{109 \times 1}{\pi \times 3.15^2 \times 9.5^2} + 447.9$$

$$\therefore V_c = 9.5 + 447.9$$

$$\therefore \underline{V_c = 457.4}$$

$$\therefore V_p = V - V_c - V_a$$

$$\text{i.e. } V_p = 650 - 457.4 - 11.2$$

$$V_p = 181.4$$

Length of positive column.

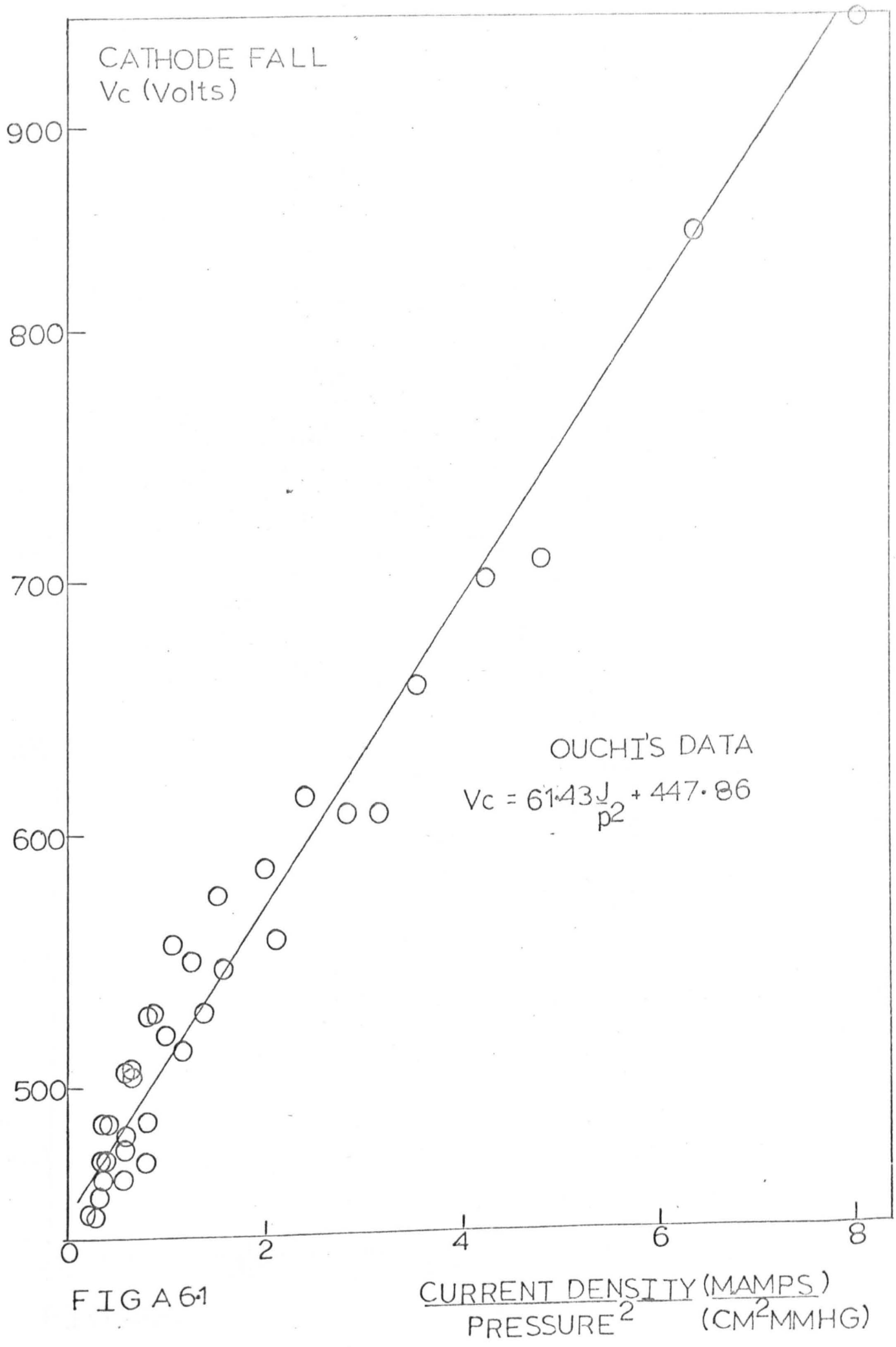
L = inter-electrode distance - 10.87 d.

where d = (0.9536 - 0.0008 Vc) p⁻¹

$$\therefore L = 6.5 - 10.87 \left(\frac{0.9536 - (0.0008 \times 457.4)}{9.5} \right) = \underline{5.82 \text{ cm.}}$$



FIG. A. 1



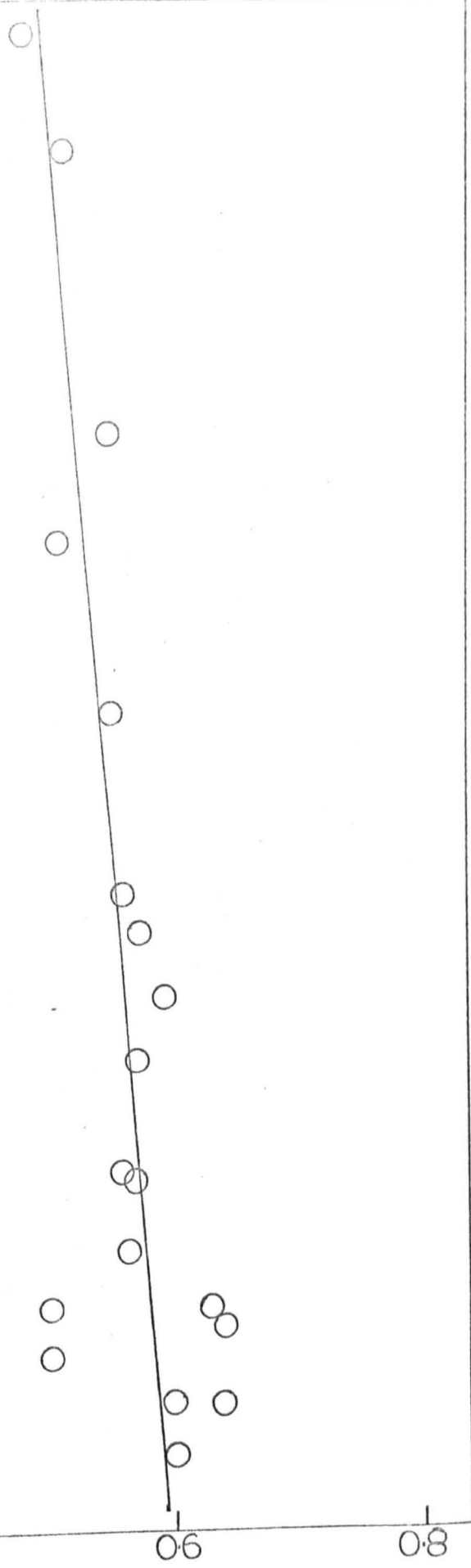
CATHODE FALL
 V_c (Volts)

OUCHI'S DATA
Dark Space Width \cdot Pressure
 $= -0.0008 \cdot V_c + 0.9536$

560
540
520
500
480
460
0
0.2
0.4
0.6
0.8

DARK SPACE WIDTH \cdot PRESSURE
(cm.mmHg)

FIG A6.2



APPENDIX 7.0.

Appendix 7.0

Specimen Calculations.

A7.1 Nett rate of formation of hydrazine (r)

Hydrazine produced in a Run.

In all runs hydrazine was absorbed in 50 mls of ethylene glycol.

A sample of this material was diluted then analysed for ppm hydrazine.

Thus if the reading obtained from the calibration curve was α ppm

hydrazine then in t minutes

$$\text{grams of hydrazine} = \alpha \times 10^{-6} \times \text{dilution} \times 50 \text{ (volume of ethylene glycol)}$$

$$\therefore \text{nett rate of formation of hydrazine} = \frac{\text{gms. of hydrazine}}{(t \times 60) \text{ secs} \times \frac{(\pi D^2 L)}{4}} \text{ cm}^3$$

where D = reaction tube diameter

L = length of the positive column

$\frac{\pi D^2 L}{4}$ = volume of the positive column

Typical Case.

All typical case examples presented in this appendix refer to

run number 1, table A4.1.

$$\alpha = 0.402 \text{ ppm} \quad \text{volume of ethylene glycol} = 50.0 \text{ mls.}$$

$$D = 3.15 \text{ cm} \quad \text{volume of analysis sample} = 2.0 \text{ mls.}$$

$$L = 5.82 \text{ cm} \quad \text{volume of water and/or}$$

$$t = 2 \text{ mins.} \quad \text{colour reagent added} = 20.0 \text{ mls.}$$

$$\text{grams of hydrazine} = 0.402 \times 10^{-6} \times \frac{20+2}{2} \times 50 = 2.2154 \times 10^{-4} \text{ grams.}$$

$$\therefore \text{nett rate of formation of hydrazine} = \frac{2.2154 \times 10^{-4} \times 4}{120 \times 3.15^2 \times 5.82} = 4.07410^{-8} \frac{\text{gms}}{\text{cm}^3 \text{ sec}}$$

A7.2 $\frac{(r \times 10^8) D^3}{FC}$

$$\frac{(r \times 10^8) D^3}{FC} = \frac{(\text{nett rate of formation of hydrazine} \times 10) \times (\text{Diam. of Reaction tube})^3}{(\text{Ammonia flow at op. conditions}) \times (\text{Concen. of ammonia gas})}$$

Typical Case.

$$(r \times 10^8) = 4.07 \text{ gm cm}^{-3} \text{ sec}^{-1}$$

$$D = 3.15 \text{ cm.}$$

$$F = 1.84 \text{ cm}^3 \text{ sec}^{-1}$$

$$C = 2.9 \times 10^{-5} \text{ gms cm}^{-3} \text{ (see A7.3).}$$

$$\frac{(rx10^8)D^2}{FC} = \frac{4.07 \times 3.15^2}{1.84 \times \frac{762}{9.5} \times 2.9 \times 10^{-5}} = 29644 \text{ (dimensionless)}$$

A7.3. Concentration of ammonia gas.

$$C = \frac{\text{Flow of ammonia gas } \left(\frac{\text{cm}^3}{\text{sec}}\right) \times \text{density of ammonia gas } \left(\frac{\text{gms}}{\text{cm}^3}\right)}{\text{volume of positive column (cm}^3\text{)}}$$

volume of positive column (cm³)

Typical Case.

$$F = 1.84 \text{ cm}^3 \text{ sec}^{-1}$$

$$\rho = 0.000716 \text{ gm cm}^{-3}$$

$$L = 5.82 \text{ cm}$$

$$C = \frac{1.84 \times 0.000716 \times 4}{\pi \times 3.15^2 \times 5.82} = 2.9 \times 10^{-5} \frac{\text{gms}}{\text{cm}^3 \text{ sec}}$$

$$A7.4. \frac{(V_p I D^4)}{(F^3 C)}$$

$$\frac{V_p I D^4}{F^3 C} = \frac{(\text{Voltage difference across positive column})(\text{Current})(\text{Diam. of reaction tube})^4}{(\text{Ammonia flow at operating conditions})^3 \times (\text{Concentration of ammonia gas})}$$

Typical Case.

$$\frac{V_p I D^4}{F^3 C} = \frac{181.4 \times 109 \times 3.15^4}{(1.84 \times \frac{762}{9.5})^3 (2.9 \times 10^{-5})} = 21067 \text{ (dimensionless).}$$

A7.5 $\frac{(D^4 P)}{(F^2 C)}$

$$\frac{(D^4 P)}{(F^2 C)} = \frac{(\text{Diameter of reaction tube})^4 (\text{Pressure in reaction tube})}{(\text{Ammonia flow at operating conditions})^2 (\text{Concentration of ammonia gas})}$$

Typical Case.

$$\frac{(D^4 P)}{(F^2 C)} = \frac{3.15^4 \times 9.5}{(1.84 \times 762)^2 (2.9 \times 10^{-5})} = 1479 \text{ (dimensionless)}$$

A7.6

$$\frac{L}{D} = \frac{\text{Length of positive column}}{\text{Diameter of reaction tube}} \text{ (dimensionless)}$$

Typical Case.

$$= \frac{5.82}{3.15} = 1.84$$

A7.7

$$\left(\frac{V_p I D^4}{F^3 C}\right)^{-0.27} \times \left(\frac{D^4 P}{F^2 C}\right)^{0.71} \times \left(\frac{L}{D}\right)^{-0.59} \text{ (dimensionless)}$$

Typical Case.

$$(21067)^{-0.27} \times (1.479 \times 10^{-3})^{0.71} \times (1.84)^{-0.59} = 8.76$$

A7.8

(Reduced electric field strength) pos. col. = $\frac{E}{p}$ $\frac{\text{volts}}{\text{cm mmHg}}$

where E = volts per cm of positive column i.e. $\frac{V_p}{L}$

Typical Case.

$$\frac{E}{p} = \frac{181.4}{5.82 \times 9.5} = 3.30 \left(\frac{\text{volts}}{\text{cm mmHg}} \text{ pos. col.} \right)$$

A7.9 Chromatography Results.

Method of Calculation

a) From ammonia flow rate grams per minute calculate the number of moles entering the reactor in unit time, say one minute.

$$\text{Moles} = \frac{\text{grams}}{\text{Molecular weight.}} = \frac{\text{grams}}{17}$$

b) From chromatography results -

H ₂	N ₂	N ₂ H ₄	NH ₃
z	y	x	100 - (x+y+z) moles percent.

c) Calculate weight percent - assume one mole of gas mixture.

$$\begin{aligned} \text{Weight of H}_2 &= 0.02 z \\ \text{Weight of N}_2 &= 0.28 y \\ \text{Weight of N}_2\text{H}_4 &= 0.32 x \\ \text{Weight of NH}_3 &= 0.17 (100 - (x+y+z)) \end{aligned}$$

$$\text{therefore weight percent of hydrazine} = 100 \times \frac{0.32x}{(0.17(100-(x+y+z)) + 0.02z + 0.28y + 0.32x)}$$

d) Let Y be weight of hydrazine obtained by analysis.

Let W be weight of ammonia entering reactor

$$\therefore \frac{Y}{W} \times 100 = \frac{0.32x}{0.17(100 - (x+y+z)) + 0.02z + 0.28y + 0.32x} \times 100$$

therefore solving for x gives mole percent hydrazine in gas mixture.

e) Partial pressure of ammonia in gas collection sample vessel

$$P \times \frac{100 - (x+y+z)}{100} = P_{\text{NH}_3}$$

z and y are obtained directly from chromatography results, x is calculated as shown previously.

P = total pressure in gas collection vessel (measured at a point just down stream of reactor, i.e. just between the reactor and the collection vessel).

f) Number of moles of ammonia in collection vessel.

$$n = \frac{V}{RT} \times \frac{t \times F_{op}}{\text{Vol}} \quad \text{where } t = \text{time of discharge (60 secs.)}$$

F = Flow rate at operating press. cm³ sec⁻¹

Vol = volume of gas collection vessel

$$\therefore n = \frac{P_{\text{NH}_3} \times t \times F_{op}}{RT}$$

P = pp of NH₃

T = Temp^oC (20^oC)

$$n = \frac{\text{NH}_3 \times 60 \times (F_{op} \times 762)}{(9.5) \times R}$$

R = Gas constant

V = Volume of gas.

$$(273 + 20) \times 0.08206 \times 1000(\text{litre}) \times 760(\text{atmos})$$

$$n = 0.002501 \times \frac{F_{STP}}{P} \times P_{\text{NH}_3}$$

g) Moles of NH₃ decomposed is given by moles going into reactor - moles

going out of reactor .

h) % hydrazine formed from ammonia decomposed

$$= \frac{\text{gms hydrazine} / 32}{\text{Moles Ammonia decomposed}} \times 100$$

Example Calculation. Run No. 50 (A4.3) and (A7.1)

Conversion based upon ammonia entering reactor = 0.229

Chromatography analysis $H_2 = 2.25\%$ $N_2 = 0.5\%$

Hydrazine analysis $2.1725 \times 10^{-4} \text{ gms min}^{-1}$

Ammonia entering $0.0948 \text{ gms min}^{-1}$

1) Molal % hydrazine

$$0.229 = \frac{32x}{0.17 (100 - (x+0.5 + 2.25) + 0.02(2.25) + 0.28(0.5) + 0.32x)}$$

$$0.229 = \frac{32x}{16.7175 + 0.15x}$$

$$\therefore x = 0.119763\%$$

2) Partial pressure of ammonia in collection vessel.

Reactor operating pressure = 9.5 mmHg

$$\therefore p_{NH_3} = 9.5 \times \left(100 - \frac{(2.25 + 0.5 + 0.119763)}{100} \right)$$

$$P_{NH_3} = 9.5 \times 0.9713$$

$$P_{NH_3} = 9.22735 \text{ mmHg}$$

3) Number of moles of ammonia coming out of reactor.

$$\begin{aligned} n &= 0.002501 \times \frac{F}{P} \times P_{NH_3} \\ &= 0.002501 \times \frac{2.207}{9.5} \times 9.22735 \\ &= 0.005361 \text{ Moles} \end{aligned}$$

4) Moles of ammonia decomposed.

$$\begin{array}{r} \text{Moles in} - \text{Moles out} \\ \underline{0.948} \quad - \quad \underline{0.005361} \\ 17 \\ \text{i.e. } 0.005576 \quad - \quad 0.005361 \end{array}$$

i.e. 0.000215

i.e. 2.15×10^{-4} Moles of ammonia decomposed.

5) % Hydrazine based upon ammonia decomposed.

$$100 \times \frac{2.1725 \times 10^{-4}}{32}$$

- moles of hydrazine formed

$$2.15 \times 10^{-4}$$

- moles of ammonia decomposed.

$$\therefore \% = \frac{6.789}{2.15}$$

$$= \underline{3.15\%}$$

Table 2

Run No.	Flow (gpm)	Flow (m ³ /hr)	Flow (m ³ /min)	Flow (m ³ /sec)	Flow (m ³ /hr)	Flow (m ³ /min)	Flow (m ³ /sec)	Flow (m ³ /hr)	Flow (m ³ /min)	Flow (m ³ /sec)
1	0.1	0.000278	0.00000464	0.000000773	0.000278	0.00000464	0.000000773	0.000278	0.00000464	0.000000773
2	0.2	0.000556	0.00000928	0.000001546	0.000556	0.00000928	0.000001546	0.000556	0.00000928	0.000001546
3	0.3	0.000833	0.00001392	0.000002319	0.000833	0.00001392	0.000002319	0.000833	0.00001392	0.000002319
4	0.4	0.001111	0.00001856	0.000003092	0.001111	0.00001856	0.000003092	0.001111	0.00001856	0.000003092
5	0.5	0.001389	0.00002320	0.000003865	0.001389	0.00002320	0.000003865	0.001389	0.00002320	0.000003865

6-20-54

Table A7.1

Run No.	Pressure (mmHg)	Flow (gms min)	N ₂ H ₄ (gms x 10 ⁴)	H ₂ peak height	Mole % H ₂	N ₂ peak height*	Mole % N ₂	Mole % N ₂ H ₄	Partial press. of NH ₃ in collection vessel.	Moles of NH ₃ entering C.V. x 10 ³	Moles of NH ₃ leaving C.V. x 10 ³	Moles of NH ₃ decomposed x 10 ⁴	% NH ₃ decomposed
50.	9.5	0.0948	2.1725	0.8	2.25	0.8	0.5	0.119763	9.22735	5.576	5.361	2.15	3.86
56.	9.5	0.07011	1.8975	1.5	4.40	0.8	0.5	0.104535	9.025	4.12415	3.876	2.4815	6.02
99.	8.0	0.0474	1.8400	1.45	4.2	1.1	0.65	0.076117	7.606	5.576	5.247	3.29	5.90
100.	9.0	0.04845	0.913	4.75	14.1	10.7	4.4	0.00007	7.335	2.7809	2.2299	5.51	19.81
108.	9.5	0.070111	2.052	0.40	1.05	0.8	0.5	0.15493	9.338	4.12415	4.0	1.2415	3.01

Table A7.1
(cont'd)

Run No.	Moles of N ₂ H ₄ x 10 ⁶	Moles of H ₂ x 10 ⁵	Moles of N ₂ x 10 ⁵	Mole % N ₂ H ₄ from NH ₃ decomposed.	Mole % H ₂ based on NH ₃ decomposed	Mole % N ₂ based on NH ₃ decomposed	Weight % N ₂ H ₄ based on NH ₃ entering. (0.20)
50.	6.789	12.40	2.75	3.15	57.7	12.79	0.229
56.	5.9296	17.90	2.04	2.40	72.13	8.22	0.271
99.	5.75	23.10	3.50	1.748	70.21	10.64	0.196
100.	2.85312	39.70	12.40	0.520	72.05	22.51	0.188
108.	6.4125	4.20	1.90	5.165	33.83	15.30	0.293

* corrected for air leakage.